Molecular analysis of rare patients with bone marrow failure syndromes highlights a role of epigenetic regulation and chromatin biology in hematopoiesis

A thesis submitted for the degree of Doctor rerum naturalium (Dr. rer. nat.)

In the subject of clinical Immunology

By

Ehsan Bahrami

Ludwig-Maximilians-Universität

Department of Biology

Munich, 2017

Diese Dissertation wurde angefertigt unter der Leitung von Prof. Dr. Christoph Klein und Prof. Dr. Heinrich Leonhardt im Bereich von der Fakultät für Biologie der Ludwig-Maximilians-Universität München

Erstgutachter: Prof. Dr. Heinrich Leonhardt

Zweitgutachter: Prof. Dr. Thomas Cremer

Tag der Abgabe: 14. April. 2017

Tag der mündlichen Prüfung: 21.Juli. 2017

I dedicate this PhD thesis to our patients, Dr. Jacek Puchalka, and

my family

Eidesstattliche Erklärung

Ich versichere hiermit an Eides statt, dass die vorgelegte Dissertation von mir selbständig und ohne unerlaubte Hilfe angefertigt ist.

München, Apr 2017

Ehsan Bahrami

Table of Contents

1. List of figures

2. List of abbreviations

Amino acid	aa
AR	Autosomal recessive
ATM	Ataxia-telangiectasia mutated
BM	Bone marrow
BMF	Bone marrow failure
CMP	Common myeloid progenitor
CRC	Chromatin remodeling complexes
DBA	Diamond–blackfan anemia
DC	Dyskeratosis congenita
DDR	DNA damage response
EBF	Early B cell factor
E2A	E protein 2-alpha
FA	Fanconi anemia
GFP	Green fluorescent protein
GMP	Granulocyte-macrophage progenitor
HSC	Hematopoietic stem cell
HSCT	Hematopoietic stem cell transplantation
H2A	Histone 2A
Phospho-H2AX	ɣ-H2AX
Ig	Immunoglobulin
MDS	Myelodysplastic syndrome
MLP	Monocyte-lymphoid progenitor
MYMS1	Myb-like, SWIRM and MPN domains 1
ROS	Reactive oxygen species
SBDS	Shwachman-Bodian-Diamond Syndrome
SCN	Severe congenital neutropenia
SFFV	Spleen focus forming virus
TAR	Thrombocytopenia absent radii
TF	Transcription factors
Ub	Ubiquitine
Ub-H2A	Ubiquitinated Histone 2A
UCH	Ubiquitin carboxy-terminal hydrolases

3. Summary

Inherited bone marrow failure (BMF) syndromes comprise a heterogeneous group of genetic disorders characterized by dysfunction of hematopoietic stem cells. Studying the genetic lesions causing these diseases is critical for the development of better diagnostic tools, the understanding of underlying pathogenic pathways and the development of novel therapeutic strategies. In recent years, approximately 50 genes have been identified to be involved in pathogenesis of BMF syndromes. However, there are still many patients with BMF manifestations where the underlying gene mutation has not been identified.

Myb-Like, SWIRM and MPN domains 1 (MYSM1) is a transcriptional regulator mediating histone deubiquitination. Its role in human immunity and hematopoiesis is poorly understood. Targeted deletion of murine Mysm1 results in severe hematopoietic defects associated with an early block of B cell development, defective stem cell-maintenance, -self-renewal and -differentiation, as well as NK cell dysfunction. In humans, exome-sequencing studies have revealed potentially disease-causing mutations in MYSM1 in two families with BMF and immunodeficiencies.

We comprehensively investigated the clinical, cellular and molecular features in two siblings presenting with progressive BMF, immunodeficiency and developmental aberrations. Genome-wide homozygosity mapping combined with whole-exome sequencing (WES) and Sanger sequencing revealed a premature stop codon mutation in MYSM1 (NM_001085487: c.1168G>T: p.E390*) resulting in absence of MYSM1 protein in patient cells. MYSM1-deficient cells are characterized by increased sensitivity to genotoxic stress associated with sustained induction of phosphorylated p38 protein, increased reactive oxygen species (ROS) production and decreased survival upon UV light-induced DNA damage.

In summary MYSM1 deficiency is associated with developmental aberrations, progressive BMF with myelodysplastic features and increased susceptibility to genotoxic stress. HSCT represents a curative therapy for patients with MYSM1 deficiency. Our data further expand the spectrum of inherited human bone marrow failure disorders and highlight the role for MYSM1 in regulating genotoxic stress responses in human hematopoiesis.

4. Introduction:

4.1. Human hematopoiesis

In a healthy human bone marrow (BM), approximately one trillion (10^{12}) cells per day arise. This indicates that the blood system is one of the most highly regenerative tissues in our body. The presence of a regenerative cellular hierarchy system, later called hematopoietic stem cell (HSC), in BM was hypothesized in the early 20s by Maximow [1], but the first evidence of the existence of such a system came only during the second world war, when atomic bombs revealed the devastating effects of nuclear irradiation. After atomic violation in Japan, it has been discovered that the lethal consequence of radiation was due to BM and blood failure which was curable by injection of spleen or marrow cells of unirradiated donor [2]. By that time, it was still unclear whether there are multiple stem cells restricted to each blood cell lineage or all of the blood cells arise from a single multipotential HSC. A big move forward in understanding the hematopoietic system was achieved by Till and McCulloch in 1961. They could show that the regenerative potential of HSC can be tested with clonal in vivo repopulation assays [3]. Subsequently, other groups developed in vitro clonal expansions [4, 5].

HSCs are defined by their special ability to durably self-renewal, while at the same time contribute to the pool of differentiating cells and are therefore critical for guaranteeing lifelong blood regeneration. Nowadays, surface markers are used to define HSCs as well as a variety of differentiated cell subtypes in bone marrow. CD34 (cluster of differentiation 34), which is expressed only on less than 5% of all nucleated bone marrow cells, was the first marker found to enrich human HSCs and other blood progenitors [6]. CD34+ cells can also be found in cord blood (about 1%) and peripheral blood cells (<0.1%) [6, 7]. Further investigations identified other markers which could be used to either positively or negatively select human HSCs. Human HSCs are defined as $CD34^+$ $CD38^-$ $CD90^+$ (thymocyte differentiation antigen 1: Thy1) $CD45RA^-$ [8]. HSC first differentiate into cells called multipotent progenitors (MPPs) which lack self-renewal capability but are able to differentiate into all blood progenitors. In contrast to HSCs, human MPPs lack the expression of CD90 and CD49f. In addition, MPPs also differ from HSC in their epigenetic landscape. In HSCs the transcription factors (TFs) SOX8 (SRY-related HMG-box 8), SOX18 and NFIB (nuclear factor I B) are upregulated. In contrast,

MYC (myelocytomatosis viral oncogene homolog) and IKZF1 (IKAROS family zinc finger 1) are upregulated during differentiation into MPPs [9]. Moreover, other TFs such as Polycomb-group gene BMI1 (B lymphoma Mo-MLV insertion region 1 homolog), HLF (hepatic leukemia factor) and HES1 (hairy and enhancer of split 1) are reported to be involved in HSCs quiescence [10, 11]. MPP cells can then differentiate into CMP (common myeloid progenitor) or MLP (monocyte-lymphoid progenitor) which can be distinguished by cell surface markers. CMPs are $CD34^+$ $CD38^-$ $CD45RA^-$ $CD10^-$ $CD7^-$ while MLPs are known to be $CD34^+$ $CD38^-$ $CD45RA^+$ $CD10^+$ $CD7^-$ [8]. CMPs give rise to MEPs (Megakaryocyte-Erythroid progenitor) which are able to fully differentiate into megakaryocytes and erythrocytes. Activation of PU.1 is required for differentiation of CMPs into GMP (granulocyte-macrophage progenitor) [12]. GMP cells which are $CD45RA^+$ and $CD135^+$ give rise to granulocytes, monocytes and dendritic cells.

MLPs are responsible to generate B and T lymphocytes as well as NK cells. This process is orchestrated by GATA2 (GATA binding protein 2), PU.1, NOTCH1 and PAX5 (paired box 5) [13].

The main TFs involved in human hematopoiesis, as well as surface markers are depicted in figure 1.

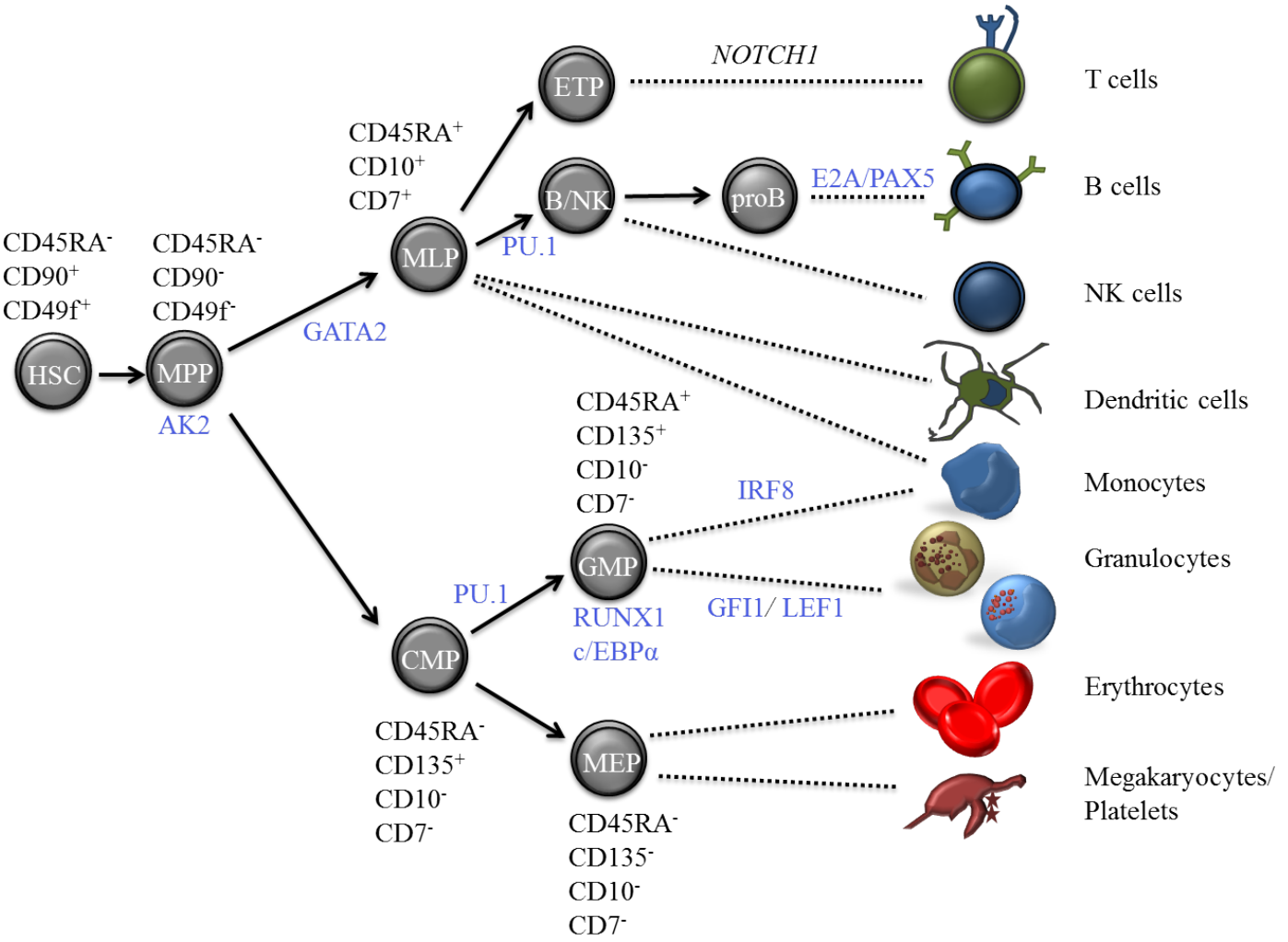

Figure 1: Schematic representation of human hematopoietic hierarchies. HSCs give rise to MPP which later differentiate to MLP and CMP. All lymphoid cells, including B and T cells and NK cells, arise from MLP, while CMP fully differentiate into monocytes, granulocytes, erythrocytes and megakaryocytes. Surface markers (black) and transcription factors (blue) of each cell population are depicted.

4.1.1. B cell development

Development of B cells has been well dissected into several distinct stages based on cell surface markers and expression of TFs. In the initial step, E2A (E protein 2-alpha) and EBF (Early B cell factor) are critical TFs that specify B cell fates. B cell progenitors in this step, called Pre-pro-B cells, can be isolated from BM using $CD34^+$ $CD38^+$ $CD10^+$ $CD19^-$ markers. Further development into pro-B cells is coupled with immunoglobulin-gene (Ig) rearrangement events and expression of CD19 and CD24 markers. Pre-B cells start to express CD20 surface marker but became negative for CD34 stem cell marker. At the end of this step, VDJ (variable, diverse, joining) Ig rearrangement is completed and IgM (immunoglobulin M) can be expressed on cell surface. These cells are called immature B cells which are immunophenotypically defined as $CD38^+$ $CD10^+$ $CD19^+$ IgM^+ IgD^- cells [13, 14]. Immature B cells exist in BM and are able to react to T cell–independent type 1 antigens [15]. Immature B cells undergo negative selection in bone marrow in order to exclude strongly self-recognizing cells. Following negative selection, immature B cells leave the BM and proceed to further maturate in the spleen and other lymphoid organs [14]. Surface expression of IgD in addition to IgM is the hallmark of mature B cells. They are responsive to antigens and unless the cells encounter foreigner antigens, they die within a few weeks [16].

Figure 2 depicts different stages of human B cell development in bone marrow.

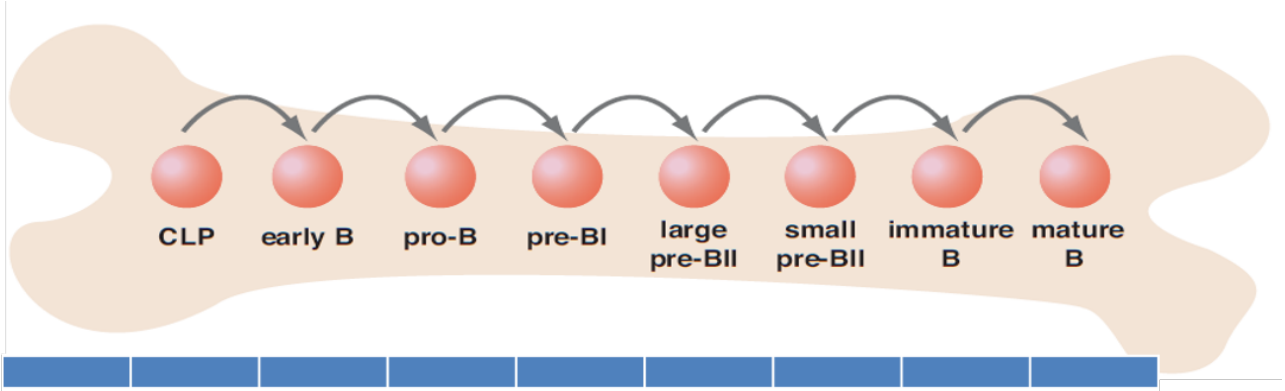

CD34	+	+	+	-	-	-	-	-
PU.1	+	-	-	-	-	-	-	-
CD10	+	+	+	+	+	+	+	-
IL-7Ra	+	+	+	-	-	-	-	-
CD19	-	-	+	+	+	+	+	+
CD79a	-	+	+	+	+	+	+	+
TdT	-	-	+	-	-	-	-	-
RAG	-	-	+	+	-	+	+	-
Vpre-B	-	+	+	+	+	-	-	-
µH	-	-	+/-	+	+	+	+	+
Pre-BCR	-	-	-	-	+	-	-	-
IgH	GL	DJ_H	V_HDJ_H	V_HDJ_H	V_HDJ_H	V_HDJ_H	V_HDJ_H	V_HDJ_H
κL	GL	GL	GL	GL	GL	V_LJ_L	V_LJ_L	V_LJ_L
cycling	-	-	-	+	+	-	-	-
Pax-5	-	-	+	+	+	+	+	+
sIgM	-	-	-	-	-	-	+	+
sIgD	-	-	-	-	-	-	-	+

Figure 2: B cell development in humans. Differentiation of CLP into the mature B cells occurs in the bone marrow. CLPs pass through a $CD34^+CD19^-CD10^+$ early B, $CD34^+CD19^+CD10^+$ pro-B, large $CD34^+CD19^+CD10^+$ pre-BI, large $CD34^-CD19^+CD10^+$ pre-BII, small $CD34^-CD19^+CD10^+$ pre-BII cell developmental pathway. Gene activation at each step has been characterized. This model has been adapted from reference [17].

4.1.2. Transcription factors and epigenetic regulation of B cell development

During cellular differentiation, changes in gene expression as well as chromatin status occur, reflecting genetic and epigenetic regulation [18]. The transition process from HSCs to B cells is coupled with loss of self-renewal and multilineage potential. Once early B cell fate is established, a shift from low-level gene expression associated with HSCs to high expression level of lymphoid specific genes (such as Tdt and Rag1/2) occurs [19, 20]. Activation of lymphoid specific genes is also accompanied by a sequential loss of megakaryocyte/erythroid and myeloid potentials [21, 22].

TFs have been recognized as key regulators of hematopoiesis and their function ensures a precise and successful developmental transition from one stage of progenitor cell differentiation to the next. TFs function in a network or a cascade fashion rather than acting alone [23]. Activation of a fate specific TF leads to suppression of unwanted TFs of the alternate fates as well as activation of lineage-specific target genes [24].

One of the first TFs reported to be involved in lymphopoiesis was PU.1. PU.1 was originally identified as the target gene of proviral integration of the spleen focus forming virus (SFFV) in erythroleukemia [25]. PU.1 has a highly dynamic expression pattern that is restricted only to hematopoietic system. Using GFP (green fluorescent protein) reporter mice, it was shown that the expression of PU.1 is downregulated in HSCs and sequentially increasing along myeloid lineage (ST-HSCs > LMMP > GMP > macrophages and neutrophils) [12, 26]. Targeted disruption of *Pu.1* in mice is fatal [27], while conditional deletion of *Pu.1* in adult mice results in failure to generate CMPs and GMPs, indicating the necessity of this TF for specification of the myeloid lineage [28, 29]. Interestingly, De Koter *et al.* showed that enforced expression of *Pu.1* in PU.1-deficient progenitors, drove lineage determination in a dose-dependent manner demonstrating that low versus high expression of PU.1 favors generation of B cells versus macrophages, respectively [30]. Their studies implied an essential role for PU.1 in generation of B cells, but only when expressed at reduced concentrations. It has been hypothesized that low expression of PU.1 might prime modification of chromatin structure to facilitate transcription activation required for B cells development [31].

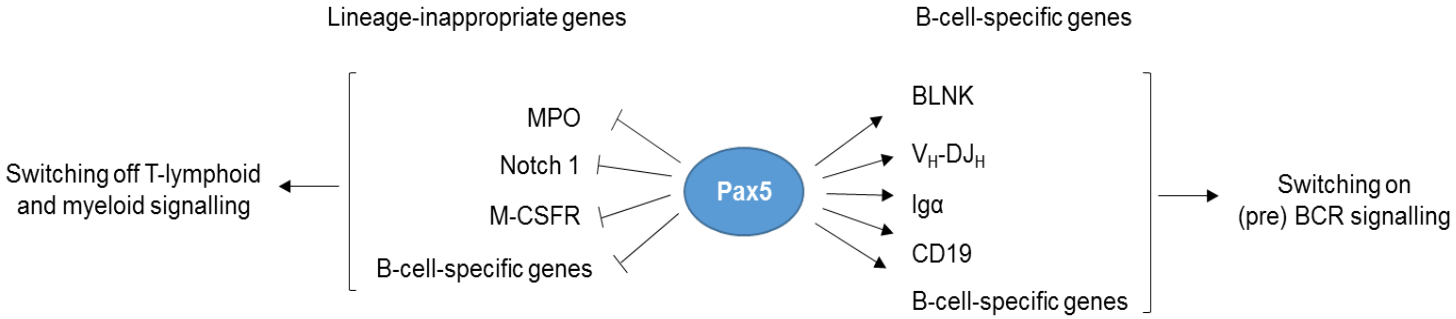

Figure 3: Different faces of Pax5. Pax5 expression has repression effect on T-lymphoid and myeloid specific genes including MPO, Notch1 and M-CSFR. Induction of B cell-specific target genes by Pax5, such as CD19, Igα and Ig genes leads to activation of BCR signaling pathways. The figure adapted from reference [32].

Another important player orchestrating CLP differentiation into B cells is PAX5. It has been shown that CLP (common lymphoid progenitors: $CD34^+$ $CD10^+$ $CD19^-$ $CD7^{-)}$ cells have upregulated expression of PAX5 [33]. This observation correlates well with findings in mouse, where CLPs already express different lymphoid-specific TFs including PAX5 [34]. Conditional ablation of *Pax5* in $CD19^+$ splenocytes results in loss of a B cell differentiation program and a striking conversion to T cell fate [35]. At the transcriptional level, PAX5 plays a dual role by repressing lineage-inappropriate genes and simultaneously activating B-cell-specific genes (figure 3). Expression of at least 170 genes are regulated by PAX5 in which a significant number of them are important for B-cell signaling, adhesion, and migration of mature B cells [36].

E2A, EBF and their target genes are still expressed in $PAX5^{-/-}$ pro-B cells, indicating that PAX5 functions downstream of E2A and EBF in controlling of B cell development (figure 4) [37, 38]. The E2A genetic locus encodes E12 and E27 by differential splicing events. These proteins are widely expressed and they all belong to the class I family of basic helix-loop-helix (bHLH) proteins [39, 40]. Early studies on $E2A^{-/-}$ mice revealed B cell development arrest at the early pro-B cell stage, prior to the onset of Ig heavy chain rearrangement, demonstrating requirement for E2A activation at the earliest detectable stages of B cell commitment [41, 42]. Further investigation suggested that E2A is not only important for B lineage commitment, but also that it plays multiple roles at later stages of B cell maturation [43]. Ectopic expression of E2A in non-lymphoid cells activated B cell specific genes indicating the importance of E2A as a master regulator of B lymphopoiesis. For instance, in fibroblast cells, ectopic expression of E2A resulted in transcription of B cell-specific Ig heavy chain transcripts [44] and overexpression of E12 in a macrophage cell line also led to the

activation of a variety of B lineage genes, including the transcription factor EBF, the surrogate light chain lambda 5 and Rag-1 [45]. At later stages of B cell maturation, E2A acts to regulate class switching of immunoglobulin recombination in peripheral mature B cells [46].

Like EBF$^{-/-}$ mice, E2A depletion results in a similar arrest of early B cell development [47]. The similarity of the B cell developmental arrest in E2A and EBF mutant mice strongly suggests a concerted action of these two TFs in controlling the earliest phase of B lymphopoiesis. Since pro-pre B cells in EBF$^{-/-}$ mice express almost normal level of E2A mRNA, whereas EBF transcription appear to be reduced in BM cells of E2A$^{-/-}$ mice, it has been concluded that E2A may act upstream of EBF in the genetic hierarchy of B cell development (figure 4) [47, 48].

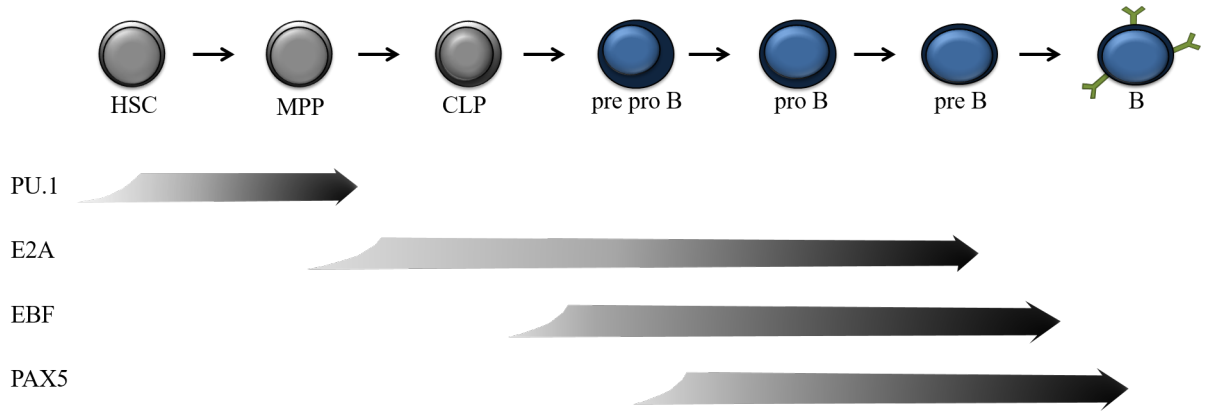

Figure 4: Transcription factors in B cell development. Sequential activation of four TFs involved in B cell development, including PU.1, E2A, EBF and PAX5 has been depicted. Figure adapted from reference [35] .

During B-cell development, besides the activation of the TFs, accessibility to the genomic region of the target genes is also required. This is achieved via epigenetic regulations and chromatin remodeling mechanisms. Murre *et al*. showed E2A occupancy near transcription start sites is associated with activating Histone H3K4 monomethylation marks (H3K4me1) at enhancers and H3K4 trimethylation marks (H3K4me3) at promoters. Moreover, E2A-occupied sites co-localize with binding motifs of TFs essential to the B lineage fate including

EBF and PU.1 [49]. Following activation of other TFs, such as *EBF*, co-occupancy of these two TFs correlates with H3K4 methylation status and an abundance of the hallmark B lineage transcripts *VpreB*, *Cd19*, *Foxo1*, *Pou2f1*, *Cd79a*, and *Pax5* [35]. These data prove that functional synergy between E2A and EBF at the epigenome level is critical for orchestrating B cell lineage-gene activation. In line with these data, genome-wide analyses demonstrated different sets of genes being activated or repressed by EBF TFs across defined stages of B cell development [50]. All EBF-activated target genes, including *Cd79a* and *Pax5*, gained the activating epigenetic marks H3K9me and H3ac (acetylated histone H3), whereas EBF-repressed genes acquire repressive H3K27me3 marks. Another epigenetic regulation of B cell development was discovered by Busslinger *et al*. Their studies revealed that the *Pax5* enhancer is demethylated during HSC and MMP transitions, while it gains the active chromatin mark by the pro-B cell stage. Moreover, they could show that in the absence of E2A and EBF, the promoter region of *Pax5* fails to acquire activating histone mark H3K9ac, demonstrating sequential and synchronized activation of TFs in B cell development [51].

Other studies documented that the induction of CD19 expression in pro-B cells occurs upon acquisition of the H3K4me3 activating marks in the promoter regions and simultaneous activation of *E2a*, *Ebf* and *Pax5* [52]. However, the effect of other histone modifications including ubiquitination and de-ubiquitination in B cells development remains elusive.

In summary, B cell-lineage commitment and development is highly determined by activation of specific TFs, including PU.1 E2A EBF and PAX5, which leads to induction of B cell-specific target genes and silencing of HSCs and the other lineage-specific genes through epigenetic regulation of regulatory elements (promoter, enhancer and silencer regions).

4.2. Bone marrow failure syndromes; defect of hematopoiesis

The inherited bone marrow failure syndromes (BMF) are characterized as a heterogeneous group of disorders representing bone marrow failure usually in association with one or more somatic abnormality. The failure in BM might affect either only a single or all three blood lineages and normally presents in early childhood. For instance, Fanconi anemia (FA) and dyskeratosis congenita (DC) usually affect all three blood lineages, whereas patients with Diamond–Blackfan anemia (DBA) initially present with single-lineage cytopenia affecting erythroid cells. Studying the genetic lesions causing these diseases is critical to better

understand underlying pathogenic pathways and to potentially define new therapeutic approaches.

About 50 genes have been identified to be involved in pathogenesis of BMF syndromes [53, 54]. Germline mutations in these genes results in the disruption of the key biological processes such as DNA repair and genome integrity (Fanconi anemia), telomere biology (Dyskeratosis congenital syndromes), or ribosomal biogenesis (Diamond Blackfan anemia, Shwachman Diamond syndrome) [55].

4.2.1. Fanconi anemia

The Swiss pediatrician Dr. Guido Fanconi, first described a rare aplastic anemia disorder associated with growth anomalies, later called Fanconi anemia [56]. The disease is characterized as an inherited progressive BMF associated with congenital abnormalities and a pronounced susceptibility to malignancies [57]. In approximately 60% of the reported cases of FA, at least one physical abnormality is documented. Among all the growth aberrations in FA, short stature as well as café au lait and hyper- and hypo-pigmented areas are the most common findings. The other reported abnormalities in FA are radial ray anomalies especially in thumb, microcephaly, microphthalmia, structural renal and endocrine anomalies [55].

In the majority of cases, FA follows an autosomal recessive (AR) inheritance pattern, but some cases of X-linked inheritance have been reported as well (table 1). Hypersensitivity of the cells from FA patients to DNA cross-linking agents such as mitomycin C, which results in chromosomal breakage and genome instability, is the cytogenetic hallmark of this disease. The increased genome instability in FA is due to defective proteins involved in DNA repair mechanisms encoded by Fanconi anemia genes [58]. It has been discovered that at least eight of the Fanconi anemia proteins (FANCA, FANCB, FANCC, FANCE, FANCF, FANCG, FANCL and FANCM) interact with each other and form a nuclear complex called the “Fanconi anemia core complex”. This core complex is needed to activate the FANCI-FANCD2 protein complex to a monoubiquitinated form (FANCI-FANCD2-Ub). FANCI-FANCD2-Ub directly interacts with DNA repair proteins such as BRCA2, BRCA1, NBS1 (Nijmegen breakage syndrome 1), PCNA (proliferating cell nuclear antigen) and RAD51, resulting in repair of damaged DNA. Of note, BRCA2 (also called FANCD1) is a human tumor suppressor gene critically involved in repair of DNA damage through homologous

recombination [55, 59]. FANCC also has been shown to be the co-interacting partner of BRCA2 [60, 61]. Certain variations in *BRCA2* increase risks for breast cancer as part of a hereditary breast-ovarian cancer syndrome [62] while biallelic mutation in this gene cause FA (table 1) [53]. Patients with FA have an increased risk of developing Myelodysplastic syndrome (MDS) and leukemia [63]. In particular patients with mutation in *FANCD1* (*BRCA2*) have the highest risk for cancer with a cumulative probability of 97% by the age of 6 years [55]. In regard to progressive bone marrow failure and increased risk of developing cancer in patients with FA, the life expectancy of FA patients is reduced to an average of 29 years [55].

Despite significant recent advances in understanding the molecular function of FA proteins, it is still not fully understood why such a large multiprotein FA core complex is required for DNA repair.

Table 1: List of mutated Fanconi anemia genes. FA mutated genes as well as chromosomal location, inheritance pattern and frequency of the mutations have been summarized. Data from reference [55].

Table 1. List of mutated FA genes

Genes	Chromosome locus	Mode of inheritance	Frequency (% of patients)
FANCA	16q24.3	AR	60
FANCB	Xp22.31	XLR	2
FANCC	9q22.3	AR	14
FANCD1/BRCA2	13q12.3	AR	3
FANCD2	3p25.3	AR	3
FANCE	6p21.3	AR	3
FANCF	11p15	AR	2
FANCG/XRCC9	9p13	AR	10
FANCI	15q25–26	AR	1
FANCJ/BACH1/BRIP1	17q22.3	AR	2
FANCL	2p16.1	AR	0.2
FANCM	14q21.3	AR	0.2
FANCN/PALB2	16p12.1	AR	0.7
FANCO	17q22	AR	1 single case
FANCP	16p13.3	AR	1 single case

4.2.2. Dyskeratosis congenita

Dyskeratosis Congenita (DC) is characterized by skin pigmentation changes, leukoplakia, and nail dystrophy as well as BMF development in about 80% of cases by the age of 20 years [64]. The other less common physical aberrations in DC patients are constant tearing from lacrimal duct stenosis, sparse and/or early grey hair and eyebrows, poor dentition and developmental delay. Pulmonary and hepatic complications are also common. However, it has been noted that most of the physical findings in DC are age-dependent and thus absence of common symptoms in a young patient by no means eliminates DC from probable consideration [55]. Except for two very severe subtypes of DC (called Hoyeraal-Hreidarsoon syndrome and Revesz syndrome suffering from microcephaly, neurological findings, immunodeficiency and intrauterine growth retardation), DC is less severe compared to FA., The median age at diagnosis for DC is 14 years, which is more than double the age in FA [55].

The hallmark laboratory diagnostic test for DC is detection of very short telomeres (less than the 1st percentile for age in a large number of normal controls) in blood leukocyte subsets [65]. Telomeres are the end of linear chromosomes which are composed of tandem hexanucleotide (TTAGGG) repeats as well as associated proteins (figure 5). Telomeres get shorter with every cell division and genome replication. The telomerase enzyme, a ribonucleoprotein complex, elongates telomeres by adding telomeric repeats to the end of telomeres in early progenitor cells [66]. All seven DC genes encode proteins that are either part of the telomerase complex or associated telomere protein called shelterin complex. DKC1 (dyskeratosis congenita 1, dyskerin) encodes a highly conserved nucleolar protein called dyskerin which plays an important role in telomerase function. DC can be inherited in an X-linked pattern (mutation in *DKC1*) or in an autosomal recessive/dominant pattern. The other genes which have been discovered to be mutated in DC are *TINF2* (TERF1 interacting nuclear factor 2), *TERC* (telomerase RNA component), *TERT* (telomerase reverse transcriptase), *NOP10* (nucleolar Protein 10 also called NOLA3), *NHP2* (ribonucleoprotein homolog 2 also called NOLA2) and *TCAB1* (telomerase Cajal body protein 1 also called *WRAP53*). It has been shown that mutations in *NOP10*, *NHP2* and *TCAB1* cause autosomal recessive DC, but mutations in *TERC*, *TERT* and *TINF2* can cause DC in both children and adults. Loss of function of only one alleil is sufficient to reduce telomerase activity and accelerate telomere shortening [67].

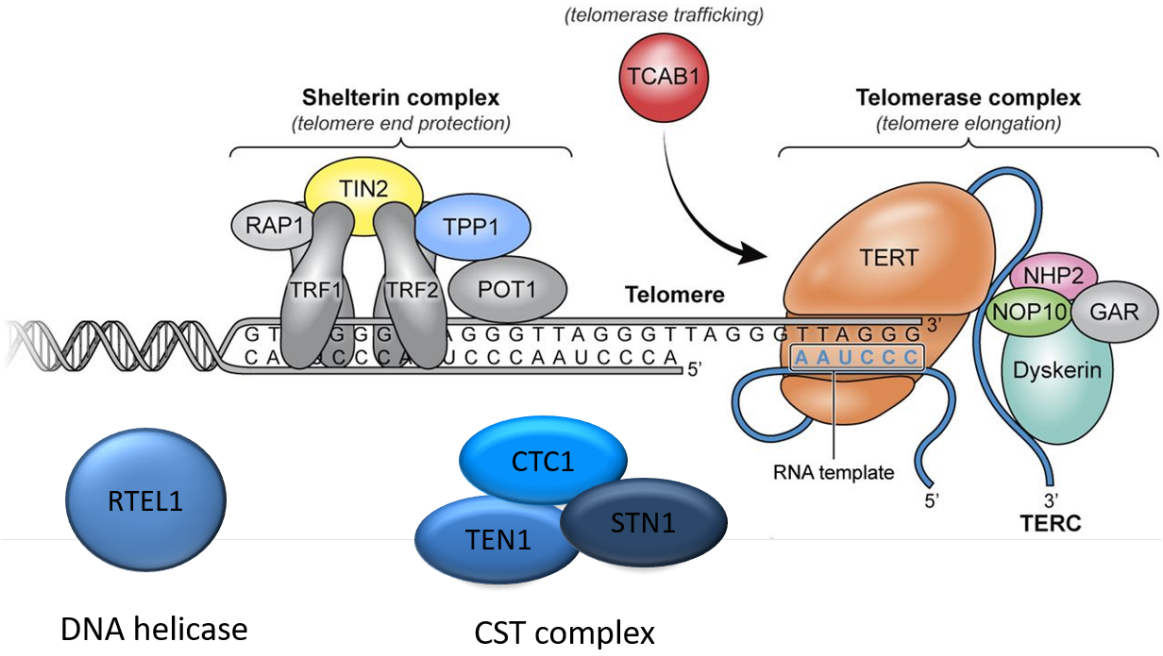

Figure 5: Human telomere and telomerase complexes. Human telomerase consists of the large molecules;telomerase reverse transcriptase (TERT) telomerase RNA (TR or TERC) and dyskerin (DKC1). The accessory compartments including DNA helicase (RTEL), Shelterin and CST complexes coordinate telomerase function. This schematic figure has been adapted from reference [67].

4.2.3. Diamond–Blackfan anemia

Diamond–blackfan anemia (DBA) usually presents in early infancy and is characterized by selective red cell aplasia associated with a variable number of somatic abnormalities. The most common growth aberrations are craniofacial, thumb abnormalities, cardiac and urogenital malformation [68]. In a few patients with DBA, MDS and acute leukemia have been reported, which suggests an increased susceptibility to hematologic malignancies [53]. The median age of diagnosis and the median overall survival of the patients are about 3 months and 40 years, respectively. Unlike FA and DC, there is not a clear-cut diagnostic method for DBA, however in blood counts of suspected cases, macrocytic anemia with reticulocytopenia, often with increased Hb F, as well as elevated red cell adenosine deaminase can be indicative of DBA. Erythroblastopenia with normal or reduced cellularity of BM is documented in BM evaluations of DBA patients [55].

DBA was the first human disease described to be directly linked to defective ribosome biogenesis. However, there was an initial incredulity that an erythropoiesis deficiency may be caused by a defect in a housekeeping pathway essential for every dividing cell. *RPS19* (ribosomal protein S19) was the first gene identified to be mutated in DBA [69]. Later several heterozygous mutations in other genes encoding for ribosomal proteins of the small (RPS24, RPS17, RPS7, RPS10, RPS26) and large (RPL5, RPL11, RPL35A) ribosomal subunits have also been documented to be causative of BDA [53]. To date however, approximately half of all DBA cases lack identifiable genetic alterations. The inheritance pattern of DBA is autosomal dominant with some ethnic differences in phenotypic expression [53]. Haploinsufficiency in ribosome biogenesis is thought to be the responsible mechanism for DBA [70].

4.2.4. Shwachman–Diamond syndrome

Shwachman–Diamond syndrome (SDS, also known as Shwachman-Bodian-Diamond syndrome) is an AR disorder characterized by BMF, pancreatic insufficiency associated with somatic abnormalities, in particular short stature and metaphyseal dysostosis [55, 71]. Signs of malabsorption and pancreatic insufficiency are apparent early in infancy (the median age of diagnosis is about 2 weeks). Neutropenia is the most common presenting hematological abnormality in SDS (~20%). Evolution of MDS and leukemia are observed in SDS patients as well [53].

In more than 90% of SDS cases, biallelic mutation in *SBDS* (Shwachman-Bodian-Diamond Syndrome) is causative of the disease. SBDS is a highly conserved protein, shuttles in and out of nucleolus. In mammals, SBDS can bind to 60S large ribosomal subunit and is involved in ribosome maturation and mitotic spindle stabilization [55]. Studies of bone marrow cells of SDS patients revealed that hematopoietic cells of the patients exhibit cell intrinsic defect in proliferation and differentiation [72] which was also confirmed in *Sbds* knockdown mice [73]. The studies demonstrated hypersensitivity to multiple types of DNA damage as well as endoplasmic reticulum stress in SBDS-deficient cells [74]. Moreover, SDS marrow stromal cells exhibit an impaired ability to support hematopoiesis of progenitor cells from healthy donors [72]. Abnormal B and T cell numbers and function as well as F-actin polymerization/depolymerization defects of neutrophils have been reported in SDS [75, 76].

4.2.5. Severe congenital neutropenia

Severe congenital neutropenia (SCN) was first described by Rolf Kostmann in 1950 as a disease affecting maturation of neutrophil granulocytes [77]. Classical definition for SCN is an absolute neutrophil count of less than 500 per microliter, associated with invasive bacterial infections such as omphalitis, skin abscesses, pneumonia, or septicemia [78]. Typically, SCN is not associated with any physical abnormalities in childhood, but in some patients decreased bone mineral density, leading to osteopenia or osteoporosis and increased propensity to fracture, is a common clinical problem [78]. BM examination in patients suffering from SCN shows an arrest in neutrophil maturation at the promyelocyte/myelocyte stage (figure 6), however cellularity of BM is normal or slightly reduced, and other cell lineages have normal maturation [55].

SCN can be distinguished from cyclic neutropenia through sequential assessment of neutrophil counts over a 6 week period, equivalent to two 21 cycles [55].

Due to the lack of comprehensive epidemiological studies, evaluation of SCN prevalence is difficult. Recent surveys in Iranian, French and some other ethnicities revealed that the minimal prevalence of congenital neutropenia appears to be 6 cases per one million [79]. SCN is most frequently caused by dominant mutations in the neutrophil elastase gene (*ELANE*) [80]. However, the original SCN disease which was first described by Kostmann appeared to be due to AR mutations in *HAX1* (HS1-Associating Protein X-1) [81]. Recent studies revealed new genetic mutations causing SCN, including *G6PC3* (glucose phosphatase catalytic subunit 3), *GFI1* (growth factor independence 1), *WAS* (Wiskott–Aldrich syndrome; causing X-linked SCN), *JAGN1* (jagunal homolog 1), *GCSF3R* (granulocyte colony-stimulating factor 3 receptor) and *VPS45* (vacuolar protein sorting 45 homolog) [82-87]. Nevertheless, the genetic cause of many SCN cases remains elusive [78].

Hematopoietic stem cell transplantation (HSCT) is the only definitive cure for SCN patients. First line therapy is based on administration of recombinant G-CSF (Granulocyte-colony stimulating factor). Patients who are non-responders or who develop MDS/AML after G-CSF administration are candidates for allogeneic HSCT [55].

Figure 6: Myeloid maturation arrest. Bone marrow smears in patients suffering from SCN, typically reveal a severe paucity of mature neutrophils. Since the arrest occurs normally after promyelocyte, myeloblasts and promyelocytes are present and detectable.

4.2.6. Other less common BMF syndromes

There are other BMF syndromes, including amegakaryocytic thrombocytopenia (CAMT), thrombocytopenia absent radii (TAR), radioulnar synostosis (RUS) and Pearson syndrome (PS), that are not as prevalent as the syndromes previously described. CAMT presents usually with petechiae or hemorrhages and sometimes evolves into aplastic anemia. Blood counts show thrombocytopenia with or without pancytopenia. Cellularity of BM may be normal, but decreased numbers or complete absence of megakaryocytes is evident. All CAMT patients carry AR mutation in MPL (myeloproliferative leukemia virus oncogene), which encodes the receptor for thrombopoietin. The only curative therapy for CAMT patients is HSCT [55].

Thrombocytopenia at birth associated with physical abnormalities of bilateral absent radii has been reported in patients suffering from TAR. The presence of thumbs makes these patients distinguishable from FA, however, chromosomal breakage test helps to better differentiate FA from TAR. The bone marrow of the patients with TAR shows reduced numbers or lack of megakaryocytes while the other lineages are normal. Genetic studies have failed to define a consistent finding in all 100 reported cases of therefore and the causative gene(s) remains elusive [55, 88].

Autosomal dominant mutations in *HOXA11* (homeo box A11) have been reported in two patients with RUS which is characterized with thrombocytopenia or aplastic anemia, and patients are noted to have limited pronation/supination of the arms due to proximal radioulnar synostosis [55].

Pearson syndrome is characterized by malabsorption, refractory sideroblastic anemia/aplastic anemia and lactic acidosis. BM cellularity in PS patients, in contrast to SDS, is normal but cytoplasmic vacuoles in myeloid and erythroid precursors and ringed sideroblasts can be noted. The disease shows maternal inheritance pattern and all the patients carrying mutations in mitochondrial genes involved in respiratory chain function [89].

Despite recent advances in genetic etiology of BMF syndromes, there are still many patients that exhibit features consistent with an inherited BMF syndrome however the causative gene mutation remains unknown and required further investigations [54].

4.3. Histone H2A ubiquitination and de-ubiquitination

Histones are subject to the various types of modifications, modulating chromatin accessibility during gene transcription, DNA repair and chromosome condensation. Methylation, acetylation, phosphorylation, ubiquitination and sumoylation are the most common post-translational modifications of histones [90]. Histone H2A was the first protein shown to be ubiquitinated (Ub) [91], and the site of modification was demonstrated to be in the highly conserved C-terminal containing Lys 119 residue [91, 92]. Approximately 5-10% of the total H2A present in mammalian cells are mono-ubiquitinated. [93] mono-Ub correlates with gene silencing pattern [94-96]. A growing body of evidence supports an additional critical role for Ub-H2A in the maintenance of genome integrity and stability [97].

Ubiquitin is a polypeptide composed of 76 amino acids that is covalently attached to histone lysines via the sequential action of three enzymes, E1-activating, E2-conjugating and E3-ligating enzymes. This large enzyme complex determines both substrate specificity (meaning which lysine is targeted) and the degree of ubiquitination (mono or poly-Ub) [98]. The major E3 ligase that mediates H2A mono-Ub is RING1b. RING1a/b- BMI1 (also called RNF2; Ring Finger Protein 2) is a component of the PRC (Polycomb repressive complex) that mediates silencing of the genes via histone modifications and chromatin remodeling [94].

Analysis of global Ub-H2A levels during cell cycle showed that Ub of H2A is very dynamic [99, 100]. Several mammalian H2A deubiquitinating enzymes (DUBs) have been identified. Based on homology of catalytic domains of DUBs, five different families, including

Otubain/Ovarian tumor-domain containing proteins (OTU), ubiquitin carboxy-terminal hydrolases (UCH), ubiquitin specific proteases (Usp), Machado-Joseph Domain (Josephin domain)-containing proteins (MJD) and Jab1/MPN domain associated metalloprotease domain proteins (JAMM) have been described [101]. Among the DUBs, only the JAMM family utilizes a zinc metalloproteinase domain to break the bond between target proteins and Ub. Nine different DUBs have been classified in the JAMM family including PSMD7 (proteasome 26S subunit, non-ATPase 7), PSMD14 (proteasome 26S subunit, non-ATPase 14), EIF3H (eukaryotic translation initiation factor 3 subunit H), BRCC36 (BRCA1/BRCA2-containing complex subunit 3), AMSH (associated molecule with the SH3 domain), AMSH-LP (AMSH-like protein), MPND (MPN domain containing), PRPF8 (pre-mRNA processing factor 8), and MYSM1 (Myb-like, SWIRM and MPN domains 1) [102].

USP16, USP3, and MYSM1 specifically deubiquitinate histone proteins [99]. Disruption of USP3 and USP16 leads to aberrant cell cycle progression and delayed S-phase [103].

4.3.1. MYSM1

MYSM1 was originally discovered in research attempts screening for potential transcription coregulators of androgen receptor-dependent gene activation [104]. MYSM1 is the only DUB enzyme which contains a SANT (switching-defective protein 3, adaptor 2, nuclear receptor corepressor, and transcription factor IIIB) DNA binding domain, that enables it to directly interact with double strand DNA (figure 7).

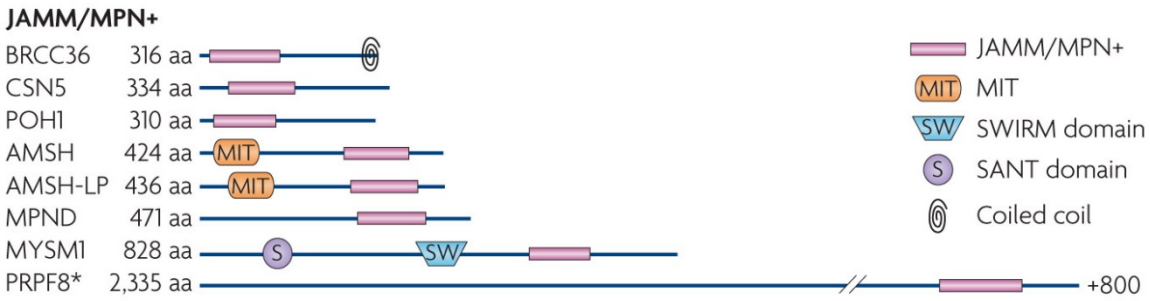

Figure 7: Domain structure of JAMM/MPN+ DUBs. SANT domain and SWIRM domain of MYSM1 is quite unique among other DUBs. Figure adapted from reference [105].

The human MYSM1 protein, previously called 2A-DUB or KIAA1915, is encoded by *MYSM1* (ENSG00000162601) mapped on chromosome 1 (1p32.1). MYSM1 is composed of 828 amino acids (aa) forming three main structural domains including a SANT domain (aa 116-167); SWIRM domain (aa 372-470) and a MPN domain (aa 572-682). The SANT domain is a well-known domain existing in many transcriptional regulators and is capable of binding directly to DNA and histones. SWIRM which is named for its presence in the proteins Swi3, Rsc8, and Moira exists in many chromatin associated proteins interacting with histones. The MPN domain is the metalloprotease catalytic site of MYSM1. The JAMM motif (aa 656-669) is located at the end of the MPN domain and is followed by a generic LXXLL motif, found in many coactivators for interaction with agonist-bound nuclear receptors. The complete X-ray crystallographic structure of MYSM1 remains to be solved, but the 3D structure of SANT and SWIRM domains have been studied (figure 8).

MYSM1 can be post-translationally phosphorylated at aa residues 110, 208, 236, 242, 267, and 340 [104].

Figure 8: Schematic illustration of MYSM1 protein

Early investigations documented that MYSM1 coordinates de-ubiquitination of H2A which subsequently results in acetylation of nucleosome histones and disassociation of histone H1 [104]. It has been proposed by Zhu *et al*. that MYSM1 acts as a coactivator of androgen receptor-gene activation and is required for the activation of several target genes in prostate cancer cell lines [104].

Homozygous *Mysm1*$^{-/-}$ mice are viable and fertile. They have truncated tails, growth retardation, and reduced numbers of B220^{+} CD19^{+} B cells in bone marrow, spleen, and lymph nodes [106]. In addition to the striking defect in B cell differentiation, other groups later

reported bone marrow failure, lymphopenia, anemia, and thrombocytosis in *Mysm1*$^{-/-}$ *mice [106-108]*. In the study performed by Nijnik *et al*., *Mysm1*$^{-/-}$ mice showed more severe phenotypes including increased levels of embryonic mortality, reduced body size and weight, and some growth abnormalities. In bone marrow of the *Mysm1*$^{-/-}$ mice, functionally impaired HSCs was reported to be associated with elevated DNA damage marker and increased reactive oxygen species (ROS) production. This study highlighted a critical role for MYSM1 in maintenance of BM stem cell, lymphocyte development and genome stability [107].

Bone marrow failure, HSC dysfunction in maintenance and self-renewal as well as defective hematopoiesis in *Mysm1*$^{-/-}$ mice has also been documented by other groups [109-111]. Further investigations have revealed that mice lacking MYSM1 represent defective NK maturation and dendritic cells development as well as problems in skin pigmentation and bone formation [110, 112-114].

During the course of our investigations, which started in 2011, three patients with homozygous mutations in MYSM1 suffering from bone marrow failure, anemia and lymphopenia associated with mild growth aberrations have been reported [115, 116].

4.3.2. MYSM1 in hematopoiesis

HSC dysfunction and defective hematopoiesis, mainly in B cells, were the most prominent finding of the initial *Mysm1*$^{-/-}$ mice studies that led investigators to search for a transcriptional regulatory function for MYSM1 in hematopoiesis.

The fact that the B cell developmental block caused by MYSM1 loss occurred at a similar stage (pre-pro-B cell) that had been described for the *Ebf1*$^{-/-}$ mice, led the investigators to connect Mysm1 and Ebf1 functionally. Indeed, MYSM1 regulates EBF1 transcription in early B cell commitment by controlling histone modifications and TF recruitment at the *Ebf1* promoter locus [106].

Further studies revealed that MYSM1, in coordinated action with GATA2 and RUNX1, regulates expression of GFI1. Reduced binding of GATA2 and RUNX1 TFs to the GFI1 locus and increased recruitment of Ring1B and Bmi1 (components of PCR1) have been associated with loss of MYSM1 [109].

The importance of MYSM1 in the development of dendritic cells was studied by Won *et al.* They showed that MYSM1 is selectively required for *Flt3L*-induced DC development and upregulates expression of *Flt3* through direct binding at the promoter locus [110].

It has been hypothesized that depletion of HSC and impaired hematopoiesis in *Mysm1*$^{-/-}$ mice likely results from activation of the DNA damage response (DDR) and uncontrolled production of ROS [117]. The same functions, such as regulation of HSC quiescence and self-renewal, antioxidant and DNA repair functions, as well as HSC differentiation checkpoints have been demonstrated for p53 [118-120]. Therefore, a possible connection between *Mysm1* and *p53* was studied by two independent groups, which brought new insights into the molecular biology of MYSM1. Growth retardation and neurological abnormalities as well as defective lymphopoiesis of *Mysm1*$^{-/-}$ mice could be almost fully rescued by deletion of p53 [117, 121]. Mechanistically, it has been shown that Mysm1 has the potential to directly bind to the prompter region of *Cdkn2a/p19ARF*, one of the major regulator of p53, and suppresses activation of p53 [117]. Colocalization of MYSM1 and p53 on the promoters of the classical p53-target genes *Bbc3* (BCL2 binding component 3 also known as PUMA (p53 upregulated modulator of apoptosis)) and *Cdkn1a/p21* has also been reported, suggesting a critical functional relationship between MYSM1 and p53 [122].

The findings derived from *Mysm1*$^{-/-}$ and *p53*$^{-/-}$ mice strongly suggest that molecular mechanism of BMF and defective hematopoiesis in MYSM1 deficiency is p53 mediated and indicates the importance of MYSM1 in DNA damage and apoptosis protection. However, the exact molecular mechanism of MYSM1 function in DNA damage response in human is still unknown (see manuscript #1)

4.4. SMARCD2-deficiency; role of chromatin remodeling complex in hematopoiesis and neutropenia

The human genome is organized into chromosome structures composed of DNA, packaging proteins (primarily histones), factors for histone deposition and removal, histone modification enzymes and a set of chromatin remodeling complexes (CRCs). The chromatin remodelers work in concert with other chromatin factors to control packaging and unpackaging of DNA and regulate DNA replication, gene transcription, DNA repair and recombination [123]. Four

different families of CRCs have been described, including SWI/SNF (switching defective/sucrose nonfermenting), ISWI (imitation switch), CHD (chromodomain, helicase, DNA binding) and INO80 (inositol requiring 80) family (figure 9).

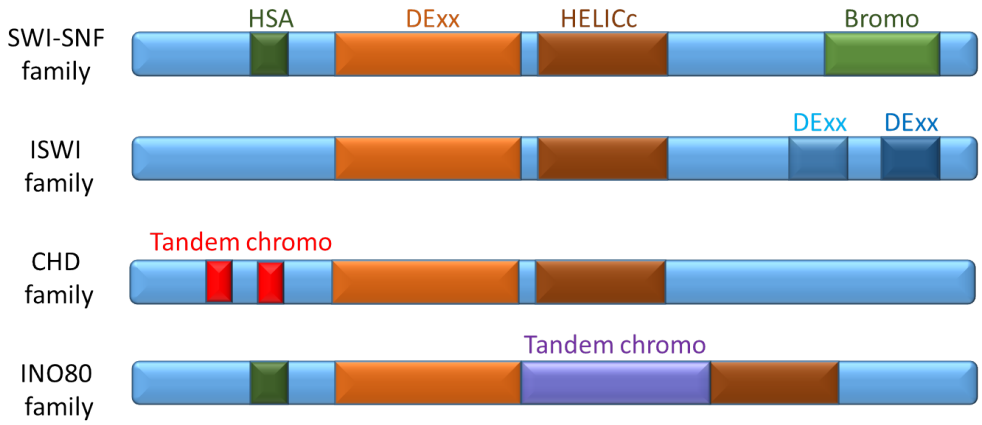

Figure 9: The families of chromatin remodeling complexes. Figure adapted from reference [123].

In mammals, two SWI/SNF multiprotein complexes have been described, called BAF (BRG1-accosiated factor) and PBAF (polybromo-BRG1-associated factors). The complexes share multiple proteins, such as BAF170, BAF155, BAF60a/b/c, BAF57, BAF53a/b, BAF47, BAF45a/b/c/d and β-actin. The main difference between the BAF and PBAF complexes is the ATPase subunit. In BAF, the ATPase subunit can be either BRG1 or BRM, whereas in PBAF it is only BRG1 [123, 124]. The role of the SWI/SNF remodeler family in embryonic differentiation and organs development as well as in DNA damage response, genome stability, cancer and tumorigenesis have been studied extensively [124, 125].

One of the core components of the BAF remodeler complex is a 60 kDa subunit called BAF60 that can be represented by the paralogous proteins BAF60a, BAF60b or BAF60c, encoded by the *SMARCD1*, *SMARCD2* and *SMARCD3* genes, respectively [126]. It has been documented that BAF60c is essential to activate both skeletal and cardiac muscle programs. BAF60c deficiency in mice leads to severe cardiac defects and in zebrafish causes heart developmental deficiencies [127, 128]. Studies have revealed that BAF60a has a pleiotropic role in cells, varying from regulation of metabolic gene programs in the liver and skeletal

muscles to association with lung cancer risk, binding to p53 and steroid receptor function [129-131].

SGD (neutrophil-specific granule deficiency) is a rare inherited disorder characterized by frequent and severe bacterial infections, lack of secondary granule proteins and defensins as well as neutrophils dysfunction and impaired bactericidal activity. SGD is caused by biallelic mutations in *C/EBPε* (CCAAT/enhancer binding protein E) [132]. However, there are very rare cases associated with specific granule deficiency who have no mutations in *CEBPE*.

C/EBPs are a family of TFs involved in cellular differentiation and function in a variety of tissues [133]. At least six different members of this family (C/EBPα—C/EBPζ) have been isolated and characterized [134]. C/EBPε is a 281 aa protein, exclusively expressed in myeloid cells and T cell lineages [135, 136]. Mice lacking C/EBPε show a similar phenotype seen in patients with CEBPE-deficiency [137].

Genetic studies are ongoing to identify mutations causing SCN and SGD.

5. Manuscript # 1

Myb-like, SWIRM, and MPN domains 1 (MYSM1) deficiency: Genotoxic stress-associated bone marrow failure and developmental aberrations

Ehsan Bahrami, MSc,[a] Maximilian Witzel, MD,[a] Tomas Racek, PhD,[a] Jacek Puchałka, PhD,[a]† Sebastian Hollizeck, MSc,[a] Naschla Greif-Kohistani, MD,[a] Daniel Kotlarz, MD, PhD,[a] Hans-Peter Horny, MD,[b] Regina Feederle, PhD,[c] Heinrich Schmidt, MD,[a] Roya Sherkat, MD,[d] Doris Steinemann, PhD,[e] Gudrun Göhring, MD,[e] Brigitte Schlegelbeger, MD,[e] Michael H. Albert, MD,[a] Waleed Al-Herz, MD,[f] and Christoph Klein, MD, PhD[a] *Munich and Hannover, Germany, Isfahan, Iran, and Kuwait City, Kuwait*

GRAPHICAL ABSTRACT

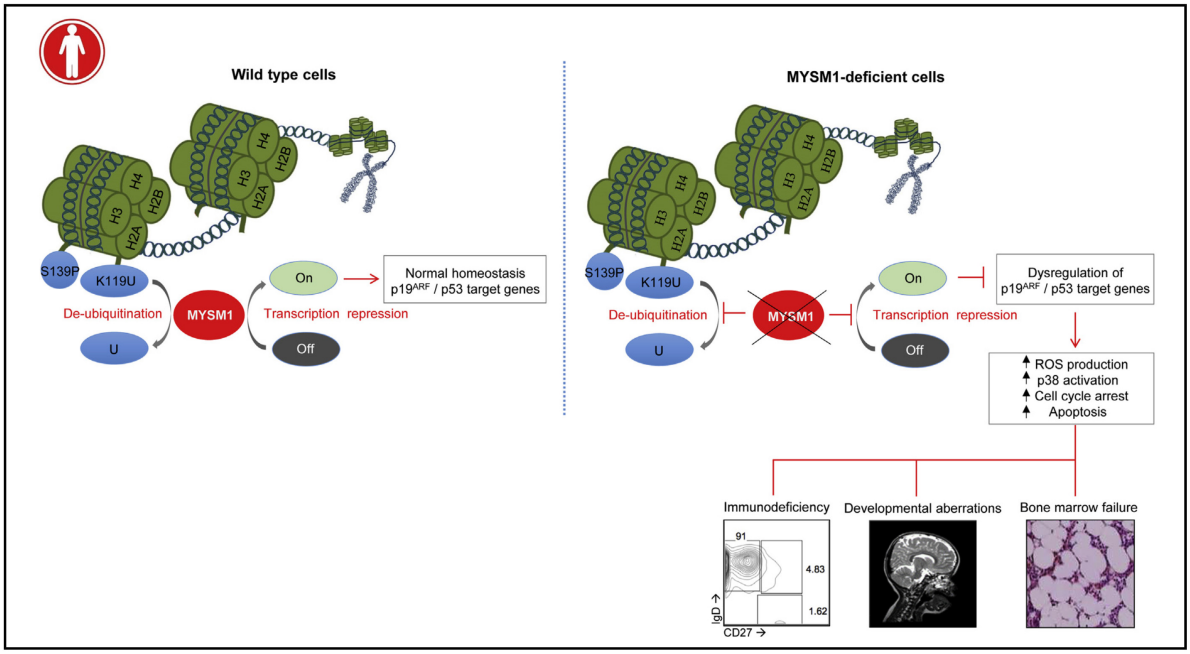

Background: Myb-like, SWIRM, and MPN domains 1 (MYSM1) is a transcriptional regulator mediating histone deubiquitination. Its role in human immunity and hematopoiesis is poorly understood.

Objectives: We sought to investigate the clinical, cellular, and molecular features in 2 siblings presenting with progressive bone marrow failure (BMF), immunodeficiency, and developmental aberrations.

From [a]the Department of Pediatrics, Dr. von Hauner Children's Hospital, and [b]the Institute for Pathology, Faculty of Medicine, Ludwig-Maximilians-Universität, Munich; [c]Helmholtz Zentrum München, German Research Center for Environmental Health, Core Facility Monoclonal Antibody Development, Munich; [d]the Acquired Immunodeficiency Research Center, Isfahan University of Medical Sciences; [e]the Institute of Human Genetics, Hannover Medical School, Hannover; and [f]the Department of Pediatrics, Faculty of Medicine, Kuwait University, and Department of Pediatrics, Al-Sabah Hospital, Kuwait City.

†Deceased.

Supported by grants from the BMBF (German PID-NET, #01GM0894), the Leona M. and Harry B. Helmsley Charitable Trust (#2015PG-IBD008), the German Research Society (Gottfried Wilhelm Leibniz Program [#KL 877/11-1], SFB 1054 [#SFB 1054/1 A05]), German Research Foundation (DFG) through the excellence cluster REBIRTH (DFG #EXC 62), the European Research Council (ERC, Advanced Grant Explore [#268608-EXPLORE]), Reinhard-Frank Stiftung, the Else Kröner-Fresenius-Stiftung (#2013_Kolleg.18), DZIF/EKFS (#TTU 07.801), and the Care-for-Rare Foundation (#C4R/PrNr.140042).

Disclosure of potential conflict of interest: The authors declare that they have no relevant conflicts of interest.

Received for publication April 13, 2016; revised September 22, 2016; accepted for publication October 17, 2016.

Corresponding author: Christoph Klein, MD, PhD, Dr. von Hauner Children's Hospital, Lindwurmstrasse 2a, D-80337 München, Germany. E-mail: christoph.klein@med.uni-muenchen.de.

0091-6749/$36.00

http://dx.doi.org/10.1016/j.jaci.2016.10.053

Methods: We performed genome-wide homozygosity mapping, whole-exome and Sanger sequencing, immunophenotyping studies, and analysis of genotoxic stress responses. p38 activation, reactive oxygen species levels, rate of apoptosis and clonogenic survival, and growth in immune and nonimmune cells were assessed. The outcome of allogeneic hematopoietic stem cell transplantation (HSCT) was monitored.
Results: We report 2 patients with progressive BMF associated with myelodysplastic features, immunodeficiency affecting B cells and neutrophil granulocytes, and complex developmental aberrations, including mild skeletal anomalies, neurocognitive developmental delay, and cataracts. Whole-exome sequencing revealed a homozygous premature stop codon mutation in the gene encoding MYSM1. MYSM1-deficient cells are characterized by increased sensitivity to genotoxic stress associated with sustained induction of phosphorylated p38 protein, increased reactive oxygen species production, and decreased survival following UV light–induced DNA damage. Both patients were successfully treated with allogeneic HSCT with sustained reconstitution of hematopoietic defects.
Conclusions: Here we show that MYSM1 deficiency is associated with developmental aberrations, progressive BMF with myelodysplastic features, and increased susceptibility to genotoxic stress. HSCT represents a curative therapy for patients with MYSM1 deficiency. (J Allergy Clin Immunol 2017;■■■;■■■-■■■.)

Key words: *Immunodeficiency, stem cells, hematopoiesis, rare disease, transplantation*

Inherited bone marrow failure (BMF) syndromes comprise a heterogeneous group of disorders associated with dysfunction of hematopoietic stem or progenitor cells. Genetic analysis of these rare diseases has provided important insight into the fundamental biological principles governing genomic integrity in stem cells, such as DNA repair, telomere maintenance, or ribosomal biogenesis.[1] Although the hierarchical control of hematopoiesis by transcription factors is well studied, the relevance of epigenetic regulation remains less well understood. Myb-like, SWIRM, and MPN domains 1 (MYSM1) has originally been identified in a search for transcriptional regulators and was found to mediate histone deubiquitination, specifically at position lysine 119 (K119) of histone 2A (H2A), a common chromatin modification associated with gene silencing.[2] Targeted deletion of murine Mysm1 results in severe hematopoietic defects associated with an early block of B-cell development[3]; dysfunction of stem cell maintenance, self-renewal, and differentiation[4]; and natural killer (NK) cell defects.[5] In human subjects exome sequencing studies have revealed potentially disease-causing mutations in *MYSM1* in 2 families with BMF and immunodeficiencies.[6,7] Here we study 2 patients with MYSM1 deficiency, including genetic reconstitution data and cellular studies illustrating decreased genotoxic stress resistance in patients with this rare genetic disorder.

METHODS

Patient information and study approval

Patients were referred to the Department of Pediatrics, Al-Sabah Hospital, Kuwait, and the Dr. von Hauner Children's Hospital at Ludwig-Maximilians-Universität Munich, Germany. Informed consent was obtained according to current ethical and legal guidelines. This study was conducted in accordance with the Declaration of Helsinki and was approved by the institutional review board of the Ludwig-Maximilians-Universität Munich.

Abbreviations used
BMF: Bone marrow failure
EBV-LCL: Epstein-Barr virus transformed B lymphoblastoid cell line
H2A: Histone 2A
γ-H2AX: Phospho-histone H2AX
HD: Healthy donor
HSCT: Hematopoietic stem cell transplantation
MAPK: Mitogen-activated protein kinase
MYSM1: Myb-Like, SWIRM, and MPN domains 1
RFP: Red fluorescent protein

Next-generation sequencing and genetic analysis

Next-generation sequencing was performed, as previously described.[8] Briefly, genomic DNA isolated from whole blood of both patients and their parents were first analyzed with the Affymetrix Genome-wide Human SNP array 6.0 (GEO Platform GPL6801), according to the manufacturer's instructions (Affymetrix, Santa Clara, Calif). Remaining DNA has been used for generation of whole-exome libraries using the SureSelect XT Human All Exon V4 + UTRs kit (Agilent Technologies, Santa Clara, Calif). Barcoded libraries were sequenced with the SOLiD 5500 XL next-generation sequencing platform (Life Technologies, Grand Island, NY) to an average coverage depth of 80. Bioinformatic analysis and subsequent filtering of called variants led to identification of a potentially causative homozygous mutation (see Table E1 in this article's Online Repository at ww.jacionline.org). All relevant variants were confirmed by using Sanger sequencing.

Cell culture

Epstein-Barr virus transformed B lymphoblastoid cell lines (EBV-LCLs) were generated by infecting freshly isolated PBMCs with B95-8 cell supernatant in the presence of cyclosporine and maintained in RPMI 1640 medium supplemented with 10% heat-inactivated FBS, 1% penicillin/streptomycin, 1% HEPES, and 2 mmol/L L-glutamine at 37°C in the presence of 5% CO_2. Fibroblasts were derived from skin or foreskin biopsy specimens, with continuous cultivation in Dulbecco modified Eagle medium and supplementation with 10% heat-inactivated FBS, 1% penicillin/streptomycin, and 2 mmol/L L-glutamine at 37°C in a 5% CO_2 atmosphere.

Further clinical data and methods are provided in the Methods section in this article's Online Repository at ww.jacionline.org.

RESULTS

Clinical phenotype

We studied 2 siblings of a consanguineous Arab pedigree (Fig 1, *A*) with early-onset progressive BMF and myelodysplastic features.

Patient IV-1 was born prematurely and presented with severe anemia (hemoglobin, 3 g/dL) at birth, requiring immediate red blood cell transfusion. In her first 2 years of life, she was treated for recurrent upper respiratory tract infections. During one episode of severe infection, she was hospitalized, treated with intravenous antibiotics, and maintained on co-trimoxazole prophylaxis thereafter. She presented with BMF, short stature, and mild dysmorphic features, including thoracic asymmetry, a short left humerus, shortness of the metacarpal bone, dry skin, trigonocephaly, midface hypoplasia, gingiva hyperplasia, bilateral cataracts, and neurodevelopmental delay correlating

TABLE I. Clinical phenotype of human MYSM1 deficiency

	Patient IV-1	Patient IV-2	Patient (Le Guen et al[7])	Patient 1 (Alsultan et al[6])	Patient 2 (Alsultan et al[6])
Ethincity	Arabic	Arabic	Turkish	Arabic	Arabic
Mutation	c.1168G>T:pE390*	c.1168G>T:pE390*	c.1967A>G, somatic reversion in peripheral blood (T, B, and NK cells and monocytes)	c.1168G>T:pE390*	c.1168G>T:pE390*
Infections/ prophylaxis	Infant hospitalized for severe infections; consequently, co-trimoxazole, upper airway infections	Co-trimoxazole; free of infections	IVIG, co-trimoxazole; free of infections	NA	NA
Neonatology	Preterm 33rd gestational week, 1400 g, postpartum anemia Hb = 3 g/dL, RBC transfusion	Preterm 33rd gestational week 2120 g, postpartum anemia = Hb 2 g/dL, RBC transfusion, postpartum cardiopulmonary resuscitation	At term, 2620 g, Hb = 5 g/dL at birth, leukopenia respiratory stress because of choanal atresia	Normal growth parameters	ND
Growth	At 2 y, 4 mo*: Weight, 11 kg (percentile: 8.2%) Length, 81.5cm (percentile: 1.3%) Head, 47 cm (percentile, 30.9%)	At 3 mo*: Weight, 5.7 kg (percentile: 16.8%) Length, 53 cm (percentile: 0.0%) Head, 38 cm (percentile: 1.8%)	At birth*: Weight, 2.62 kg (percentile: 5.4%) Length, 47 cm (percentile: 6.4%) Head, 32 cm (percentile: 0.0%)	ND	ND
Hematology	IBMF, aregenatory anemia tricytopenia, B-cell deficiency, dysplastic signs of granulopoiesis, erythropoiesis, megakaryopoiesis	IBMF, aregenatory anemia tricytopenia, G6PDH eficiency B-cell deficiency, dysplastic signs of granulopoiesis, erythopoiesis, megakaryopoiesis	Aregeneative anemia BM: absence of erythroid precursors, normal granulopoiesis, B-cell deficiency	IBMF, pallor at 4 mo with Hb = 6 g/dL, transfusion dependent, until 9 mo, hypocellular bone marrow, thrombocytopenia 60,000/μL, spontaneous recovery of erythropoiesis	IBMF, pallor at 15 mo with Hb = 4.4 g/dL, transfusion dependent until 33 mo, pronounced erythropoiesis, reduced granulopoiesis, reduced megakaryopoiesis, dysplasia of erythoid precursors and megakaryoctes, negative HAM test result
Bones	Thoracic asymmetry, short left humerus, brachymetacarpia D1 left and broad metacarpia D1 left, osteopenia	Rhizomelic shortening of arms, short fingers	NA	NA	NA
Skin	Dry, itching skin, thin hair	Dry skin, eczema, leaf-like hypopigmentation on trunk, accessory papilla of breast	NA	NA	NA
Face	Trigonocephaly, hypoplasia of orbital floor, hypoplasia of zygomatic bones, midface hypoplasia, pointed chin, short neck, bilateral cataract	Midface hypoplasia, hypoplasia of orbital floor, short neck	NA	Facial dysmorphy†	NA
Heart	TI I°, dPmax 26 mm Hg, PFO with laminar LRS (incidental finding)	Cardiomegaly, left ventricle dilatation, reduced FS 16-20%, noncompaction cardiomyopathy	NA	NA	NA
Dental/mouth	Gingiva hyperplasia	Gingiva hyperplasia, delayed dentition	NA	NA	NA

(Continued)

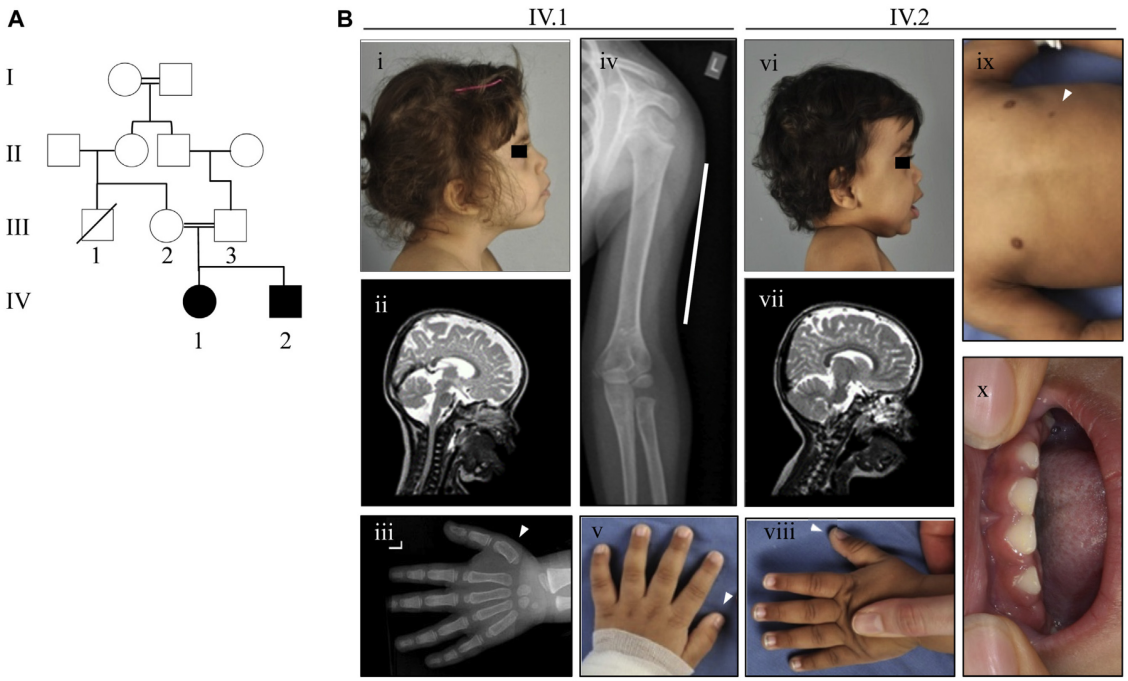

FIG 1. Pedigree, clinical, and immunologic phenotype of MYSM1-deficient patients. **A,** Pedigree of the family. **B,** Clinical phenotype of MYSM1-deficient patients with facial features, including midface hypoplasia, low-set ears, hypoplasia of the orbital floor, short neck (*i* and *vi*), magnetic resonance imaging correlates of increased liquor space and reduction of cerebral volume (*ii* and *vii*), short left humerus (*iv, white line*) and osteopenia *(iv),* brachymetacarpia/broad metacarpal bone D1 left (*iii, arrowhead*) and deep-set thumb (*v* and *viii, arrowhead*), accessory papilla of the breast (*ix, arrowhead*), and gingiva hyperplasia *(x).*

with reduced cerebral volume (Fig 1, *B*, *i-v*; Table I; and see Fig E1, *i-ii*).

Patient IV-2 was delivered preterm and had anemia (hemoglobin, 2 g/dL), as well as cardiac insufficiency requiring immediate cardiopulmonary resuscitation and transfusion. Until his second year of life, 2 episodes of upper airway infection were noted, but no further infections developed under co-trimoxazole prophylaxis. In our center he presented with BMF, short stature, and dysmorphic features, including rhizomelic shortening of the arms, short fingers, bilateral protrusions on collar bones, dry skin, eczema, accessory papilla of the breast, noncompaction cardiomyopathy, midface hypoplasia, gingiva hyperplasia, delayed dentition, and neurodevelopmental delay associated with reduced cerebral volume (Fig 1, *B*, *vi-x*; Table I; and see Fig E1, *iii-vi*).

Table I provides a comprehensive synopsis of known clinical feature courses in human MYSM1 deficiency. In both patients BMF manifested with transfusion-dependent anemia, mild thrombocytopenia, lymphopenia, and moderate-to-severe neutropenia (see Fig E3 in this article's Online Repository at ww.jacionline.org). Further investigations on sequential bone marrow biopsy specimens of the patients revealed hypocellularity, increased adipocytes (Fig 2, *A*, *i* and *v*), siderosis (see Fig E2, *A*, *i-iii*, in this article's Online Repository at ww.jacionline.org), and reduced numbers of megakaryocytes with pleomorphic aberrations (see Fig E2, *A*, *iv-vi*) and normal myeloperoxidase levels (see Fig E2, *A*, *vii-ix*).

Bone marrow cytology showed dysplastic findings of red and white blood cell precursors. Pseudo–Pelger-Huet anomaly, as well as dysplastic findings of erythroid lineages, including multinucleated erythroblasts, cytoplasmic bridges, and ectopic nuclear morphology of erythroblasts, was noted in both patients. No blast excess was noted (Fig 2, *A*, *ii-iv* and *vi-ix*, and se Fig E2, *B*, *i-iv*). We searched for mutations in genes frequently mutated in patients with myelodysplastic syndromes but could not identify any in the exome data set (see Table E2 in this article's Online Repository at ww.jacionline.org). Cytogenetic studies in myeloid precursor cells, as well as in mitomycin C–treated lymphoid cells, showed a normal karyogram according to chromosomal banding. Array-CGH data did not reveal a disease-causing copy number variation (data not shown).

Immunostaining of bone marrow samples was performed to further characterize early B- and T-cell development. Lymphoid TdT^+ progenitor and early B-cell progenitor ($CD10^+$ PAX^+CD79a^+) cell counts were markedly reduced, whereas $CD3^+$ cell counts were only mildly reduced (see Fig E2, *A*, *x-xxiv*). In line with these data, immunophenotypic analysis disclosed marked reduction of peripheral $CD19^+$, marginal, and switched memory B-cell counts, which is consistent with B-cell deficiency. Further analysis of the B-cell compartment showed an increase in transitional ($CD19^+CD38^{Hi}IgM^{Hi}$), activated $CD19^+CD21^{low}CD38^{low}$, and plasmablast ($CD19^+CD38^{high}IgM^-$) B cells (Fig 2, *B*).[9,10] T-cell immunophenotyping studies

TABLE I. *(Continued)*

	Patient IV-1	Patient IV-2	Patient (Le Guen et al[7])	Patient 1 (Alsultan et al[6])	Patient 2 (Alsultan et al[6])
Neurology	Neuro developmental delay: increased liquor space and reduction of cerebral volume	Neuro developmental delay: increased liquor space and reduction of cerebral volume	Deafness, agenesis of choleovestubolar nerves, cerebral MRI without further pathologic findings	NA	NA

BM, Bone marrow; *dPmax*, left ventricular contractility index; *HAM test*, acid hemolysin test; *Hb*, hemoglobin; *IVIG*, intravenous immunoglobulin; *IBMF*, inherited bone marrow failure; *LRS*, left to right shunt; *MRI*, magnetic resonance imaging; *NA*, not applicable; *ND*, not determined; *PFO*, patent foramen ovale.
*World Health Organization percentile calculator at http://www.infantchart.com.
†Not specified.

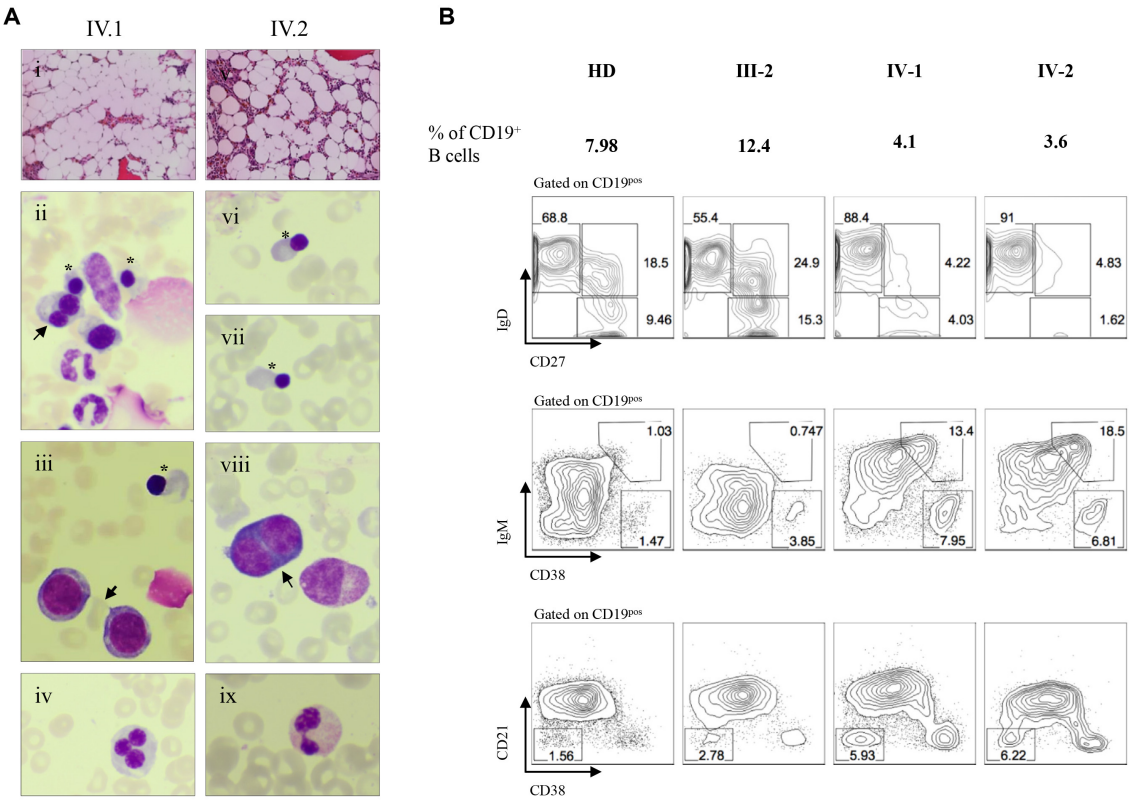

FIG 2. Cytohistopathological analysis of bone marrow (BM) samples. **A,** Histopathological analyses of BM biopsy specimens (hematoxylin and eosin staining) depicting hypocellular BM with increase in adipocyte values (Pat IV.1:i and Pat IV.2:vii). Cytological studies of BM aspirates (May-Grunwald-Giemsa) showing myelodysplastic features with binucleated and trinucleated erythroblasts (*ii [arrow]* and *iv*) and proerythroblast (*viii [arrow]*), ectopic nuclear morphology of erythroblasts (*ii, iii, vi,* and *vii [all asterisks]*), cytoplasm bridge between proerythroblasts *(iii [arrow]),* and pseudo–Pelger-Huet anomaly *(ix).* **B,** Immune phenotype of peripheral blood cells in MYSM1-deficient patients compared with a healthy donor and a parent (III-2).

provided inconsistent results. At several time points, patients were slightly lymphopenic, with decreased absolute numbers of $CD4^+$ or $CD8^+$ T cells, but at other time points, relative and absolute numbers of T cells were normal (see Fig E4 and Table E3 in this article's Online Repository at ww.jacionline.org). Proliferation studies of B and T cells did not reveal any significant alterations compared with reference values of healthy age-matched children (see Table E3).

Comprehensive immunohematologic findings of all MYSM1-deficient patients are listed in Table E3.

Identification of mutations in *MYSM1*

To investigate the underlying genetic alteration, we performed whole-exome sequencing in patients and their parents according to previously described protocols.[8] On variant filtering, we identified 9 potentially disease-causing variants (see Table E1). Of note, we found a variant in *MYSM1* (NM_001085487: c.1168G>T: p.E390*) in a large homozygous interval. The sequence variant c.1168G>T could be confirmed by Sanger sequencing and segregated with the disease phenotype in an autosomal recessive inheritance pattern (Fig 3, *A*).

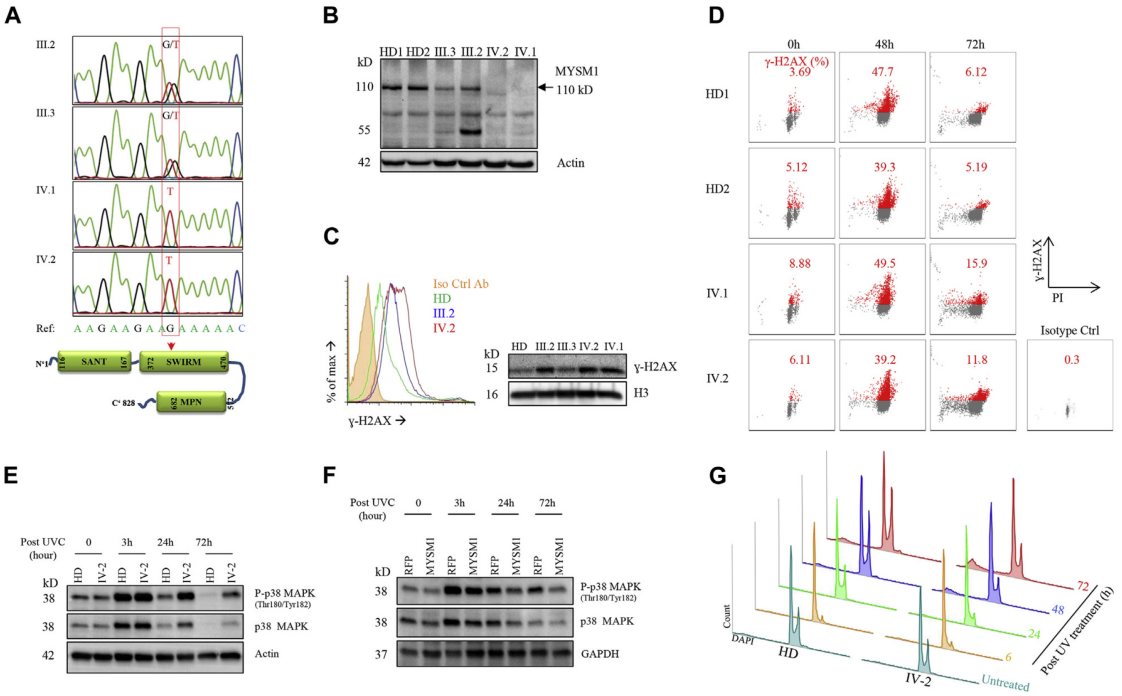

FIG 3. Mutation analysis and increased genotoxicity. **A,** Segregation of *MYSM1* mutation in the family. **B,** Western blot (WB) analysis of MYSM1 protein expression in EBV-LCLs of MYSM1-deficient patients compared with that seen in the heterozygous cells of their parents and 2 healthy control subjects (representative data of 3 independent experiments). **C,** Flow cytometry and WB detection of γ-H2AX in EBV-LCLs of an MYSM1-deficient patient in comparison with a parent (heterozygous for the mutation) and a healthy control subject (representative data of 3 independent experiments). **D,** Flow cytometric analysis of γ-H2AX levels in PBMCs of MYSM1-deficient patients compared with healthy control subjects before and after UV-induced DNA damage induction (50 J/m^2, representative data of 3 independent experiments). **E,** WB analysis of p38 MAPK and phospho-p38 (Thr180/Tyr182) MAPK expression in primary fibroblasts of MYSM1-deficient patients and healthy control subjects in response to genotoxic stress (UV irradiation, 50 J/m^2; representative data of 2 independent experiments). **F,** Reconstitution analysis of p38 MAPK activation (phospho-p38, Thr180/Tyr182) in patient IV-2's primary fibroblast transduced by bicistronic lentiviruses expressing MYSM1-RFP or RFP only. After transduction, RFP-expressing cells were sorted and irradiated by UVC, and phospho-p38 and total p38 MAPK (Thr180/Tyr182) expression was analyzed by using WB (representative data of 3 independent experiments). The same results were observed on patient IV-1's MYSM1-corrected fibroblasts. **G,** Representative experiment of 3 independent flow cytometry–based cell-cycle analyses of MYSM1-deficient fibroblasts from a patient and a healthy control subject after UV irradiation–induced DNA damage (50 J/m^2).

To study the consequences of this mutation leading to a premature stop codon in exon 9 (SWIRM domain), we generated anti-MYSM1 mAbs. As shown in Fig 3, *B*, MYSM1 could not be detected at the expected size in EBV-LCLs generated from the patients, whereas a 110-kDa band representing wild-type MYSM1 was seen in cells from parents.

Increased genotoxic stress in MYSM1-deficient cells

Murine Mysm1 deficiency results in increased genomic instability in blood cells.[11,12] Therefore we were interested to see whether MYSM1-deficient human patients had similar aberrations. We measured levels of phospho-histone H2AX (γ-H2AX) as a marker for DNA damage in PBMCs and EBV-LCLs. In MYSM1-deficient cells from patients, baseline levels of γ-H2AX were increased in comparison with those of heterozygous parents and healthy donors (HDs) (Fig 3, *C* and *D*, and see Fig E5 in this article's Online Repository at www.jacionline.org). Upon UV irradiation–induced DNA damage, γ-H2AX levels were upregulated independent of MYSM1 expression. In contrast to control cells, however, patients' cells had a slower decay rate and expressed high γ-H2AX levels, even after 72 hours (Fig 3, *D*).

The hematopoietic phenotype in Mysm1-deficient mice can be reverted by ablation of p53.[12,13] Because p53 is linked to mitogen-activated protein kinase (MAPK) signaling,[14] we next hypothesized that increased cellular stress and genotoxicity in the setting of MYSM1 deficiency can be associated with increased activation of p38. We induced genotoxic stress in primary fibroblasts by means of UV irradiation and determined expression levels of phosphorylated p38 using Western blotting. Both MYSM1-deficient and control cells exhibited increased expression of p38

and phosphorylated p38 in response to UV exposure. In contrast to HD cells, MYSM1-deficient cells had delayed re-equilibration of these stress-associated marks after 24 and 72 hours (Fig 3, *E*). Moreover, MYSM1-deficient fibroblasts showed increased reactive oxygen species (ROS) production on UV treatment in comparison with control fibroblasts (see Fig E6 in this article's Online Repository at ww.jacionline.org).

To unequivocally prove that the increased susceptibility to genotoxic stress is caused by MYSM1 deficiency, we aimed to reconstitute the cellular phenotype using retrovirus-mediated *MYSM1* gene transfer. We cloned human *MYSM1* in a bicistronic vector expressing red fluorescent protein (RFP) as a reporter gene and transduced fibroblasts from control subjects and patients. As shown in Fig 3, *F*, and Fig E7 in this article's Online Repository at ww.jacionline.org, (partial) protection against the damaging effects induced by UV light, as seen by a more rapid decrease of phosphorylated p38 MAPK, was observed after MYSM1 transduction, whereas transduction of the control vector expressing RFP only had no effect.

In view of a putative role of MYSM1 in DNA-damage checkpoint control,[15] we next analyzed cell-cycle progression and the rate of apoptosis in MYSM1-deficient human fibroblast cells. Six hours after UV irradiation, we observed an arrest in the G1 phase and a reduced number of cells in the G2-M phase in all cells independent of MYSM1 expression. HD cells re-equilibrated their regular distribution of cell-cycle phases, whereas MYSM1-deficient cells showed prolonged G1 arrest and a slower recovery (G2/M: 32.8% and 16.5%, respectively). The percentage of apoptotic cells (sub-G1) was increased in cells from patients in contrast to the percentage in cells from HDs (27.8% vs 11.9%; Fig 3, *G*). In line with these data, MYSM1-deficient EBV-LCLs also had increased sensitivity to etoposide-induced apoptosis when compared with heterozygous parent or HD cells (see Fig E8 in this article's Online Repository at ww.jacionline.org).

Finally, we asked whether increased UV-induced genotoxic stress would lead to decreased clonogenic survival of fibroblasts. We plated 100 to 4000 cells followed by UV exposure and enumerated surviving cell clones after 20 days. MYSM1-deficient fibroblasts had reduced clonogenic growth when compared with cells from HDs (see Fig E9 in this article's Online Repository at ww.jacionline.org).

Allogeneic hematopoietic stem cell transplantation

In view of progressive BMF with trilineage cytopenia, both patients underwent allogeneic hematopoietic stem cell transplantation (HSCT) from HLA-matched adult family donors at the age of 42 and 23 months, respectively (see Fig E3). The reduced-intensity conditioning regimen[16] included fludarabine (150 mg/m^2), treosulfan (42 g/m^2), and alemtuzumab (0.4 mg/kg). Graft-versus-host disease prophylaxis included cyclosporine and mycophenolate mofetil. The early posttransplantation course was uneventful in both patients. Two years after transplantation, they are full donor chimeras with normal peripheral blood counts and without signs of graft-versus-host disease (see Fig E3). In patient IV-1 1 year after transplantation, hyperthyroidism (Graves-Basedow disease) has been diagnosed, probably reflecting a complication after transplantation. In patient IV-2 cardiomyopathy, which is currently treated with captopril, and neurological development show a favorable course.

DISCUSSION

We here report on clinical, immunologic, and molecular features in 2 siblings with MYSM1 deficiency. MYSM1 was originally discovered as a member of the histone H2A deubiquitinase complex coordinating histone acetylation and H1 dissociation in transcriptional regulation.[2] Subsequent studies in Mysm1-deficient mice have revealed that Mysm1 plays a critical role in B-cell maturation through derepression of transcription of early B-cell factor 1 (Ebf1), paired box 5 (Pax5), and other B-lymphoid genes.[3] Jiang et al[3] suggested that MYSM1 mechanistically antagonizes action of the polycomb repressive complex 1 (PRC1) on the EBF1 promoter region, resulting in activation of transcription factor E2-α and PAX5.[3] In line with mouse data, we here report human MYSM1 deficiency causes BMF associated with B-cell deficiency. B-cell defect in MYSM1 deficiency has also recently been reported by 2 other groups.[6,7]

Further investigations of Mysm1-deficient mice disclosed that the epigenetic regulatory function of Mysm1 is not restricted to B cells but might also affect other immune and nonimmune cells.[5,17-20] Moreover, Panda et al[21] reported that MYSM1, beyond its crucial role in the nucleus, can function in the cytoplasm as a deubiquitinating enzyme regulating innate immunity responses. In line with these data, we also observed impaired vaccination and antibody titers, but in contrast, T-cell immunity was not affected in our patients.

DNA damage triggers cellular repair activities associated with accumulation of ubiquitin-H2A at γ-H2AX containing foci.[22,23] Upon successful completion of DNA repair, dephosphorylation and removal of γ-H2AX and ubiquitin-H2A are essential for resuming coordinated progression of the cell cycle.[24,25]

Deubiquinating enzymes, such as ubiquitin-specific peptidase 3 (Usp3) and Usp16, might regulate the cellular response toward DNA damage.[26-28] Our data show that in the absence of MYSM1, the cellular re-equilibration of cell-cycle progression is perturbed, suggesting that MYSM1 is involved in DNA damage–induced repair.

Cross-activation of p38 and p53 has been shown to play a key role in stress responses, in particular after genotoxic stress.[14,29-31] When Nijnik et al[11] discovered increased levels of γ-H2AX, ROS, and p53 in Mysm1-deficient murine hematopoietic cells, they hypothesized a critical role for p53 linked to Mysm1. In fact, the generation of Mysm1$^{-/-}$p53$^{-/-}$ double-deficient mice confirmed this idea because the hematopoietic defects observed in Mysm1-deficient mice were completely reversed in the absence of p53.[12,13] Subsequent studies have recently shown that p53 and Mysm1 colocalize to genomic loci known to be transcriptionally controlled by p53,[32] suggesting that Mysm1 controls accessibility of defined genomic loci to transcription factors. However, the exact sequence of events remains to be elucidated. Our data show that MYSM1-deficient cells are characterized by a state of increased stress (evidence by phosphorylation of p38) and delayed return to a coordinated cell-cycle progression. We assume that these effects are linked to both altered histone deubiquitination and imbalanced transcriptional regulation, but at this point, we cannot yet define the molecular steps in greater detail.

Two previous reports of patients with MYSM1 deficiency have implicated its importance in adequate hematopoiesis and B-cell development.[6,7] We expand on these observations and show that MYSM1 deficiency is associated with developmental aberrations, myelodysplastic features, and increased susceptibility to

genotoxic stress. We also document that the hematopoietic defects in patients with MYSM1 deficiency can be cured by allogeneic HSCT. Conditioning regimens for allogeneic HSC transplants must be carefully selected in patients with increased susceptibility to genotoxicity, such as Fanconi anemia and Nijmegen breakage syndrome. Our regimen based on fludarabine and treosulfan appeared to be safe and effective for stable engraftment of allogeneic stem cells without undue toxicity.

In summary, our results expand the spectrum of rare BMF syndromes associated with immunodeficiency and developmental aberrations.

We thank the family for participating in this study and the medical and nursing staff for excellent clinical care. We dedicate this work to Dr Jacek Puchałka, who died in a tragic accident in the Bavarian Alps while these investigations were ongoing.

Key messages

- **MYSM1 deficiency causes B-cell immunodeficiency associated with complex developmental aberrations and inherited BMF syndrome.**
- **MYSM1 controls genotoxic stress responses.**
- **The immunologic and hematologic aberrations in patients with MYSM1 deficiency can be cured by using allogeneic HSCT.**

REFERENCES

1. Shimamura A, Alter BP. Pathophysiology and management of inherited bone marrow failure syndromes. Blood Rev 2010;24:101-22.
2. Zhu P, Zhou WL, Wang JX, Puc J, Ohgi KA, Erdjument-Bromage H, et al. A histone H2A deubiquitinase complex coordinating histone acetylation and H1 dissociation in transcriptional regulation. Mol Cell 2007;27:609-21.
3. Jiang XX, Nguyen Q, Chou YC, Wang T, Nandakumar V, Yates P, et al. Control of B cell development by the histone H2A deubiquitinase MYSM1. Immunity 2011; 35:883-96.
4. Wang T, Nandakumar V, Jiang XX, Jones L, Yang AG, Huang XF, et al. The control of hematopoietic stem cell maintenance, self-renewal, and differentiation by Mysm1-mediated epigenetic regulation. Blood 2013;122:2812-22.
5. Nandakumar V, Chou YC, Zang LD, Huang XF, Chen SY. Epigenetic control of natural killer cell maturation by histone H2A deubiquitinase, MYSM1. Proc Natl Acad Sci U S A 2013;110:E3927-36.
6. Alsultan A, Shamseldin HE, Osman ME, Aljabri M, Alkuraya FS. MYSM1 is mutated in a family with transient transfusion-dependent anemia, mild thrombocytopenia, and low NK- and B-cell counts. Blood 2013;122:3844-5.
7. Le Guen T, Touzot F, Andre-Schmutz I, Lagresle-Peyrou C, France B, Kermasson L, et al. An in vivo genetic reversion highlights the crucial role of Myb-Like, SWIRM, and MPN domains 1 (MYSM1) in human hematopoiesis and lymphocyte differentiation. J Allergy Clin Immunol 2015;136:1619-26, e1-5.
8. Triot A, Jarvinen PM, Arostegui JI, Murugan D, Kohistani N, Dapena Diaz JL, et al. Inherited biallelic CSF3R mutations in severe congenital neutropenia. Blood 2014;123:3811-7.
9. Piatosa B, Wolska-Kusnierz B, Pac M, Siewiera K, Galkowska E, Bernatowska E. B cell subsets in healthy children: reference values for evaluation of B cell maturation process in peripheral blood. Cytometry B Clin Cytom 2010;78: 372-81.
10. Morbach H, Eichhorn EM, Liese JG, Girschick HJ. Reference values for B cell subpopulations from infancy to adulthood. Clin Exp Immunol 2010;162:271-9.
11. Nijnik A, Clare S, Hale C, Raisen C, McIntyre RE, Yusa K, et al. The critical role of histone H2A-deubiquitinase Mysm1 in hematopoiesis and lymphocyte differentiation. Blood 2012;119:1370-9.
12. Gatzka M, Tasdogan A, Hainzl A, Allies G, Maity P, Wilms C, et al. Interplay of H2A deubiquitinase 2A-DUB/Mysm1 and the p19(ARF)/p53 axis in hematopoiesis, early T-cell development and tissue differentiation. Cell Death Differ 2015;22: 1451-62.
13. Belle JI, Langlais D, Petrov JC, Pardo M, Jones RG, Gros P, et al. p53 mediates loss of hematopoietic stem cell function and lymphopenia in Mysm1 deficiency. Blood 2015;125:2344-8.
14. Gong XW, Liu AH, Ming XY, Deng P, Jiang Y. UV-induced interaction between p38 MAPK and p53 serves as a molecular switch in determining cell fate. FEBS Lett 2010;584:4711-6.
15. Nishi R, Wijnhoven P, le Sage C, Tjeertes J, Galanty Y, Forment JV, et al. Systematic characterization of deubiquitylating enzymes for roles in maintaining genome integrity. Nat Cell Biol 2014;16:1016-26.
16. Myers KC, Howell JC, Wallace G, Dandoy C, El-Bietar J, Lane A, et al. Poor growth, thyroid dysfunction and vitamin D deficiency remain prevalent despite reduced intensity chemotherapy for hematopoietic stem cell transplantation in children and young adults. Bone Marrow Transplant 2016;51:980-4.
17. Won H, Nandakumar V, Yates P, Sanchez S, Jones L, Huang XF, et al. Epigenetic control of dendritic cell development and fate determination of common myeloid progenitor by Mysm1. Blood 2014;124:2647-56.
18. Jiang XX, Chou Y, Jones L, Wang T, Sanchez S, Huang XF, et al. Epigenetic regulation of antibody responses by the histone H2A deubiquitinase MYSM1. Sci Rep 2015;5:13755.
19. Huang XF, Nandakumar V, Tumurkhuu G, Wang T, Jiang X, Hong B, et al. Mysm1 is required for interferon regulatory factor expression in maintaining HSC quiescence and thymocyte development. Cell Death Dis 2016;7:e2260.
20. Li P, Yang YM, Sanchez S, Cui DC, Dang RJ, Wang XY, et al. Deubiquitinase MYSM1 is essential for normal bone formation and mesenchymal stem cell differentiation. Sci Rep 2016;6:22211.
21. Panda S, Nilsson JA, Gekara NO. Deubiquitinase MYSM1 regulates innate immunity through inactivation of TRAF3 and TRAF6 complexes. Immunity 2015;43: 647-59.
22. Huen MS, Grant R, Manke I, Minn K, Yu X, Yaffe MB, et al. RNF8 transduces the DNA-damage signal via histone ubiquitylation and checkpoint protein assembly. Cell 2007;131:901-14.
23. Mailand N, Bekker-Jensen S, Faustrup H, Melander F, Bartek J, Lukas C, et al. RNF8 ubiquitylates histones at DNA double-strand breaks and promotes assembly of repair proteins. Cell 2007;131:887-900.
24. Keogh MC, Kim JA, Downey M, Fillingham J, Chowdhury D, Harrison JC, et al. A phosphatase complex that dephosphorylates gammaH2AX regulates DNA damage checkpoint recovery. Nature 2006;439:497-501.
25. Chowdhury D, Keogh MC, Ishii H, Peterson CL, Buratowski S, Lieberman J. gamma-H2AX dephosphorylation by protein phosphatase 2A facilitates DNA double-strand break repair. Mol Cell 2005;20:801-9.
26. Lancini C, van den Berk PC, Vissers JH, Gargiulo G, Song JY, Hulsman D, et al. Tight regulation of ubiquitin-mediated DNA damage response by USP3 preserves the functional integrity of hematopoietic stem cells. J Exp Med 2014;211:1759-77.
27. Nicassio F, Corrado N, Vissers JH, Areces LB, Bergink S, Marteijn JA, et al. Human USP3 is a chromatin modifier required for S phase progression and genome stability. Curr Biol 2007;17:1972-7.
28. Shanbhag NM, Rafalska-Metcalf IU, Balane-Bolivar C, Janicki SM, Greenberg RA. ATM-dependent chromatin changes silence transcription in cis to DNA double-strand breaks. Cell 2010;141:970-81.
29. She QB, Chen N, Dong Z. ERKs and p38 kinase phosphorylate p53 protein at serine 15 in response to UV radiation. J Biol Chem 2000;275:20444-9.
30. Bulavin DV, Saito S, Hollander MC, Sakaguchi K, Anderson CW, Appella E, et al. Phosphorylation of human p53 by p38 kinase coordinates N-terminal phosphorylation and apoptosis in response to UV radiation. EMBO J 1999;18:6845-54.
31. Huang C, Ma WY, Maxiner A, Sun Y, Dong Z. p38 kinase mediates UV-induced phosphorylation of p53 protein at serine 389. J Biol Chem 1999;274:12229-35.
32. Belle JI, Petrov JC, Langlais D, Robert F, Cencic R, Shen S, et al. Repression of p53-target gene Bbc3/PUMA by MYSM1 is essential for the survival of hematopoietic multipotent progenitors and contributes to stem cell maintenance. Cell Death Differ 2016;23:759-75.

Supplemental figures

Figure S1

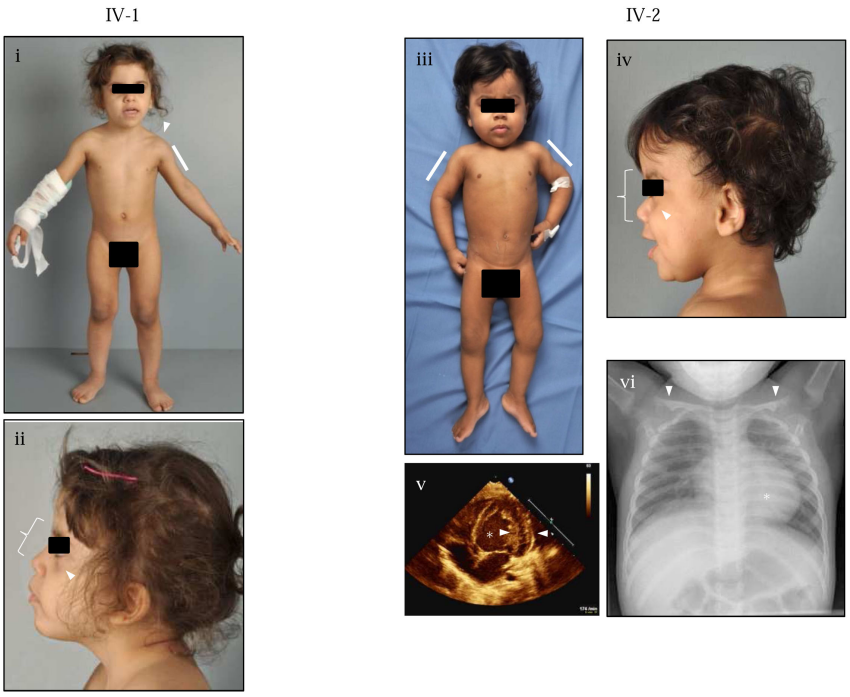

Figure S2A

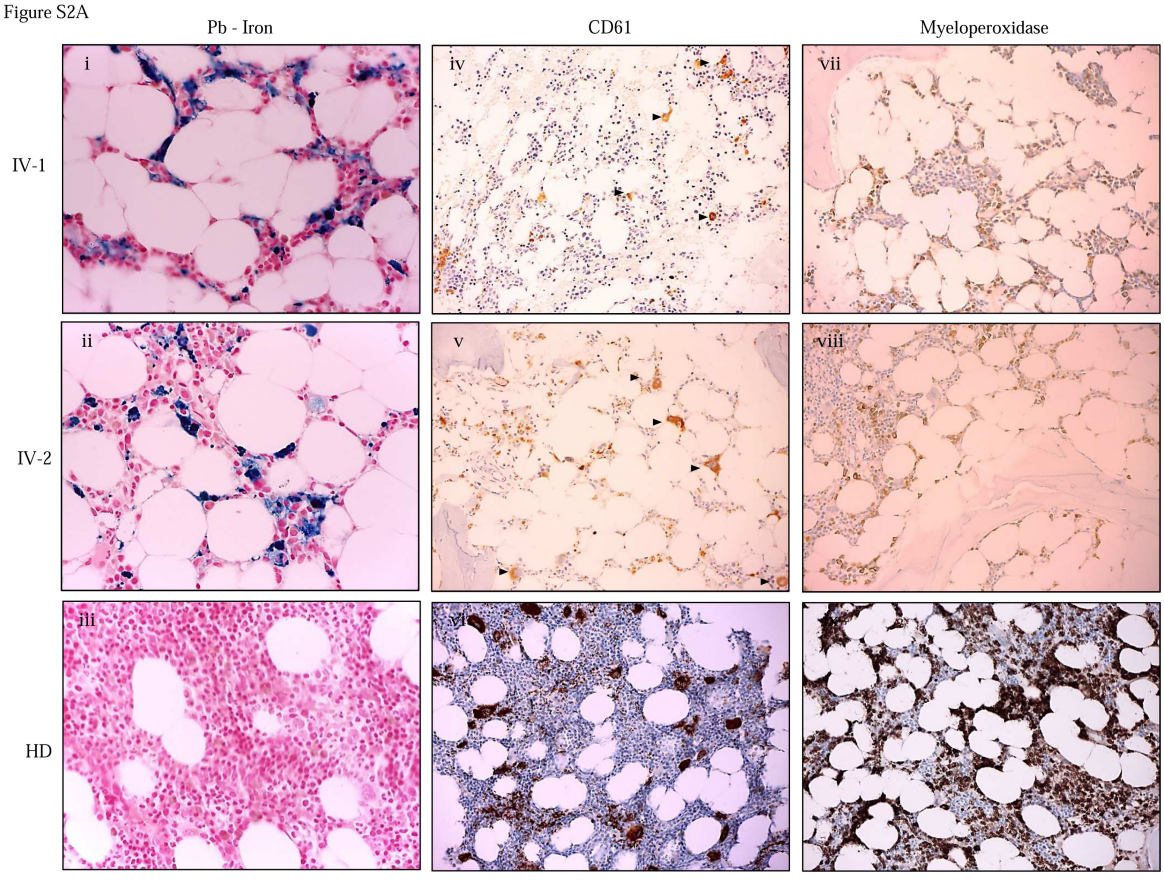

Figure S2A, continued

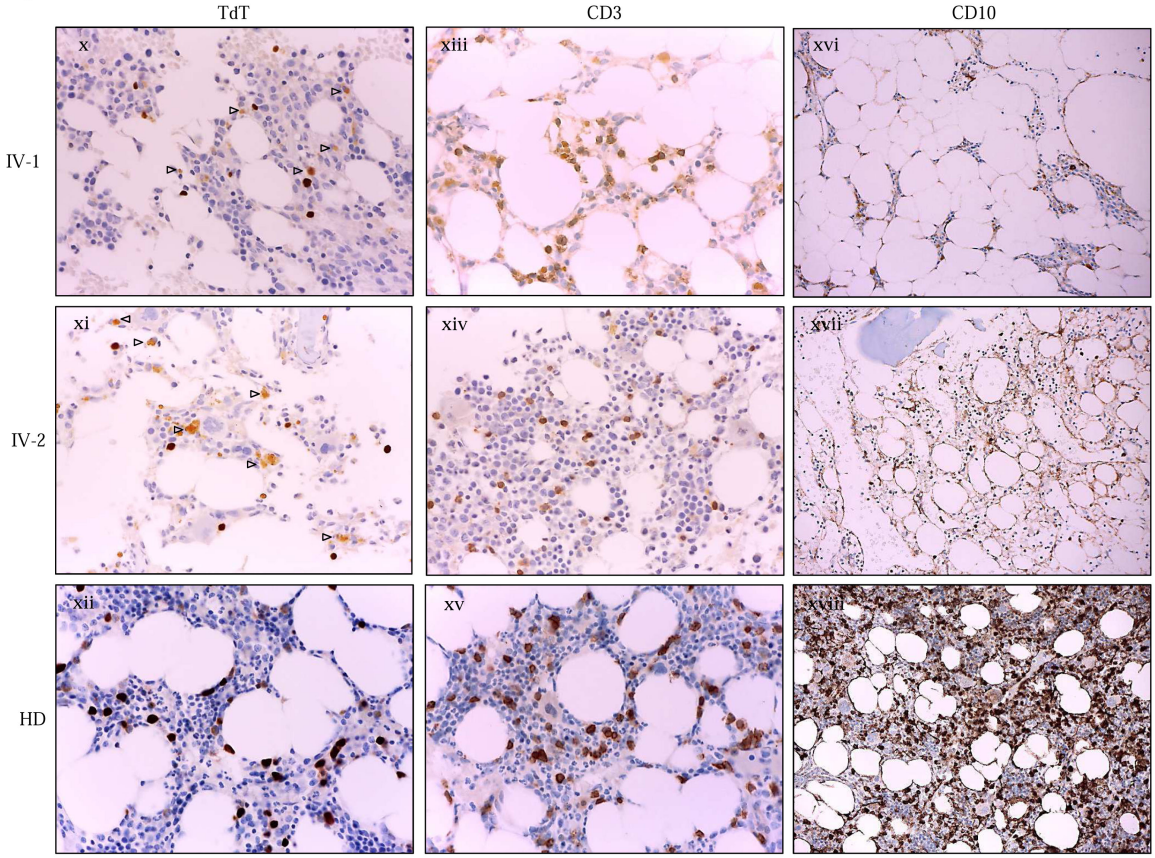

Figure S2A, continued

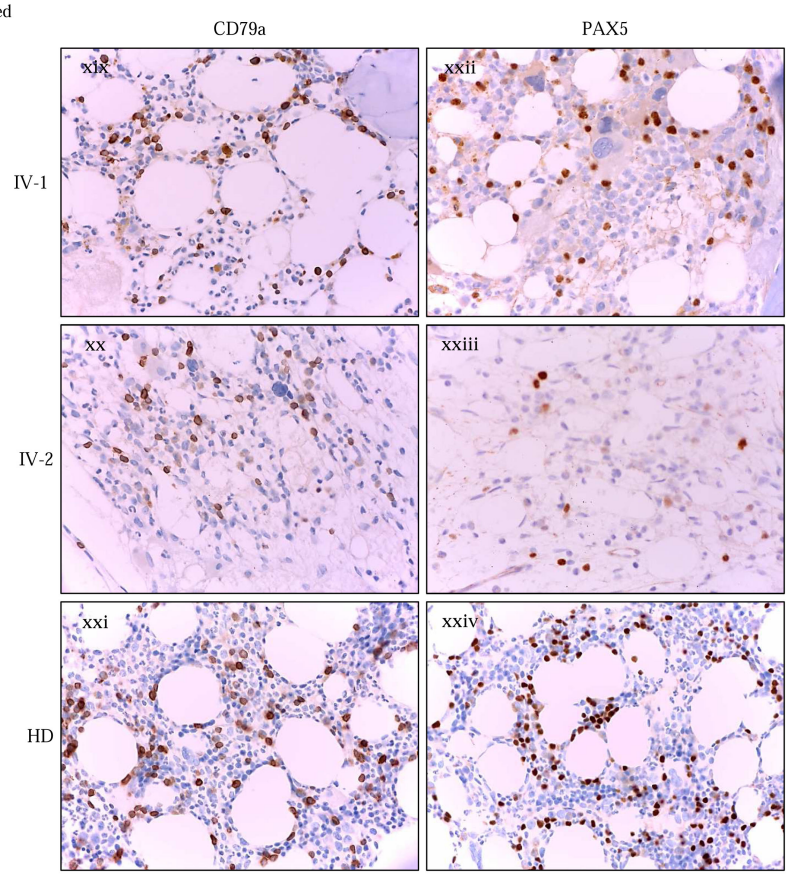

Figure S2B

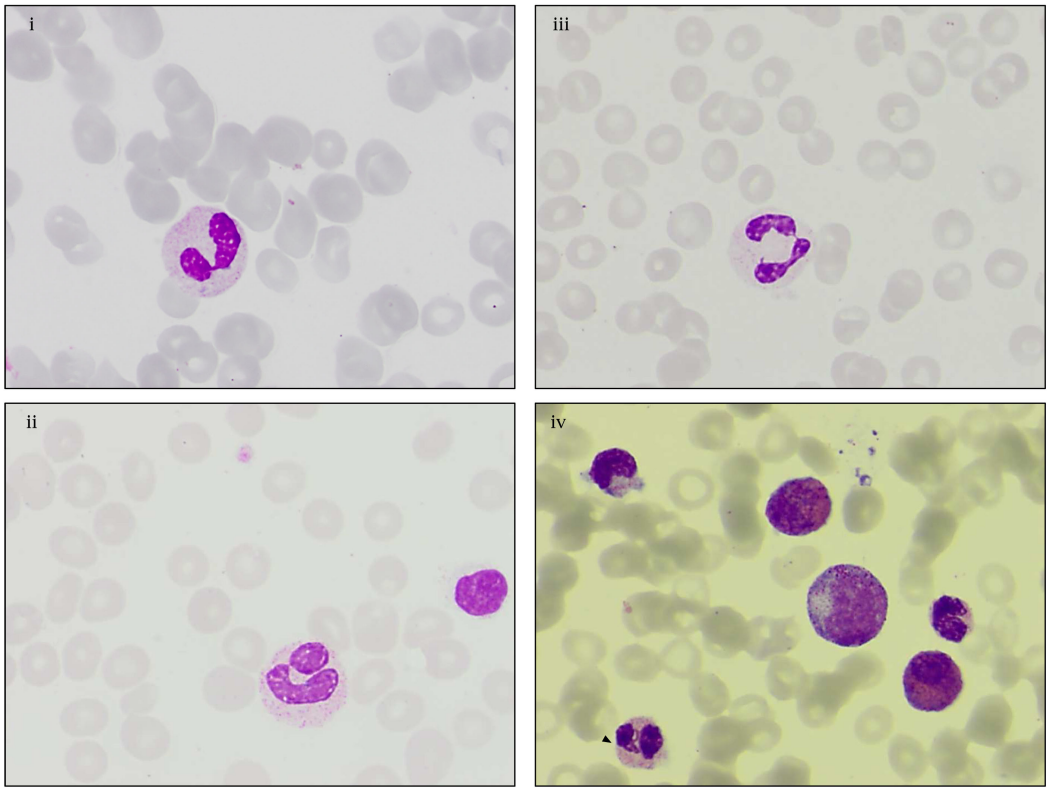

Figure S3

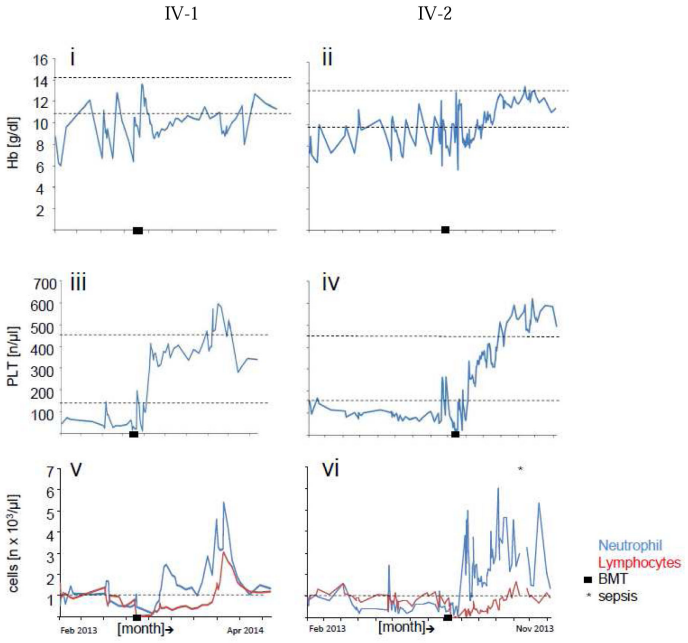

Figure S4

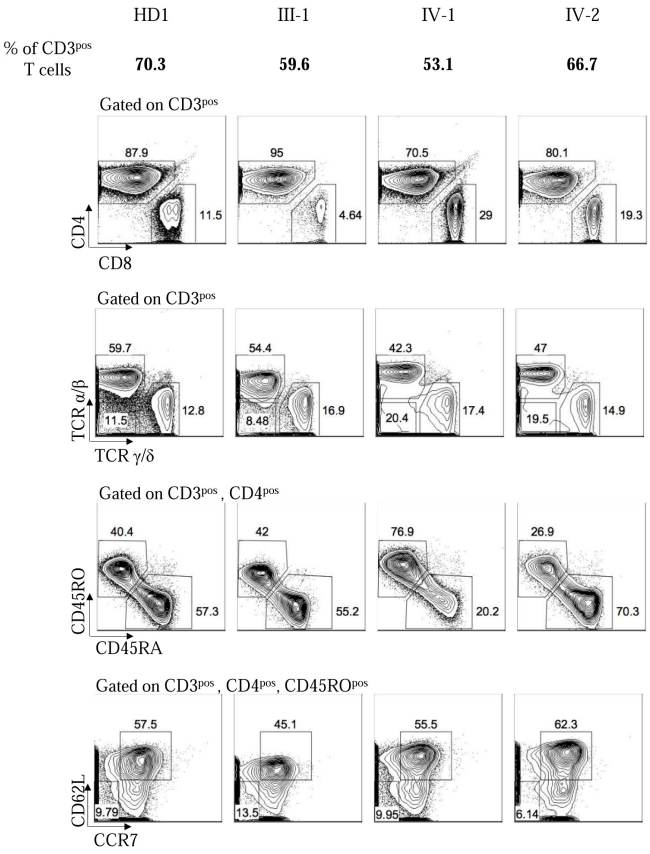

Figure S5

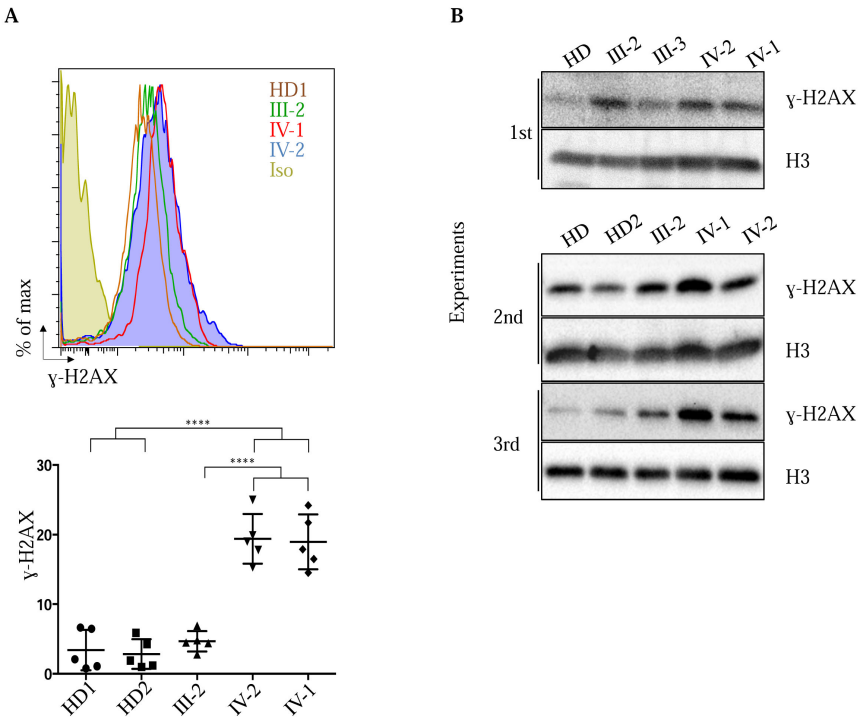

Figure S6

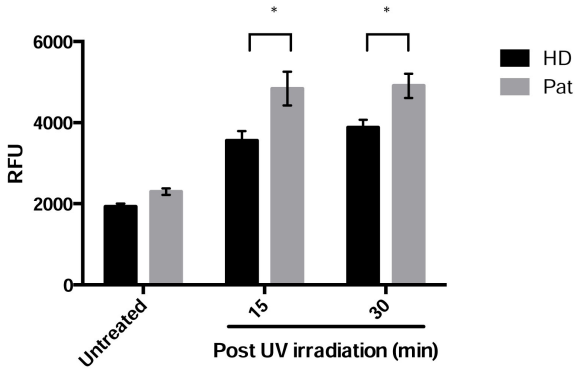

Figure S7

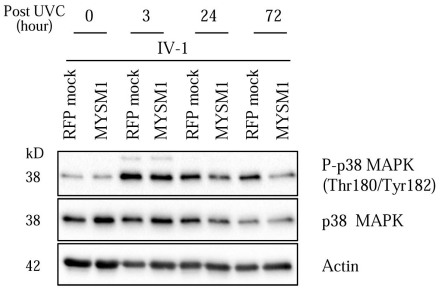

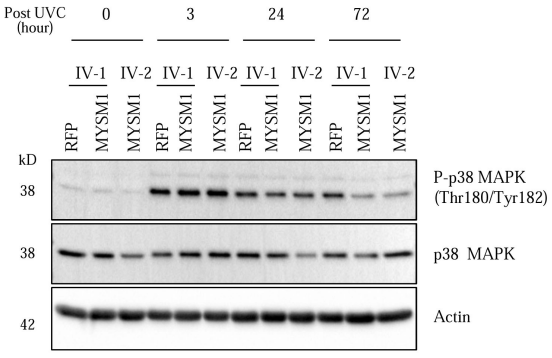

Figure S8

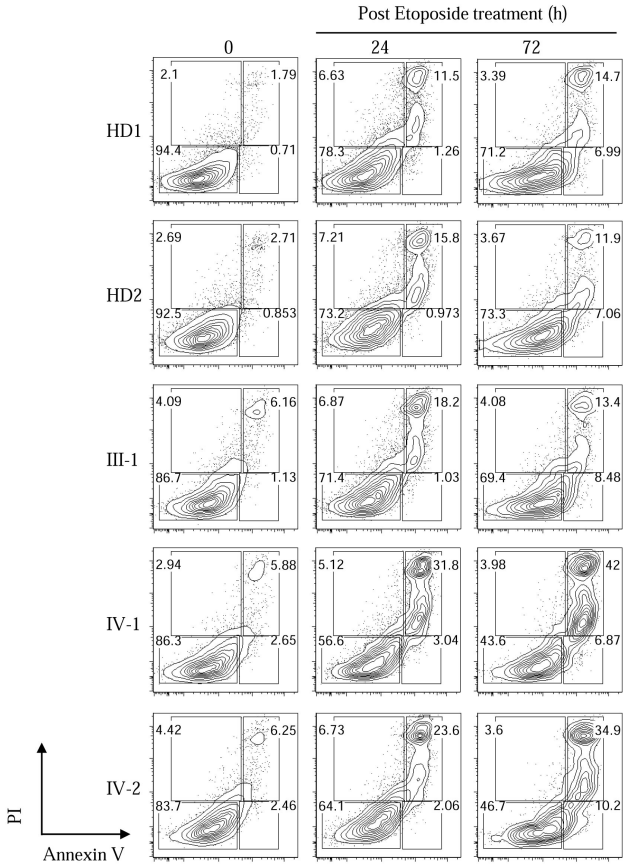

Figure S9

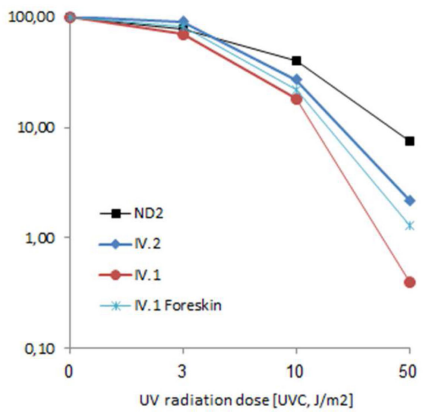

6. Manuscript # 2

nature genetics

Chromatin-remodeling factor SMARCD2 regulates transcriptional networks controlling differentiation of neutrophil granulocytes

Maximilian Witzel[1,2], Daniel Petersheim[1], Yanxin Fan[1], Ehsan Bahrami[1], Tomas Racek[1], Meino Rohlfs[1], Jacek Puchałka[1,13], Christian Mertes[2], Julien Gagneur[2,3], Christoph Ziegenhain[4], Wolfgang Enard[4], Asbjørg Stray-Pedersen[5], Peter D Arkwright[6], Miguel R Abboud[7], Vahid Pazhakh[8], Graham J Lieschke[8], Peter M Krawitz[9], Maik Dahlhoff[10], Marlon R Schneider[10], Eckhard Wolf[10], Hans-Peter Horny[11], Heinrich Schmidt[1], Alejandro A Schäffer[12] & Christoph Klein[1,2]

We identify SMARCD2 (SWI/SNF-related, matrix-associated, actin-dependent regulator of chromatin, subfamily D, member 2), also known as BAF60b (BRG1/Brahma-associated factor 60b), as a critical regulator of myeloid differentiation in humans, mice, and zebrafish. Studying patients from three unrelated pedigrees characterized by neutropenia, specific granule deficiency, myelodysplasia with excess of blast cells, and various developmental aberrations, we identified three homozygous loss-of-function mutations in *SMARCD2*. Using mice and zebrafish as model systems, we showed that SMARCD2 controls early steps in the differentiation of myeloid–erythroid progenitor cells. *In vitro*, SMARCD2 interacts with the transcription factor CEBPε and controls expression of neutrophil proteins stored in specific granules. Defective expression of SMARCD2 leads to transcriptional and chromatin changes in acute myeloid leukemia (AML) human promyelocytic cells. In summary, SMARCD2 is a key factor controlling myelopoiesis and is a potential tumor suppressor in leukemia.

Differentiation of hematopoietic stem cells (HSCs) follows a hierarchical program of transcription factor–regulated events[1–3]. Early myeloid cell differentiation is dependent on PU.1 and CEBPα (CCAAT/enhancer-binding protein α), and late myeloid cell differentiation is orchestrated by CEBPε (CCAAT/enhancer-binding protein ε)[4]. The influence of SWI/SNF (SWItch/Sucrose Non-Fermentable) chromatin-remodeling factors as novel master regulators of hematopoietic differentiation is only beginning to be explored[3,5,6]. PU.1, CEPBPα, CEBPε, and proteins in SWI/SNF complexes participate in transcription factor–mediated instructive events and less well-defined permissive events orchestrated by a variety of epigenetic modulators[7,8]. Dynamic chromatin remodeling adds another level of complexity. Embedding of promoter DNA into nucleosome landscapes restricts the accessibility of cognate binding sites for transcription factors and restricts gene expression[9–11]. The SWI/SNF complex is composed of multimeric units that use energy derived from ATP hydrolysis to unwrap or restructure nucleosomes[12]. SMARCD2 is a component of the SWI/SNF complex in HSCs and other hematopoietic cells[6,13,14]. The two paralogous proteins SMARCD1 (BAF60A) and SMARCD3 (BAF60C) control embryonic stem (ES) cell[15] and heart muscle cell[16] differentiation, respectively.

RESULTS

Clinical phenotype

Here we investigated three independent consanguineous pedigrees with four patients (for an explanation on kinship, see the Online Methods) who presented as neonates with delayed separation of umbilical cord and subsequently developed severe bacterial infections associated with neutropenia, parasitosis, or chronic diarrhea (**Supplementary Table 1**). Extrahematopoietic findings included mild-to-moderate developmental delay and dysmorphic features (**Fig. 1**, **Supplementary Fig. 1**, and **Supplementary Table 1**). The bone marrow of patients showed hypercellularity, paucity of neutrophil granulocytes, dysplastic features (**Fig. 1**), and progressive development of myelodysplasia (**Fig. 2** and **Supplementary Fig. 2**). Neutrophil granulocytes were characterized by absence of granule proteins (**Supplementary Fig. 3**).

[1]Department of Pediatrics, Dr. von Hauner Children's Hospital, Ludwig-Maximilians-Universität München, Munich, Germany. [2]Gene Center, Ludwig-Maximilians-Universität München, Munich, Germany. [3]Department of Informatics, Technical University of Munich, Munich, Germany. [4]Anthropology and Human Genomics, Department of Biology II, Faculty of Biology, Ludwig-Maximilians-Universität München, Munich, Germany. [5]Norwegian National Unit for Newborn Screening, Oslo University Hospital, Oslo, Norway. [6]Department of Paediatric Allergy and Immunology, University of Manchester, Royal Manchester Children's Hospital, Manchester, UK. [7]Department of Pediatrics and Adolescent Medicine, American University of Beirut Medical Center, Beirut, Lebanon. [8]Australian Regenerative Medicine Institute, Monash University, Clayton, Victoria, Australia. [9]Medical Genetics and Human Genetic, Charite University Hospital, Berlin, Germany. [10]Molecular Animal Breeding and Biotechnology, Gene Center Ludwig-Maximilians-Universität München, Munich, Germany. [11]Pathology Institute, Faculty of Medicine, Ludwig-Maximilians-Universität München, Munich, Germany. [12]National Center for Biotechnology Information, US National Institutes of Health, US Department of Health and Human Services, Bethesda, Maryland, USA. [13]Deceased. Correspondence should be addressed to C.K. (christoph.klein@med.uni-muenchen.de).

Received 16 August 2016; accepted 10 March 2017; published online 3 April 2017; doi:10.1038/ng.3833

Molecular genetics

In search of the underlying genetic defect, we performed homozygosity mapping and whole-exome sequencing, followed by Sanger sequencing of patients and family members (see the Online Methods and **Supplementary Note** for details). Homozygosity mapping identified an especially large perfect marker interval of over 50 Mb in family A on chromosome 17; within this interval, family B had two non-adjacent perfect intervals spanning 1.8 Mb and 0.5 Mb. The asymptotic logarithm of the odds (LOD) scores for these intervals are +4.2 (+1.8 for family A and +2.4 for family B), and peak observed LOD scores, with a more realistic disease haplotype frequency of 0.05, were 3.0 (+1.2 and +1.8). There were approximately 36 genes located in the two shared intervals, including *SMARCD2*.

We identified distinct segregating homozygous mutations in *SMARCD2* in all three pedigrees (**Fig. 3a–c**). Mutations are described by their putative effect on transcript SMARCD2-001 (ENST00000448276; NM_001098426.1). Effects on hypothetical transcripts are shown in **Supplementary Table 2**. At the DNA level, the mutations in pedigrees A and C affected splice sites, while the mutation in pedigree B was a duplication of 25 bp, leading to a frameshift and premature termination (**Supplementary Table 2**). Immunoblot analyses showed an absence of SMARCD2 protein in patient-derived cells (**Fig. 3d** and **Supplementary Data 1**). To confirm that the *SMARCD2* mutations lead to a loss of function, we sequenced reverse-transcribed mRNA from patient-derived cells (**Fig. 3e**) and determined their putatively encoded proteins. We then cloned (primers listed in **Supplementary Table 3**) two isoforms of patient AII.1 (AII.1a: p.Ile362Cysfs*3 and AII1b: p.Ser394Argfs*1), one isoform of patient BII.1 (BII.1: p.Gln147Glufs*5) and one isoform of patient CII.1 (CII.1: p.Arg73Valfs*8). FLAG-tagged expression vectors carrying mutated *SMARCD2* versions and a red fluorescence protein gene separated by an internal ribosomal entry sequence (IRES.RFP) were transfected into 293T cells, and the encoded proteins were investigated for coimmunoprecipitation with native SWI/SNF core members. As shown in **Figure 3f** (**Supplementary Data 2**), only the wild-type version of SMARCD2 was able to co-precipitate with SMARCA4 (BRG1), SMARCC2 (BAF170), SMARCC1 (BAF155), and SMARCB1 (BAF47); none of the mutant versions were able to co-precipitate with any of these proteins, suggesting that the mutations constitute loss-of-function alleles.

Because all SMARCD2-deficient patients had either been subjected to allogeneic hematopoietic stem cell therapy (HSCT) or had died from their disease, primary SMARCD2-deficient HSCs were not available for further experiments. To further study the role of SMARCD2 in neutrophil differentiation, we established several *in vivo* and *in vitro* models.

smarcd2 regulates granulopoiesis in zebrafish

As a first model organism, we used zebrafish (*Danio rerio*), in which *smarcd2* (XP_692749.2) is the ortholog of human *SMARCD2*. Using antisense morpholino oligonucleotides (MOs), we created Smarcd2-deficient zebrafish in two reporter strains with fluorescent neutrophil granulocytes: Tg(*mpx*:*EGFP*)^{i114} (**Supplementary Fig. 4a–c** and **Supplementary Data 3a**,**b**) and Tg(*lyz*:*dsRed*)^{nz50} (**Fig. 4a**)[17–19]. *smarcd2* MOs were designed to block either translation initiation (label ATG) or splicing (labels SB1 and SB2, for MOs targeting splice donor and acceptor sites, respectively) of *smarcd2*. In both fish lines, there was a significant reduction in the number of neutrophil granulocytes in comparison to controls at 72 h post fertilization (h.p.f.) for the ATG and SB1 MOs (**Fig. 4a** and **Supplementary Fig. 4c**). MO SB2, which failed to disrupt *smarcd2* splicing (**Supplementary Fig. 4a**), provided an additional negative control indicating specificity of the on-target *smarcd2* MO effect to reduce neutrophil abundance. Using CRISPR/Cas9 genome editing in zebrafish, we also created a frameshift mutant *smarcd2* allele *smarcd2*$^{1/1}$ (**Supplementary Fig. 4d**), which also showed reduced granulocyte abundance at 72 h.p.f. in comparison to wild-type controls (**Fig. 4b**,**c**). There were no marked effects of *smarcd2* MO on zebrafish granulocyte morphology (**Supplementary Fig. 5**). There were no qualitative differences in *O*-dianisidine-stained hemoglobinized erythrocytes and no quantitative differences in numbers of Tg(*mpeg1*:*mCherry*)^{gl25xc264}-marked macrophages and Tg(*cd41*:*EGFP*)^{la2}-marked thrombocytes after *smarcd2* MO knockdown (**Supplementary Fig. 6**). This underlines the lineage-specific effects of *smarcd2*. Collectively, these zebrafish models provide concordant evidence that a requirement for SMARCD2 in neutrophil granulocyte differentiation is evolutionarily conserved.

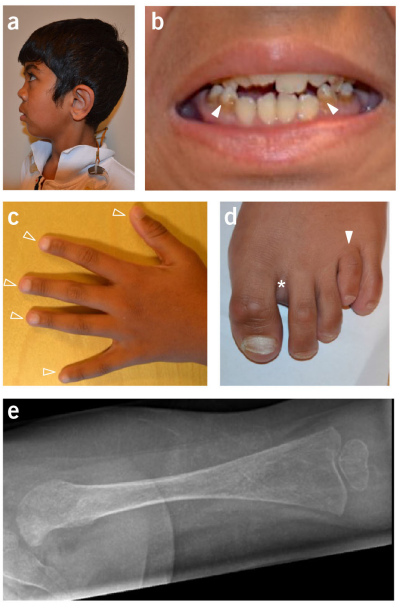

Figure 1 Syndromic features in SMARCD2 deficiency. (**a**–**e**) The phenotype of patient AII.1 includes low-set ears, posteriorly rotated, with prominent concha, hypoplastic mandibula, saddle nose, midface hypoplasia, synophris, and asymmetric face (ear to ear) (**a**), misaligned, dysplastic teeth and incomplete amelogenesis imperfecta (filled arrowheads) (**b**), brachytelephalangy (unfilled arrowheads) and longitudinal ridges on finger nails (**c**), sandal gap/increased interdigital space D1–D2 (asterisk), brachymetatarsy D4 (filled arrowhead), and brittle nails (**d**), and severe osteopenia with relative constriction of diaphysis and flaring of metaphysis (Erlenmeyer deformity) (**e**). Images have been partially cropped; please compare to **Supplementary Table 18**. Patients or their parents gave informed consent for publication of their photographs.

Knockout of *Smarcd2* in mouse embryos

A second *in vivo* model was generated by injection of *Smarcd2*$^{+/-}$ mouse ES cells (KOMP repository) into blastocysts and transfer of these cells into pseudo-pregnant mice. Chimeric offspring were mated with wild-type mice, resulting in *Smarcd2*$^{+/-}$ mice, which were intercrossed (**Supplementary Fig. 7a**,**b**). We found that *Smarcd2*$^{-/-}$ embryos died late during fetal development (**Supplementary Fig. 7c–e**

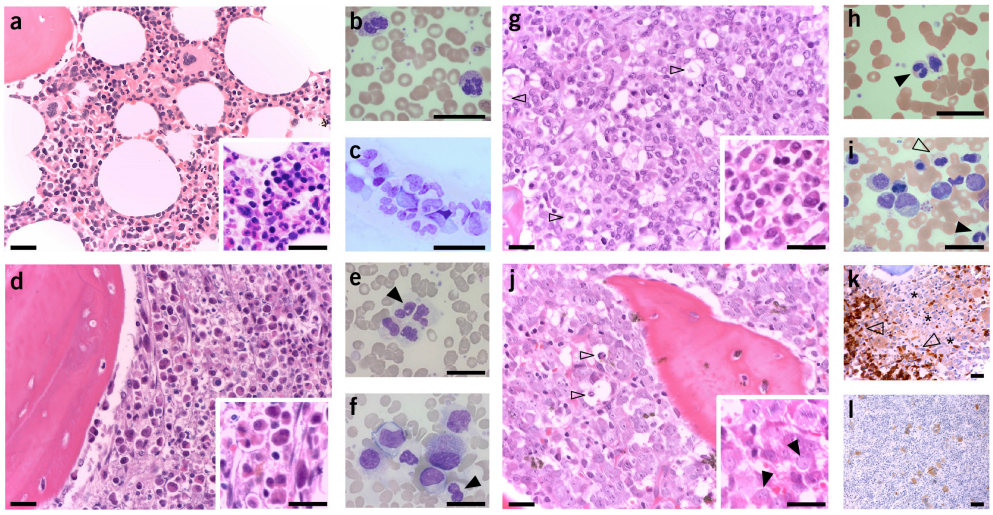

Figure 2 Bone marrow and peripheral blood cell analysis. (**a**–**c**) Healthy donor. (**a**) Regular maturation of hematopoietic lineages and no blast cell excess. Inset, magnification (bone marrow histology; hematoxylin and eosin). (**b**) Segmented neutrophil granulocytes (peripheral blood cytology; Giemsa). (**c**) Red and white blood cell maturation (bone marrow cytology; Giemsa). (**d**–**f**) AII.1. (**d**) Diffuse and compact blast cell infiltration with absence of megakaryocytes and erythroid islands. Inset, immature neutrophilic cells (bone marrow histology; hematoxylin and eosin). (**e**) Atypical neutrophilic cells with hypogranulated cytoplasm, hyposegmented nuclei, and pseudo-Pelger–Huët anomaly (PPHA) (black arrowhead) (peripheral blood cytology; Giemsa). (**f**) Left-shifted neutrophilic granulopoiesis, blast cells, and PPHA (black arrowheads) (under G-CSF) (peripheral blood cytology; Giemsa). (**g**–**i**) BII.1 and BII.2. (**g**) Hypercellularity with (sub)total adipocyte depletion and normal erythroid precursors. Diffuse infiltration by blast cells and starry sky pattern with disseminated activated macrophages (unfilled arrowheads). Inset, immature neutrophilic cells (bone marrow histology from BII.2; hematoxylin and eosin). (**h**) Circulating atypical neutrophil cells and PPHA (black arrowhead) (BII.1 peripheral blood cytology; Giemsa). (**i**) Left-shifted atypical neutrophilic granulopoiesis with increase of blast cells. PPHA (black arrowhead) and atypical neutrophils (unfilled arrowhead) (BII.1 bone marrow cytology; Giemsa). (**j**–**l**) CII.1. (**j**) Marked hypercellularity with (sub)total adipocyte depletion and normal erythrocytes. Diffuse and compact infiltration by blast cells and scattered activated macrophages (unfilled arrowheads). Inset, pleomorphic blast cells with round nuclei and small nucleoli (black arrowheads) (bone marrow histology; hematoxylin and eosin). (**k**) Glycophorin C staining shows erythropoietic islands (unfilled arrowheads) and blast infiltration (asterisks). (**l**) CD61 staining shows loosely scattered, small and immature megakaryocytes (micromegakaryocytes) (bone marrow histology; hematoxylin and eosin). Images have been cropped; see also **Supplementary Table 18**. Scale bars, approximately 20 µm.

and **Supplementary Data 3c–e**) and were characterized by reduced size, pallor, and decreased temporal vascularization (**Fig. 5a**), suggestive of a compromised hematopoietic system. However, we did find Mendelian ratios of *Smarcd2*$^{-/-}$ embryos at 14.5 d post-coitum (d.p.c.) (**Supplementary Fig. 7d**). *Smarcd2*$^{-/-}$ embryos expressed SWI/SNF core members and the SMARCD1 and SMARCD3 paralog proteins (**Supplementary Fig. 7f** and **Supplementary Data 4**). Flow cytometry analysis of fetal liver single-cell suspensions showed comparable numbers of HSCs (**Supplementary Fig. 7g**), yet a striking reduction in granulocyte–macrophage progenitors (GMPs) and of CD11b^{+}Gr1^{+} neutrophil granulocytes and CD11b^{+}Ly6c^{+} monocytes in *Smarcd2*$^{-/-}$ embryos versus *Smarcd2*$^{+/+}$ embryos (**Fig. 5b,c**).

To assess the differentiation capacity of HSCs, we next purified CD45.2^{+}Lin^{-}Mac$^{+/lo}$ Sca1^{+}c-Kit^{+} (LSK) cells from wild-type, heterozygous, and homozygous fetal livers and performed colony-forming unit (CFU) assays *in vitro*. In comparison to CFU colonies derived from wild-type or heterozygous fetal liver LSK cells, knockout CFU colonies showed a marked reduction in size and numbers (data not shown and **Supplementary Fig. 8a**) and maturation arrest (**Fig. 5d**). *Smarcd2*$^{-/-}$ myeloid CFU colonies, generated in the presence of myeloid cytokine cocktail, were deficient in cell surface expression of CD11b, Gr1, and Ly6c (**Supplementary Fig. 8b**). A block in myeloid differentiation was also seen when LSK cells (native) were exposed to any of GM-CSF, M-CSF, or G-CSF, suggesting that none of the corresponding cytokine receptors were able to induce myeloid cell growth (**Fig. 5e**).

Aberrant hematopoiesis was not restricted to the myeloid compartment in *Smarcd2*$^{-/-}$ embryos but also affected erythroid differentiation. Fetal/umbilical cord blood cytology at 14.5 d.p.c. showed marked dysplastic changes in *Smarcd2*$^{-/-}$ erythropoiesis: In contrast to wild-type embryos, characterized by normochromic, orthochromatic erythrocytes and the presence of few nucleated erythrocytes, *Smarcd2*$^{-/-}$ embryos showed extensive anisocytosis of erythrocytes, multinucleated cells, perturbed mitosis, and increased apoptosis (**Fig. 5f**). Furthermore, *in vitro* erythroid differentiation of LSK cells in the presence of recombinant mouse SCF, recombinant mouse IL-3, recombinant human IL-6, and recombinant human EPO hints at a partial differentiation block or delay at the immature S1 stage, as determined by CD71/Ter119 expression[20] in *Smarcd2*$^{-/-}$ GEMM colonies (**Fig. 5g,h**). Taken together, mouse SMARCD2-deficient hematopoietic cell differentiation is characterized by a maturation arrest in myeloid and erythroid cells *in vitro* and *in vivo*, reminiscent of the hematological phenotype in *SMARCD2*$^{-/-}$ patients.

Various previous studies found that SWI/SNF complex members increase or decrease primitive or definite hematopoiesis[6]. Hence, we hypothesize that (i) the functional effects of SMARCD2 deficiency on granulopoiesis are due to its absence from SWI/SNF complexes,

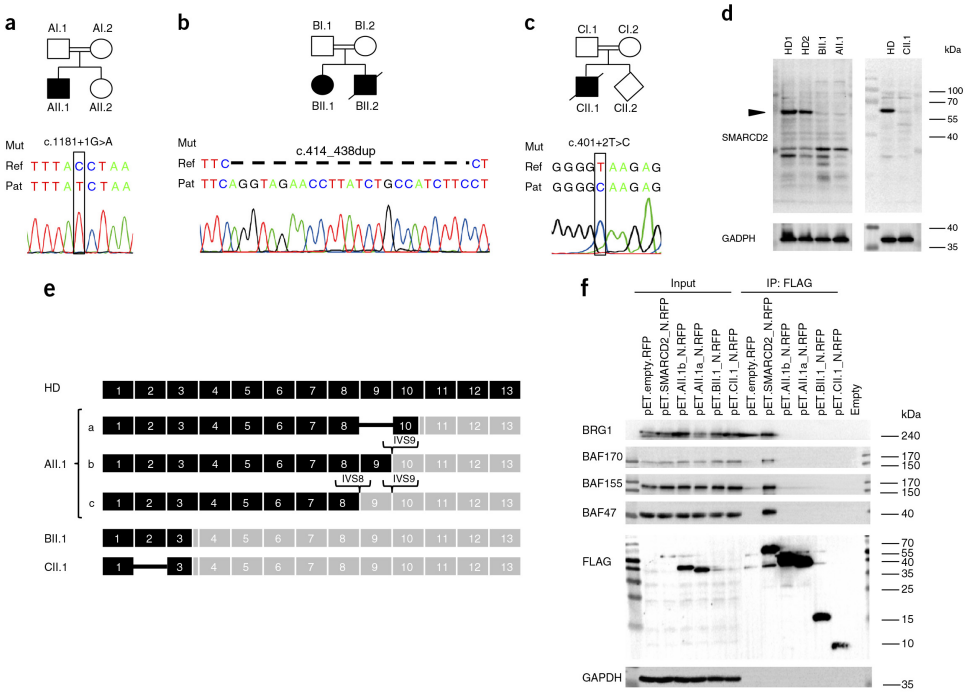

Figure 3 Identification of biallelic loss-of-function mutations in *SMARCD2*. (**a**–**c**) Pedigrees and Sanger sequencing chromatograms for patient (Pat) as compared to reference (Ref) sequences and specification of homozygous mutations (Mut). In **a**, the reverse read is shown for patient AII.1. (**d**) Immunoblot showing absence of SMARCD2 protein expression (molecular weight, 58.9 kDa; arrowhead) in fibroblasts (healthy donor 1 (HD1), healthy donor 2 (HD2), patients AII.1 and BII.1) and in Epstein–Barr virus (EBV)-transformed B cell lines (healthy donor (HD), patient CII.1). Images have been cropped; please compare to **Supplementary Data 1**. Replicates: 2. (**e**) *SMARCD2* mRNA transcripts detected in patient-derived cells; ORFs are shown in black. Healthy donor (HD) transcript ENST00000448276; NM_001098426.1; CCDS45756 is shown in comparison to transcripts in patients AII.1 (a, p.Ile362Cysfs*2; b, p.Ser394Argfs*1; c, p.Ile362Valfs*85), BII.1 (p.Gln147Glufs*4), and CII.1 (p.Arg73Valfs*8). Replicates: 2. (**f**) Immunoprecipitation showing defective binding of patient-specific mutated SMARCD2 proteins to the SWI/SNF core complex components BRG1, BAF170, BAF155, and BAF47. FLAG-tagged SMARCD2 proteins (wild type and mutant), expressed in 293T cells, were immunoprecipitated using antibody to FLAG. Coimmunoprecipitation of endogenous SWI/SNF complex components was visualized by immunoblotting of input and immunoprecipitated (IP) samples. Exposure of the membrane analyzed for FLAG shows the presence of immunoprecipitated wild-type SMARCD2, SMARCD2-AII.1a, SMARCD2-AII.1b, SMARCD2-BII.1, and SMARCD2-CII.1 proteins. Images have been cropped; please compare to **Supplementary Data 2**. Replicates: 3 Please also see **Supplementary Table 20** and the **Supplementary Note**.

(ii) SWI/SNF complexes that contain SMARCD2 have a specific role in granulopoiesis, and (iii) mechanistically, SMARCD2 governs granulopoiesis via chromatin accessibility and interaction with CEBPε.

SMARCD2 takes stage-specific roles in granulopoiesis

We continued our studies in mouse cells, taking a systems biology approach. To identify alterations in transcriptional networks controlling differentiation of fetal liver HSCs, we isolated LSK and myeloid progenitor cells (**Fig. 6a**). We profiled the transcriptome by RNA–seq of LSK cells from five *Smarcd2*$^{+/+}$ and nine *Smarcd2*$^{-/-}$ fetal livers. Among a total of 12,362 detected genes, we found 4,290 to be differentially expressed at a false discovery rate (Online Methods) lower than 10%. As expected, *Smarcd2* showed the largest fold change in expression of all genes (**Fig. 6b** and **Supplementary Table 4**). Interestingly, the majority (79%) of the 605 genes with a relatively large difference (fold change > 1.4, FDR < 1%) were upregulated and not downregulated. This had also been reported for embryonic fibroblasts deficient for SMARCB1 (Snf5) and SMARCA4 (Brg1), two other members of the SWI/SNF complex[11].

The upregulated genes were most enriched in categories related to membrane proteins, including major histocompatibility complex (MHC) proteins, immunoglobulin domains, and G-protein-coupled receptors that included signaling pathways related to immunodeficiency and host defense (**Supplementary Fig. 9a** and **Supplementary Tables 5** and **6a**). A subset of CEBPε-dependent genes (**Supplementary Table 6b**) was also deregulated in *Smarcd2*$^{-/-}$ mouse LSK cells (**Supplementary Fig. 9b**,**c** and **Supplementary Table 6c**). Consistent with the finding that CpG island (CGI) promoters can facilitate promiscuous induction without a requirement for SWI/SNF[21], we found that genes containing CGI promoters were significantly under-represented within the group of differentially expressed genes (Fisher's exact test, $P = 0.004$; odds ratio = 0.71). Thus, a considerable fraction of the genes that were found to be differentially expressed are directly dependent on SWI/SNF and/or transcription factors.

We next compared LSK cells with myeloid progenitor cells. During their maturation, neutrophil granulocytes pass through various stages of development. These stages include LSK cells ($CD45^+Lin^-Sca\text{-}1^+c\text{-}Kit^+$), common myeloid progenitors (CMPs) defined as $CD45^+Lin^-Sca\text{-}1^-c\text{-}Kit^+CD34^+CD16/32\ (FCGR)^{int}$, and GMPs defined as $CD45^+Lin^-Sca\text{-}1^-c\text{-}Kit^+CD34^+CD16/32\ (FCGR)^{high}$ or megakaryocyte–erythroid progenitors (MEPs) defined as $CD45^+Lin^-Sca\text{-}1^-c\text{-}Kit^+CD34^-CD16/32\ (FCGR)^{low}$ (**Fig. 6a** and **Supplementary Fig. 10a–c**). In contrast to the LSK, CMP, or MEP compartments, GMP cells were almost absent in *Smarcd2*$^{-/-}$ fetal livers (compare **Supplementary Fig. 10a** and **Supplementary Fig. 10b**). The distinct subpopulations were FACS sorted and analyzed by RNA–seq. As shown in **Figure 6b–e**, SMARCD2 is a transcriptional suppressor in immature cells (LSK and CMP cells), while it adopts the role of a transcriptional activator in further differentiated stages (MEP and GMP cells). Among a total of 15,465 detected genes in CMP cells, we found 852 to be differentially expressed at an FDR lower than 10%; the majority (59%) of the 170 genes with a relatively large difference in expression (fold change > 0.8, FDR < 1%) were upregulated and not downregulated (**Fig. 6c**). In contrast, among a total of 26,595 detected genes in GMP cells, we found 136 to be differentially expressed at an FDR lower than 10%; the majority (70%) of the 56 genes with a relatively large difference in expression (fold change > 1.5, FDR < 1%) were downregulated and not upregulated (**Fig. 6d**). A similar pattern was observed in MEP cells. Among a total of 13,049 detected genes in MEP cells, we found 150 to be differentially expressed at an FDR lower than 10%; again, the majority (84%) of the 37 genes with a relatively large difference in expression (fold change > 1.5, FDR < 1%) were downregulated and not upregulated (**Fig. 6e**). For differentially expressed genes, see **Supplementary Tables 4** and **7–10**; for enriched categories, see results in **Supplementary Tables 5** and **11–14**. A relatively large proportion of CEBPε-dependent genes were deregulated in *Smarcd2*$^{-/-}$ mouse CMP cells (**Fig. 6f**).

SMARCD2 regulates human granule gene expression

The mouse experiments described in the previous subsection suggest that SMARCD2 orchestrates transcriptional networks in early HSCs, but they do not directly explain the striking absence of neutrophil granules and perturbed differentiation of mature neutrophils seen in SMARCD2-deficient human individuals. To shed light on the mechanisms of SMARCD2 in late human neutrophil maturation, we set out to establish a human *in vitro* system to further study the function of SMARCD2. We chose the promyelocytic cell line NB4 that is responsive to retinoic acid signaling and can be differentiated toward mature neutrophil granulocytes *in vitro*. Because our attempts to generate SMARCD2-deficient NB4 cells using CRISPR/Cas9 tools were unsuccessful, we decided to make use of RNA interference to establish cell lines characterized by lower SMARCD2 protein expression. We designed lentiviral short hairpin RNA (shRNA) constructs expressing a *SMARCD2*-specific shRNA and the marker gene GFP, and we transduced and flow sorted NB4 cells for further analysis NB4 cells represent a human promyelocytic leukemia cell line, derived from a patient with a T15/17 translocation.

NB4 cells express *SMARCD1*, *SMARCD2*, *SMARCD3*, and *CEBPE* mRNA/cDNA at detectable levels (**Fig. 7a** and ref. 22). RNA expression of *SMARCD2*, but not of the family members *SMARCD1* and *SMARCD3*, was significantly reduced upon lentiviral expression of shRNA directed against *SMARCD2* (**Fig. 7a**). The expression of *CEBPE* was not affected by *SMARCD2* knockdown and increased after differentiation with all-*trans* retinoic acid (ATRA) (data not shown), as previously described (for example, see ref. 23). Next, we systematically analyzed the RNA expression of genes encoding proteins that are expressed and stored in primary and specific granules in neutrophil granulocytes (**Fig. 7a**). Interestingly, during differentiation with ATRA, transcript levels of the primary granule proteins cathelicidin (CAMP) and α1-antitrypsin (AAT), also known as SERPIN A1, as well as the specific granule proteins matrix metalloproteinase 8 (MMP8), transcobalamin 1 (TCN1), and lactoferrin (LTF), were reduced in SMARCD2-deficient cells.

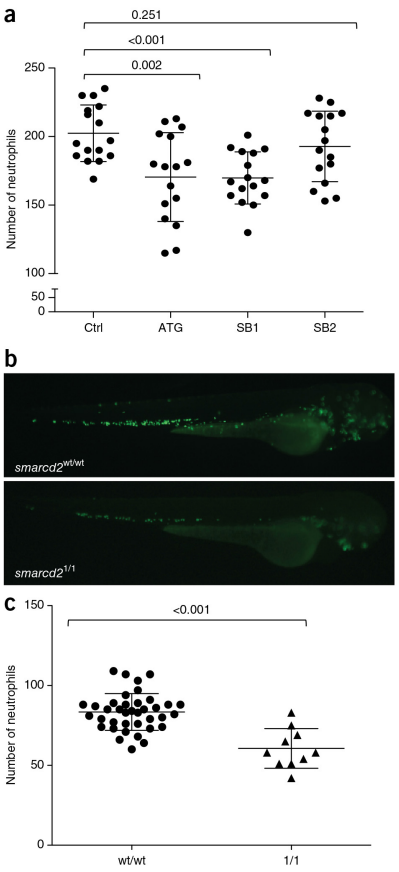

Figure 4 Smarcd2 deficiency in zebrafish. (**a**) Neutrophil numbers in Tg(*lyz:dsRed*)^{nz50} zebrafish at 72 h.p.f. after injection with MOs (control (CRTL) versus translation-start-site blocker (ATG) and splice-site blocker (SB1 and SB2) MOs targeting *smarcd2*). Data represent the numbers of fluorescence-labeled neutrophils per individual fish embryo. Pooled data from two independent MO experiments are shown: CTRL $n = 16$, ATG $n = 16$, SB1 $n = 16$, SB2 $n = 16$ fish. Center values, mean; error bars, s.d. *P* values were calculated by two-tailed unpaired *t* test. Replicates: 2. (**b**) Representative fluorescence images of zebrafish strain Tg(*mpx:EGFP*)^{i114}; *smarcd2*$^{wt/wt}$ (wild type) and *smarcd2*$^{1/1}$ (knockout). Reduced numbers of GFP-expressing neutrophils are observed in *smarcd2*$^{1/1}$ mutant fish embryos. Acquired images: *smarcd2*$^{wt/wt}$ ($n = 37$ images) and *smarcd2*$^{1/1}$ ($n = 10$ images). (**c**) Enumeration of neutrophils in *smarcd2*$^{wt/wt}$ versus *smarcd2*$^{1/1}$ zebrafish. Numbers of fluorescence-labeled neutrophils were evaluated in caudal hematopoietic tissue for individual fish embryos. $n = 38$ *smarcd2*$^{wt/wt}$ and $n = 10$ *smarcd2*$^{1/1}$ fish were evaluated in two independent CRISPR/Cas9 experiments. Center values, mean; error bars, s.d. *P* values were calculated by two-tailed unpaired *t* test. Replicates: 2. Please also see **Supplementary Tables 19** and **20**.

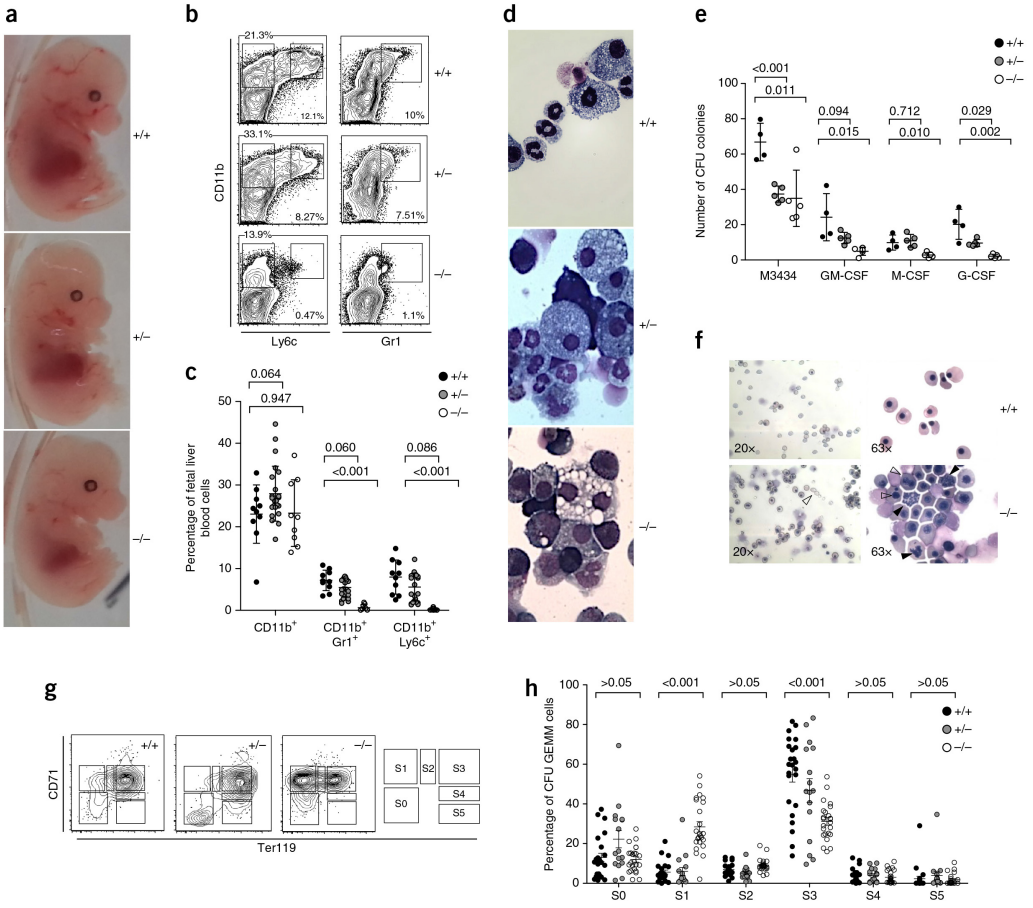

Figure 5 Defective hematopoiesis in *Smarcd2*$^{-/-}$ mouse embryos. (**a**) Morphology of *Smarcd2*$^{+/+}$, *Smarcd2*$^{+/-}$, and *Smarcd2*$^{-/-}$ littermates at 14.5 d.p.c. Images were acquired from four litters: wild type (+/+) $n = 4$, heterozygous (+/–) $n = 10$, knockout (–/–) $n = 9$. Replicates: 2. (**b**) FACS plots of CD11b, Gr1, and Ly6c expression in *Smarcd2*$^{+/+}$, *Smarcd2*$^{+/-}$, and *Smarcd2*$^{-/-}$ embryos. (**c**) Myeloid fetal liver cell quantification. Data were pooled from six litters: wild type $n = 9$, heterozygous $n = 22$, knockout $n = 9$. Center values, mean; error bars, s.d. *P* values were calculated by two-tailed unpaired *t* test. Replicates: 3. (**d**) May–Grünwald and eosin staining of CFU cells derived from *Smarcd2*$^{+/+}$, *Smarcd2*$^{+/-}$, and *Smarcd2*$^{-/-}$ HSCs. Mature mouse neutrophils (with annular-shaped nuclei) are absent in *Smarcd2*$^{-/-}$ colonies. All images were acquired at 63× magnification. Replicates: 2. (**e**) CFUs derived from *Smarcd2*$^{+/+}$, *Smarcd2*$^{+/-}$, and *Smarcd2*$^{-/-}$ LSK cells upon differentiation with cytokines MethoCult M3434 contains SCF, IL-3, IL-6, and EPO. Data were pooled for LSK cells derived from five litters: wild type $n = 4$, heterozygous $n = 5$, knockout $n = 5$. Center values, mean; error bars, s.d. *P* values were calculated by two-tailed unpaired *t* test. Replicates: 3. (**f**) Blood cytology for *Smarcd2*$^{+/+}$ and *Smarcd2*$^{-/-}$ embryos assessed by May–Grünwald and eosin staining at 20× and 63× magnification, showing anisocytosis (unfilled arrowhead, 23×), increased mitosis (black arrowheads, 63×), and multinucleated cells (unfilled arrowheads, 63×) in *Smarcd2*$^{-/-}$ embryos at 14.5 d.p.c. Replicates: 2. (**g**,**h**) FACS analysis of erythropoietic progenitors derived from *Smarcd2*$^{+/+}$, *Smarcd2*$^{+/-}$, and *Smarcd2*$^{-/-}$ CFU GEMM colonies (myeloid colonies containing granulocytes, erythrocytes, monocytes, and megakaryocytes). (**g**) FACS scatterplots and pictogram showing the distribution of CD71/Ter119 staining and erythroid stages (S0–S5). (**h**) Percentage of cells in stages S0–S5; wild type $n = 24$, heterozygous $n = 16$, knockout $n = 24$. Center values, mean; error bars, s.e.m. *P* values were calculated by two-way ANOVA (shown for wild type versus knockout). Replicates: 2.

SMARCD2 mediates transcription via CEBPε

Mice with targeted mutations in *Cebpe*[24] and human patients with rare mutations in *CEBPE*[25] are characterized by specific granule deficiency and susceptibility to bacterial infections. In view of these phenotypic similarities, we asked whether SMARCD2 controls the effects of CEBPε. RNA expression of *CEBPE* was not directly affected in SMARCD2-deficient cells. As an alternative, we hypothesized that SMARCD2 might be relevant for recruiting CEBPε to transcription start sites or open chromatin and thus facilitating expression of CEBPε-dependent genes.

CEBPε binds to the promoters of primary granule genes of *CAMP* and *SERPINA1* (*AAT*) as well as to the promoters of specific granule genes *LTF* (lactoferrin) and *MMP8* (matrix metalloproteinase 8/neutrophil

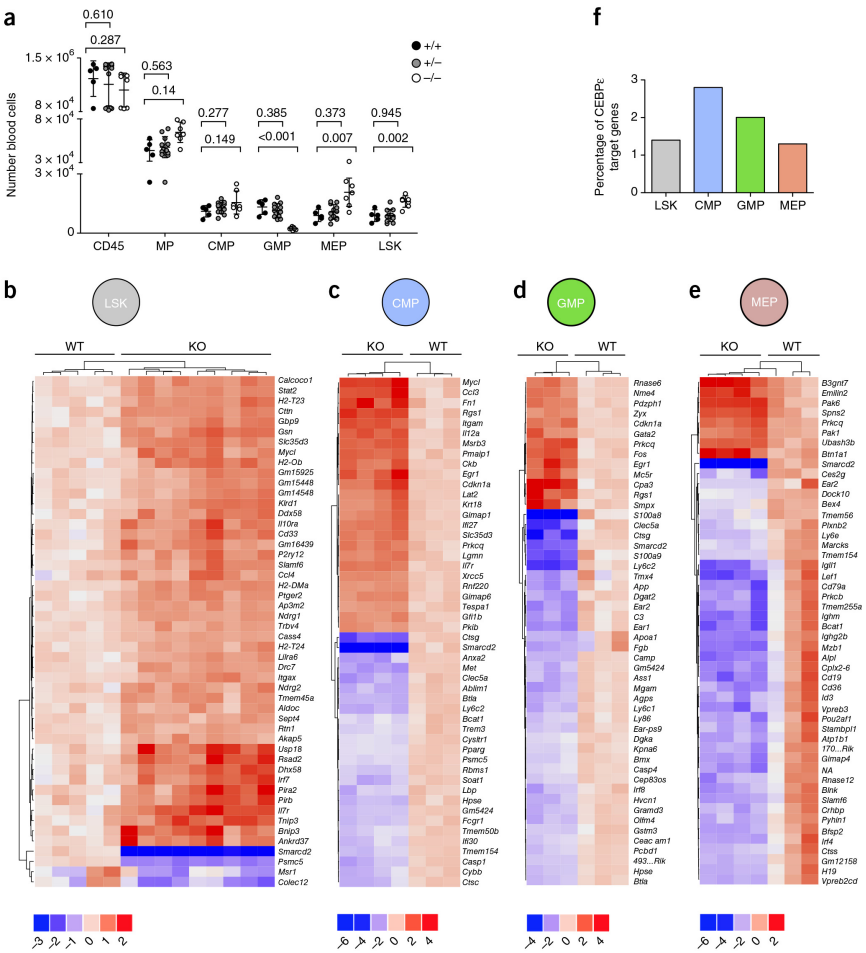

Figure 6 SMARCD2 regulates transcriptional networks in hematopoietic progenitor cells. (**a**) Quantification of fetal myeloid blood cells (CD45$^+$), progenitors (MPs, CMPs, GMPs, MEPs), and LSK stem cells at 14.5 d.p.c. Data were pooled from four litters: wild type (+/+) $n = 4$, heterozygous (+/–) $n = 14$, knockout (–/–) $n = 7$ embryos. Blood cell numbers per embryo are shown. *Smarcd2*$^{-/-}$ fetal hematopoiesis shows more cells in the LSK, MP, CMP, and MEP compartments and fewer cells in the GMP compartment. Center values, mean; error bars, s.d. *P* values were calculated by two-tailed unpaired *t* test with Welsh correction: GMP wild type versus knockout, $P = 0{,}003$. Replicates: 2. (**b**–**e**) RNA–seq analysis of *Smarcd2*$^{+/+}$ and *Smarcd2*$^{-/-}$ fetal liver hematopoietic cell samples at 14–15 d.p.c. Shown are heat maps of the 50 genes with the lowest *P* values. Each column represents a fetal liver sample from one embryo. The color keys below the heat maps show the range of $\log_2$-transformed fold change in expression. (**b**) RNA–seq analysis of *Smarcd2*$^{+/+}$ ($n = 5$) and *Smarcd2*$^{-/-}$ ($n = 9$) fetal liver LSK cell samples at 14–15 d.p.c. (**c**) RNA–seq analysis of *Smarcd2*$^{+/+}$ ($n = 3$) and *Smarcd2*$^{-/-}$ ($n = 4$) fetal liver CMP cell samples at 14–15 d.p.c. (**d**) RNA–seq analysis of *Smarcd2*$^{+/+}$ ($n = 3$) and *Smarcd2*$^{-/-}$ ($n = 3$) fetal liver GMP cell samples at 14–15 d.p.c.; *4930523C07Rik* is abbreviated as *493…Rik*. (**e**) RNA–seq analysis of *Smarcd2*$^{+/+}$ ($n = 3$) and *Smarcd2*$^{-/-}$ ($n = 4$) fetal liver MEP cell samples at 14–15 d.p.c.; *700048020Rik* is abbreviated as *170…Rik*; and *NA* is a gene without a name, described as ENSMUSG00000099065. Replicates: 1. (**f**) Percentage of CEBPε target genes among the differentially expressed genes for the different subpopulations (LSK, CMP, GMP, and MEP); see **Supplementary Table 20**.

collagenase) (**Fig. 7b** and **Supplementary Fig. 11a–c**). shRNA-mediated knockdown of SMARCD2 significantly impaired binding of CEBPε (CTRL versus shRNA 1, $P = 0.004$; CTRL versus shRNA 2, $P = 0.011$, two-tailed unpaired *t* tests) and BRG1 (CTRL versus shRNA 1, $P = 0.036$; CTRL versus shRNA 2, $P = 0.031$, two-tailed unpaired *t* tests) to the *LTF* promoter (**Fig. 7b**).

To address the question of whether SMARCD2 interacts directly with CEBPε, we performed immunoprecipitation studies in 293T cells engineered to express HA-tagged CEBPε and FLAG-tagged SMARCD2. As shown in **Figure 8a**,**b** (**Supplementary Data 5**), immunoprecipitation studies confirmed a physical interaction between both proteins. The interaction of the endogenous proteins

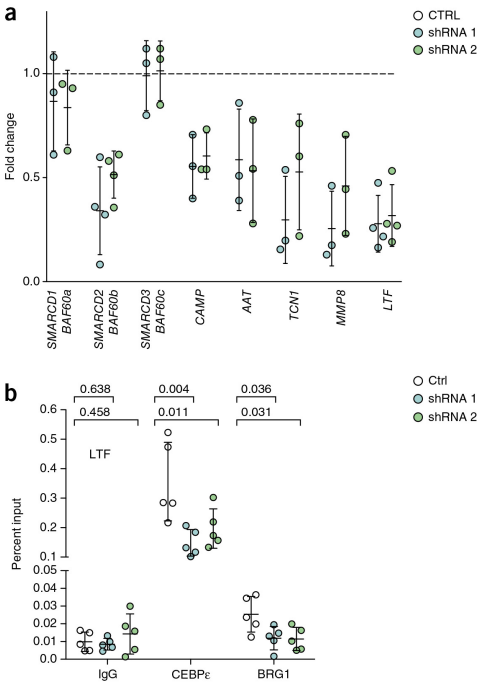

Figure 7 SMARCD2, granule formation, and transcriptional regulation. (**a**) The relative mRNA expression of SMARCD genes, primary granule genes (*CAMP*, *AAT*), and secondary granule genes (*MMP8*, *TCN1*, *LTF*) is shown in human NB4 AML cells upon shRNA-mediated knockdown of *SMARCD2*. Data points show relative expression in cells treated with shRNA 1 or shRNA 2 versus control (CTRL) in three independent experiments for *SMARCD1*, *SMARCD3*, *CAMP*, *AAT*, and *MMP8* and in four independent experiments for *SMARCD2* and *LTF*. The expression levels of *SMARCD1*, *SMARCD2*, and *SMARCD3* were determined in undifferentiated cells, and granule gene expression was measured in ATRA-differentiated NB4 cells. Center values, mean, error bars, s.d. Replicates: 3 or 4. (**b**) Chromatin immunoprecipitation (ChIP) in ATRA-differentiated NB4 cells. Shown is the percent input to describe the enrichment of CEBPε and BRG1 at the *LTF* promoter (Online Methods and **Supplementary Note**). CEBPε binds to the *LTF* promoter, and binding is significantly reduced in cells transduced with shRNA 1) or shRNA 2. BRG1 binds to the *LTF* promoter, and binding is significantly reduced in cells transduced with shRNA 1 or shRNA 2. Data from two experiments with a total of $n = 5$ independent NB4 cell cultures are shown; in total, three experiments were performed. Center values, mean; error bars, s.d. *P* values were calculated by two-tailed unpaired *t* test. Replicates: 3.

was demonstrated by immunoprecipitation with antibody to CEBPε and co-precipitation of SMARCD2 (**Supplementary Fig. 12a–j**).

A functional link between SMARCD2 and CEBPε is further supported by our finding, that documented CEPBε-dependent genes are deregulated in the absence of SMARCD2 in human (**Fig. 8c**, **Supplementary Fig. 13**, and **Supplementary Table 6d**) and mouse (**Fig. 6f** and **Supplementary Fig. 9b**,**c**) hematopoietic cells. The proportion of CEBPε-dependent genes affected by *Smarcd2*$^{-/-}$ was highest in the CMP compartment than in LSK, GMP, or MEP cells (**Fig. 6f**). This is in keeping with an established role for CEBPε in intermediate stages of differentiation[26].

SMARCD2 modulates chromatin accessibility

The consequences of defective nucleosome positioning due to dysfunctional SWI/SNF molecules may be complex. We attempted to interrogate the effects of SMARCD2 deficiency on global chromatin accessibility using the assay for transposase accessible chromatin with high-throughput sequencing (ATAC–seq) (**Fig. 8d–g**, **Supplementary Fig. 14**, and **Supplementary Tables 15** and **16**). We compared all genes that showed differential chromatin accessibility in *SMARCD2*-knockdown cells (**Supplementary Fig. 14**) with differentially expressed genes determined by RNA–seq studies both in undifferentiated (**Fig. 8d**,**e**) and ATRA-differentiated (**Fig. 8f**,**g**) promyelocytic leukemia cell line NB4. A specific subset of genes was found to be deregulated in both assays, ATAC–seq and RNA–seq. These genes are involved in vesicular trafficking, migration, and signaling. The specificity of this observation is in line with findings in mouse embryonal fibroblasts[11] and yeast[27], which show only a moderate correlation of SWI/SNF-governed chromatin accessibility and transcription in response to knockout of single SWI/SNF units. To examine the role of the discovered gene sets, further studies are needed. Differentially expressed genes in both the mouse transcriptome (**Supplementary Tables 4** and **7–10**) and the human transcriptome (**Supplementary Tables 15** and **16**) clustered significantly in signaling pathways relevant to immune system functions (**Supplementary Fig. 9a** and **Supplementary Table 6a** (mouse); **Supplementary Fig. 13a**,**b** and **Supplementary Table 6e**,**f** (human)). Taken together, DNA accessibility studies, transcriptome studies, and protein–protein interaction studies suggest that SMARCD2 has a direct role to remodel the chromatin and to mediate downstream effects partly by interaction with the myeloid transcription factor CEBPε.

DISCUSSION

In this study, we identify patients with SMARCD2 deficiency, characterized by hematopoietic defects and developmental aberrations. On the basis of our comparative studies, also involving zebrafish and mice, we conclude that SMARCD2 orchestrates HSC differentiation.

Clinically, the phenotype of SMARCD2-deficient neutrophil granulocytes is reminiscent of the phenotype of specific granule deficiency caused by mutations in *CEBPE*[28]. CEBPE-deficient neutrophil granulocytes show bilobed nuclei[29,30] with nuclear blebs and pockets[31] or pseudo-Pelger–Huët-type bilobed nuclei[32] in conjunction with a lack of specific granules[30].

Both SMARCD2 deficiency and CEBPε deficiency may be associated with decreased counts of peripheral neutrophil granulocytes, yet the capacity to mobilize neutrophils from the bone marrow remains intact.

All patients with SMARCD2 deficiency had evidence of myelodysplasia and blast excess, a feature not typically seen in CEBPε deficiency. However, allelic loss of *CEBPE* has been detected in 4 of 20 cases of evolving myelodysplastic syndromes (MDS)[33], and myelodysplasia is also a feature in *Cebpe*$^{-/-}$ mice[34,35]. CEPBε controls terminal differentiation of neutrophil granulocytes, whereas SMARCD2 appears to also control early stages of HSC differentiation, as documented by imbalances in the transcriptome in hematopoietic progenitor cells. Even though the effects of SMARCD2 deficiency on late neutrophil granulocytes are mediated, at least in part, by CEBPε, there are other less well-defined modes of action of SMARCD2.

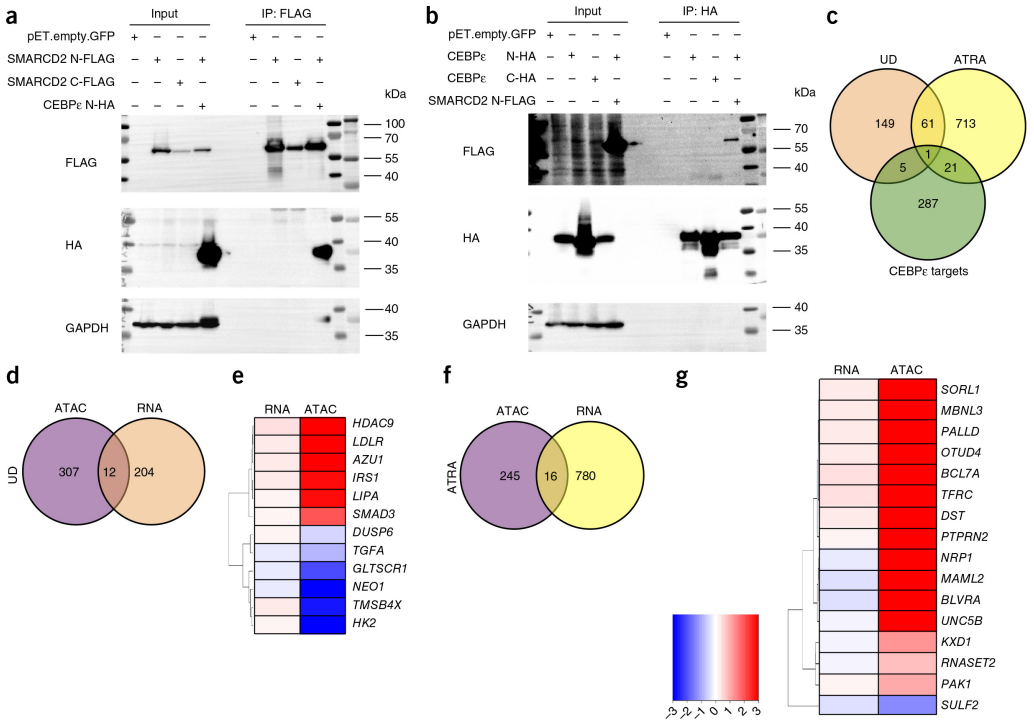

Figure 8 SMARCD2 transcriptional regulation. (**a**,**b**) Coimmunoprecipitation of FLAG-tagged SMARCD2 and HA-tagged CEBPε in 293T cells. (**a**) Immunoblot detection of immunoprecipitated FLAG-tagged SMARCD2 and coimmunoprecipitated HA-tagged CEBPε. (**b**) Immunoblot detection of immunoprecipitated HA-tagged CEBPε and coimmunoprecipitated FLAG-tagged SMARCD2. Images have been cropped; please compare to **Supplementary Data 5**. GAPDH is probed as a control. Replicates: 3. (**c**) Venn diagram showing the intersection of differentially expressed genes in undifferentiated NB4 cells (UD) and ATRA-differentiated NB4 cells (ATRA) with and without *SMARCD2* knockdown in comparison to CEBPε target genes. For a list of intersections, see **Supplementary Table 4**. (**d**–**g**) Representation of differentially expressed genes in *SMARCD2*-knockdown versus control NB4 cells. (**d**) Undifferentiated NB4 cells (*SMARCD2* knockdown versus control) analyzed by ATAC–seq and RNA–seq. An overlapping set of 12 genes was deregulated in both assays. (**e**) Heat map showing the relative expression (log_2-transformed fold change) of the genes identified in undifferentiated cells in both assays. The heat map legend is the same as in **g**. NB4 cells were transduced with shRNA 1, shRNA 2, or CTRL, mock treated with DMSO, and sequenced twice (twice for RNA–seq and twice for ATAC–seq). Technical replicates: 2. (**f**) ATRA-differentiated NB4 cells (*SMARCD2* knockdown versus control) analyzed by ATAC–seq and RNA–seq. A total of 16 genes were deregulated in both assays. (**g**) Heat map showing the relative expression (log_2-transformed fold change) of the genes identified in ATRA-differentiated cells in both assays. NB4 cells were transduced with shRNA 1, shRNA 2, or CTRL, treated with ATRA, and sequenced twice (twice for RNA–seq and twice for ATAC–seq). Technical replicates: 2.

The role of the SWI/SNF complex and SMARCD2 in leukemogenesis is intriguing. Previous studies had shown that the SWI/SNF complex controls maintenance of myeloid leukemia cells[13,36]. Specifically, knockdown of *SMARCD2* in human *MLL*-rearranged leukemia cells resulted in reduced self-renewal capacity[37]. Furthermore, mutational analysis of acute promyelocyte leukemia samples identified somatic loss-of-function mutations in *ARID1B* and *ARID1A*, encoding two components of the SWI/SNF complex[38].

The companion paper by Priam *et al.*[39] documents a specific and non-redundant role for mouse SMARCD2 in controlling granulocytopoiesis. Similar to our patients with SMARCD2 deficiency, adult mice with SMARCD2-deficient hematopoietic cells develop myelodysplasia and blast excess. It remains to be determined whether this proliferative disorder is indeed clonal.

Interestingly, our transcriptome studies in defined subpopulations of hematopoietic progenitor cells showed an evolving pattern, consistent with the concept that SMARCD2 acts as a transcriptional suppressor in early HSCs and as a transcriptional activator in later stages. We interrogated the genomic landscape in SMARCD2-deficient leukemia cells but could only identify a relatively small number of overlapping genes in ATAC–seq and corresponding RNA transcripts. This may be due to intrinsic limitations of the model system.

The complexity of SMARCD2-dependent transcriptional regulation in early and late hematopoiesis prohibits a simple mechanistic explanation of the leukemogenic disposition. Our studies in human cells and studies in mouse cells[39] documented that SMARCD2 is essential for CEBPε and SWI/SNF recruitment to the promoter of neutrophilic granule genes. Further studies are however needed to shed light on the critical role of SMARCD2 in early stages of HSC differentiation.

Systematic studies in patients with rare disorders may highlight the critical role of defined genes and pathways controlling differentiation

and function of the blood and immune system. Our clinical and molecular studies in SMARCD2-deficient patients provide an example and reveal SMARCD2 as a key factor controlling transcriptional networks governing stem cell differentiation and lineage specification in the hematopoietic system.

URLs. CHOPCHOP tool, https://chopchop.rc.fas.harvard.edu/; Cytoscape, http://wiki.reactome.org/index.php?title=ReactomeFIViz&oldid=7168; Venny, http://bioinfogp.cnb.csic.es/tools/venny/index.html; KOMP repository, http://www.komp.org/.

METHODS

Methods, including statements of data availability and any associated accession codes and references, are available in the online version of the paper.

Note: Any Supplementary Information and Source Data files are available in the online version of the paper.

ACKNOWLEDGMENTS

We thank all medical and laboratory staff members involved in taking care of patients and performing scientific experiments, in particular R. Conca (FACS sorting), J. Hinke (genomic facility), and P. Robinson and S. Mundlos for next-generation sequencing expertise. We thank S. Hollizeck, D. Kotlarz, M. Lyszkiewicz, and N. Zietara for critical scientific discussion. We thank B. Zeller, R. Abdennour, and H. Nordgarden for clinical care of patients and A. Tierens for initial FACS and histological workup. We thank J. Lessard (IRIC, Université de Montréal) for providing antibodies to SMARCD1, SMARCD2, and SMARCD3 and for critical discussion.

The study has been supported by the European Research Council (ERC Advanced Grant 'Explore'), the Else Kröner-Fresenius-Stiftung, the DZIF (German Center for Infection Research), the Deutsche Forschungsgemeinschaft (Gottfried Wilhelm Leibniz Program), the German PID-NET (BMBF), and the Care-for-Rare Foundation.

V.P. was supported by a Monash International Postgraduate Research Scholarship (MIPRS) and a Monash Graduate Scholarship (MGS). G.L. was supported by the NHMRC (1069284, 1044754). The Australian Regenerative Medicine Institute (ARMI) is supported by grants from the State Government of Victoria and the Australian Government. This research was supported in part by the Intramural Research Program of the US National Institutes of Health, NLM. W.E. and C.Z. were supported by the Deutsche Forschungsgemeinschaft (DFG) through LMUexcellent and SFB1243 (subproject A14). J.G. was supported by the Bundesministerium für Bildung und Forschung, Juniorverbund in der Sytemmedizin 'mitOmics' grant FKZ 01ZX1405A, and C.M. is supported by EU Horizon2020 Collaborative Research Project SOUND (633974).

AUTHOR CONTRIBUTIONS

M.W. designed, performed, and interpreted experiments and wrote and edited the manuscript. D.P. performed ATAC–seq and RNA–seq, Y.F., E.B., T.R., and M.R. were involved in genomic and biochemical analyses, J.P. led the computational biology efforts, C.M. and J.G. analyzed ATAC–seq and RNA–seq data, and C.Z. and W.E. performed mouse RNA–seq and digital gene expression analysis. A.S.-P., P.D.A., and M.R.A. provided clinical care for patients, V.P. and G.J.L. generated and analyzed zebrafish models, and P.M.K. analyzed whole-exome sequencing in initial patients. M.D., M.R.S., and E.W. generated mice. H.-P.H. performed immunohistochemistry analysis of bone marrow biopsies, H.S. provided expert clinical genetic consulting, and A.A.S. guided bioinformatics studies and helped write and edit the manuscript. C.K. designed and guided the study, supervised M.W., provided laboratory resources, and wrote the manuscript.

COMPETING FINANCIAL INTERESTS

The authors declare no competing financial interests.

1. Krumsiek, J., Marr, C., Schroeder, T. & Theis, F.J. Hierarchical differentiation of myeloid progenitors is encoded in the transcription factor network. *PLoS One* **6**, e22649 (2011).
2. Orkin, S.H. & Zon, L.I. Hematopoiesis: an evolving paradigm for stem cell biology. *Cell* **132**, 631–644 (2008).
3. Krosl, J. *et al.* A mutant allele of the Swi/Snf member BAF250a determines the pool size of fetal liver hemopoietic stem cell populations. *Blood* **116**, 1678–1684 (2010).
4. Friedman, A.D. Transcriptional control of granulocyte and monocyte development. *Oncogene* **26**, 6816–6828 (2007).
5. Griffin, C.T., Brennan, J. & Magnuson, T. The chromatin-remodeling enzyme BRG1 plays an essential role in primitive erythropoiesis and vascular development. *Development* **135**, 493–500 (2008).
6. Huang, H.T. *et al.* A network of epigenetic regulators guides developmental haematopoiesis *in vivo*. *Nat. Cell Biol.* **15**, 1516–1525 (2013).
7. Álvarez-Errico, D., Vento-Tormo, R., Sieweke, M. & Ballestar, E. Epigenetic control of myeloid cell differentiation, identity and function. *Nat. Rev. Immunol.* **15**, 7–17 (2015).
8. Cedar, H. & Bergman, Y. Epigenetics of haematopoietic cell development. *Nat. Rev. Immunol.* **11**, 478–488 (2011).
9. Cairns, B.R. The logic of chromatin architecture and remodelling at promoters. *Nature* **461**, 193–198 (2009).
10. de la Serna, I.L., Ohkawa, Y. & Imbalzano, A.N. Chromatin remodelling in mammalian differentiation: lessons from ATP-dependent remodellers. *Nat. Rev. Genet.* **7**, 461–473 (2006).
11. Tolstorukov, M.Y. *et al.* Swi/Snf chromatin remodeling/tumor suppressor complex establishes nucleosome occupancy at target promoters. *Proc. Natl. Acad. Sci. USA* **110**, 10165–10170 (2013).
12. Wilson, B.G. & Roberts, C.W. SWI/SNF nucleosome remodellers and cancer. *Nat. Rev. Cancer* **11**, 481–492 (2011).
13. Buscarlet, M. *et al.* Essential role of BRG, the ATPase subunit of BAF chromatin remodeling complexes, in leukemia maintenance. *Blood* **123**, 1720–1728 (2014).
14. Jojic, V. *et al.* Identification of transcriptional regulators in the mouse immune system. *Nat. Immunol.* **14**, 633–643 (2013).
15. Alajem, A. *et al.* Differential association of chromatin proteins identifies BAF60a/SMARCD1 as a regulator of embryonic stem cell differentiation. *Cell Rep.* **10**, 2019–2031 (2015).
16. Lickert, H. *et al.* Baf60c is essential for function of BAF chromatin remodelling complexes in heart development. *Nature* **432**, 107–112 (2004).
17. Hall, C., Flores, M.V., Storm, T., Crosier, K. & Crosier, P. The zebrafish lysozyme C promoter drives myeloid-specific expression in transgenic fish. *BMC Dev. Biol.* **7**, 42 (2007).
18. Liongue, C., Hall, C.J., O'Connell, B.A., Crosier, P. & Ward, A.C. Zebrafish granulocyte colony-stimulating factor receptor signaling promotes myelopoiesis and myeloid cell migration. *Blood* **113**, 2535–2546 (2009).
19. Renshaw, S.A. *et al.* A transgenic zebrafish model of neutrophilic inflammation. *Blood* **108**, 3976–3978 (2006).
20. Koulnis, M. *et al.* Identification and analysis of mouse erythroid progenitors using the CD71/TER119 flow-cytometric assay. *J. Vis. Exp.* **5**, 2809 (2011).
21. Ramirez-Carrozzi, V.R. *et al.* A unifying model for the selective regulation of inducible transcription by CpG islands and nucleosome remodeling. *Cell* **138**, 114–128 (2009).
22. Iriyama, N. *et al.* Enhancement of differentiation induction and upregulation of CCAAT/enhancer-binding proteins and PU.1 in NB4 cells treated with combination of ATRA and valproic acid. *Int. J. Oncol.* **44**, 865–873 (2014).
23. Tanaka, M., Gombart, A.F., Koeffler, H.P. & Shiohara, M. Expression of bactericidal/permeability-increasing protein requires C/EBPε. *Int. J. Hematol.* **85**, 304–311 (2007).
24. Lekstrom-Himes, J. & Xanthopoulos, K.G. CCAAT/enhancer binding protein ε is critical for effective neutrophil-mediated response to inflammatory challenge. *Blood* **93**, 3096–3105 (1999).
25. Lekstrom-Himes, J.A., Dorman, S.E., Kopar, P., Holland, S.M. & Gallin, J.I. Neutrophil-specific granule deficiency results from a novel mutation with loss of function of the transcription factor CCAAT/enhancer binding protein ε. *J. Exp. Med.* **189**, 1847–1852 (1999).
26. Hu, H. *et al.* Maturity-dependent fractionation of neutrophil progenitors: a new method to examine *in vivo* expression profiles of differentiation-regulating genes. *Exp. Hematol.* **40**, 675–681 (2012).
27. Gkikopoulos, T. *et al.* A role for Snf2-related nucleosome-spacing enzymes in genome-wide nucleosome organization. *Science* **333**, 1758–1760 (2011).
28. Wada, T. *et al.* A novel in-frame deletion in the leucine zipper domain of C/EBPε leads to neutrophil-specific granule deficiency. *J. Immunol.* **195**, 80–86 (2015).
29. Gallin, J.I. *et al.* Human neutrophil-specific granule deficiency: a model to assess the role of neutrophil-specific granules in the evolution of the inflammatory response. *Blood* **59**, 1317–1329 (1982).
30. Breton-Gorius, J., Mason, D.Y., Buriot, D., Vilde, J.L. & Griscelli, C. Lactoferrin deficiency as a consequence of a lack of specific granules in neutrophils from a patient with recurrent infections. Detection by immunoperoxidase staining for lactoferrin and cytochemical electron microscopy. *Am. J. Pathol.* **99**, 413–428 (1980).
31. Komiyama, A., Morosawa, H., Nakahata, T., Miyagawa, Y. & Akabane, T. Abnormal neutrophil maturation in a neutrophil defect with morphologic abnormality and impaired function. *J. Pediatr.* **94**, 19–25 (1979).
32. Khanna-Gupta, A. *et al.* Growth factor independence-1 (Gfi-1) plays a role in mediating specific granule deficiency (SGD) in a patient lacking a gene-inactivating mutation in the C/EBPε gene. *Blood* **109**, 4181–4190 (2007).
33. Koike, M. *et al.* C/EBP-ε: chromosomal mapping and mutational analysis of the gene in leukemia and preleukemia. *Leuk. Res.* **21**, 833–839 (1997).

34. Verbeek, W., Wachter, M., Lekstrom-Himes, J. & Koeffler, H.P. C/EBPε$^{-/-}$ mice: increased rate of myeloid proliferation and apoptosis. *Leukemia* **15**, 103–111 (2001).
35. Yamanaka, R. *et al.* Impaired granulopoiesis, myelodysplasia, and early lethality in CCAAT/enhancer binding protein ε–deficient mice. *Proc. Natl. Acad. Sci. USA* **94**, 13187–13192 (1997).
36. Shi, J. *et al.* Role of SWI/SNF in acute leukemia maintenance and enhancer-mediated *Myc* regulation. *Genes Dev.* **27**, 2648–2662 (2013).
37. Cruickshank, V.A. *et al.* SWI/SNF subunits SMARCA4, SMARCD2 and DPF2 collaborate in *MLL*-rearranged leukaemia maintenance. *PLoS One* **10**, e0142806 (2015).
38. Madan, V. *et al.* Comprehensive mutational analysis of primary and relapse acute promyelocytic leukemia. *Leukemia* **30**, 1672–1681 (2016).
39. Priam, P. *et al.* SMARCD2 subunit of the SWI/SNF chromatin-remodeling complex mediates granulopoiesis through a CEBPε- dependent mechanism. *Nat. Genet.* http://dx.doi.org/10.1038/ng.3812 (2017).

7. Manuscript # 3

Gastroenterology 2014;146:1028–1039

Mutations in Tetratricopeptide Repeat Domain 7A Result in a Severe Form of Very Early Onset Inflammatory Bowel Disease

Yaron Avitzur,[1,2,3,*] Conghui Guo,[2,*] Lucas A. Mastropaolo,[2] Ehsan Bahrami,[4] Hannah Chen,[5] Zhen Zhao,[2] Abdul Elkadri,[2,3,6] Sandeep Dhillon,[2] Ryan Murchie,[2] Ramzi Fattouh,[2] Hien Huynh,[7] Jennifer L. Walker,[8] Paul W. Wales,[1] Ernest Cutz,[9] Yoichi Kakuta,[10] Joel Dudley,[11] Jochen Kammermeier,[12] Fiona Powrie,[13] Neil Shah,[12] Christoph Walz,[14] Michaela Nathrath,[15] Daniel Kotlarz,[4] Jacek Puchaka,[4] Jonathan R. Krieger,[2] Tomas Racek,[4] Thomas Kirchner,[14] Thomas D. Walters,[2,3] John H. Brumell,[2,3,6] Anne M. Griffiths,[2,3] Nima Rezaei,[16,17] Parisa Rashtian,[18] Mehri Najafi,[18] Maryam Monajemzadeh,[19] Stephen Pelsue,[8] Dermot P. B. McGovern,[10] Holm H. Uhlig,[5] Eric Schadt,[11] Christoph Klein,[4,§] Scott B. Snapper,[20,21,§] and Aleixo M. Muise[2,3,6,§]

[1]Group for Improvement of Intestinal Function and Treatment (GIFT), Hospital for Sick Children, Toronto, Ontario, Canada; [2]SickKids Inflammatory Bowel Disease Center and Cell Biology Program, Research Institute, Hospital for Sick Children, Toronto, Ontario, Canada; [3]Division of Gastroenterology, Hepatology, and Nutrition, Department of Pediatrics, University of Toronto, Hospital for Sick Children, Toronto, Ontario, Canada; [4]Department of Pediatrics, Dr von Hauner Children's Hospital, Ludwig-Maximilians-University, Munich, Germany; [5]Translational Gastroenterology Unit and Paediatric Gastroenterology, University of Oxford, Oxford, UK; [6]Institute of Medical Science, University of Toronto, Toronto, Ontario, Canada; [7]Division of Pediatric Gastroenterology, Stollery Children's Hospital, Edmonton, Ontario, Canada; [8]Department of Immunology and Molecular Biology, University of Southern Maine, Portland, Maine; [9]Division of Pathology, The Hospital for Sick Children, Toronto, Ontario, Canada; [10]F. Widjaja Foundation Inflammatory Bowel Disease Center and Immunobiology Research Institute at Cedars-Sinai Medical Center, Los Angeles, California; [11]Icahn Institute for Genomics and Multiscale Biology, Department of Genetics and Genomics Sciences at Mount Sinai, New York, New York; [12]Gastroenterology Department, Great Ormond Street Hospital, London, UK; [13]Translational Gastroenterology Unit, Nuffield Department Clinical Medicine-Experimental Medicine Division, University of Oxford, John Radcliffe Hospital, Oxford, UK; [14]Institute for Pathology, Ludwig-Maximilians University, Munich, Germany; [15]Department of Pediatric Oncology, Kassel and CCG Osteosarcoma, Helmholtz Center Munich, Munich, Germany; [16]Research Center for Immunodeficiencies, Children's Medical Center, Tehran University of Medical Sciences, Tehran, Iran; [17]Molecular Immunology Research Center and Department of Immunology, School of Medicine, Tehran University of Medical Sciences, Tehran, Iran; [18]Department of Pediatric Gastroenterology, Children's Medical Center, Tehran University of Medical Sciences, Tehran, Iran; [19]Department of Pathology, Children's Medical Center, Tehran University of Medical Sciences, Tehran, Iran; [20]Division of Pediatric Gastroenterology, Hepatology, and Nutrition, Department of Medicine, Children's Hospital Boston, Massachusetts; and [21]Division of Gastroenterology and Hepatology, Brigham & Women's Hospital, Department of Medicine, Harvard Medical School, Boston, Massachusetts

See Covering the Cover synopsis on page 876.

BACKGROUND & AIMS: Very early onset inflammatory bowel diseases (VEOIBD), including infant disorders, are a diverse group of diseases found in children younger than 6 years of age. They have been associated with several gene variants. Our aim was to identify the genes that cause VEOIBD. **METHODS:** We performed whole exome sequencing of DNA from 1 infant with severe enterocolitis and her parents. Candidate gene mutations were validated in 40 pediatric patients and functional studies were carried out using intestinal samples and human intestinal cell lines. **RESULTS:** We identified compound heterozygote mutations in the Tetratricopeptide repeat domain 7 (*TTC7A*) gene in an infant from non-consanguineous parents with severe exfoliative apoptotic enterocolitis; we also detected *TTC7A* mutations in 2 unrelated families, each with 2 affected siblings. TTC7A interacts with EFR3 homolog B to regulate phosphatidylinositol 4-kinase at the plasma membrane. Functional studies demonstrated that TTC7A is expressed in human enterocytes. The mutations we identified in *TTC7A* result in either mislocalization or reduced expression of TTC7A. Phosphatidylinositol 4-kinase was found to co-immunoprecipitate with TTC7A; the identified TTC7A mutations reduced this binding. Knockdown of TTC7A in human intestinal-like cell lines reduced their adhesion, increased apoptosis, and decreased production of phosphatidylinositol 4-phosphate. **CONCLUSIONS:** In a genetic analysis, we identified loss of function mutations in *TTC7A* in 5 infants with VEOIBD.

*Authors share co-first authorship; §Authors share co-senior authorship.

Abbreviations used in this paper: co-IP, co-immunoprecipitate; EFR3B, EFR3 homolog B; MIA, multiple intestinal atresia; PI4KIIIα, phosphatidylinositol 4-kinase IIIα; SCID, severe combined immunodeficiency; shRNA, short hairpin RNA; TPR, tetratricopeptide repeat; TTC7A, tetratricopeptide repeat domain 7; VEOIBD, very early onset inflammatory bowel diseases; WT, wild type.

0016-5085/$36.00
http://dx.doi.org/10.1053/j.gastro.2014.01.015

Functional studies demonstrated that the mutations cause defects in enterocytes and T cells that lead to severe apoptotic enterocolitis. Defects in the phosphatidylinositol 4-kinase–TTC7A–EFR3 homolog B pathway are involved in the pathogenesis of VEOIBD.

Keywords: IBD; Intestinal Atresia; Autoimmunity; Intestine.

Very early onset inflammatory bowel diseases (VEOIBD), including forms of infantile disease, are a diverse group of diseases that are diagnosed before 6 years of age.[1] In contrast to adult-onset IBD, VEOIBD frequently encompasses a unique clinical presentation with severe, colonic disease that often has a poor response to standard therapies, including biologic agents.[2,3] Recently, several groups, including our own, demonstrated that mutations in *IL10RA/B* genes[4] cause a severe form of VEOIBD, with symptoms consistently developing in infancy.[5] Subsequently, causative variants in *IL10*,[6] *XIAP*,[7] *ADAM17*,[8] and *NCF4*,[9] and association variants in the nicotinamide adenine dinucleotide phosphate oxidase genes *NCF2/RAC2*[10] were identified in VEOIBD patients, suggesting that severe infantile colitis frequently starting immediately after birth might represent a group of heterogeneous monogenetic diseases.

Recently, mutations in the tetratricopeptide repeat domain 7 (*TTC7A*) gene were found to cause multiple intestinal atresia (MIA) with severe combined immunodeficiency (SCID), although no details about the intestinal phenotype or function of the *TTC7A* gene were provided.[11,12] In this report, we describe novel human mutations in the *TTC7A* gene (we termed *TTC7A deficiency*) identified independently by whole exome sequencing that result in severe infantile apoptotic enterocolitis with and without MIA and define the intestinal defects associated with this novel form of VEOIBD.

Materials and Methods

Whole Exome Sequencing

Genetic studies were carried out with approval from the research ethics board at the Hospital for Sick Children, University of Oxford, Cedars-Sinai Medical Center, and Dr von Hauner Children's Hospital, LMU Munich. In the index case, whole exome sequencing was performed using the SureSelect Human All Exon 50 Mb kit (Agilent, Santa Clara, CA) with high-throughput sequencing conducted using the Solid 4 System at The Center for Applied Genomics through the Hospital for Sick Children (Toronto, ON) on the complete parent–child trio set. Sanger sequencing was used to verify variant genotypes in the index patient and her family, and 40 infantile patients from the institutions named here were screened for *TTC7A* mutations.

Histologic methods are presented in the Supplementary Material.

Tandem Mass Spectrometry

Detailed methods are presented in the Supplementary Materials. Briefly, to identify potential interactors of TTC7A, M2 anti-FLAG-agarose FLAG-agarose FLAG-tagged wild type (WT), E71K, or Q526X TTC7A were transiently overexpressed in HEK293T, immunoprecipitated with FLAG-agarose, and bound proteins were trypsin digested and analyzed by tandem mass spectrometry as described previously.[13]

Knockdown of Endogenous TTC7A by Short Hairpin RNA

GIPZ human TTC7A short hairpin RNA (shRNA) (green fluorescent protein tagged) targeting coding regions and green fluorescent protein tagged control shRNA (Thermo Scientific, Logan, UT) were transfected into Henle-407 cells with Lipofectamine 2000 (Life Technologies, Carlsbad, CA). Detailed methods are provided in the Supplementary Materials.

Apoptosis Analysis

Confluent cells were starved for indicated time points. Apoptosis was assessed by both measured caspase-3 using Western blotting and cytoplasmic DNA fragments using flow cytometric analysis of Annexin V. Cells were stained with Annexin V-phycoerythrin and 7-aminoactinomycin D (BD Biosciences, San Jose, CA) according to manufacturer's instructions, and samples were run on a BD LSR II analyzer. Apoptotic cells were identified as Annexin V^+ 7-aminoactinomycin D cells.

Cell Adhesion Assay

To evaluate cellular adhesion, approximately 5×10^4 cells were seeded on 96-well plates precoated with fibronectin (20 μg/mL; Sigma-Aldrich, St Louis, MO), collagen type I (50 μg/mL; Life Technologies), or bovine serum albumin (5% in phosphate-buffered saline; Sigma) for 60 minutes at 37°C. The wells were subsequently washed with phosphate-buffered saline twice to remove nonadherent cells. After fixation with 4% paraformaldehyde, attached cells were visualized by staining with 1% crystal violet dissolved in 33% acetic acid and were quantified by measuring the absorbance at 570 nm on a Versamax microplate reader (Molecular Devices, Sunnyvale, CA).

Constructs, Western Blot, Cell Culture, and Immunoprecipitation

Details of constructs, antibodies, and methods used can be found in the Supplementary Materials.

Statistical Analysis

Data are presented as mean ± SD. Experiments were performed with a minimum of 3 replications. Statistical significance between groups was established at $P < .05$ using a 2-tailed Student t test. P values are indicated in the figure legends and text.

Results

Identification of Apoptotic Enterocolitis in a VEOIBD Patient

In Family 1 (index case), a female patient born at term to a Caucasian mother and Sudanese father presented with

high-output secretory diarrhea and hematochezia that started almost immediately after birth, requiring total parenteral nutrition. Colonoscopy demonstrated chronic inflammation with severe friability, exfoliative mucosal changes, and sloughed mucosa within the colonic lumen (Figure 1*A*). Biopsies taken from the duodenum showed villous atrophy and the duodenum and colon showed glandular dropout with crypt apoptosis and exploding crypts (Figure 1*B* and *C*). The severity of the epithelial injury was strikingly reminiscent of acute gastrointestinal graft-vs-host disease and intestine allograft rejection. There was no evidence of perianal disease or dermatological disease. The patient had clinical features of immunodeficiency, including lymphopenia and hypogammaglobulinemia. The patient was treated with 2 mg/kg methylprednisone without significant response. At 11 months of age, she developed respiratory failure and succumbed shortly afterward (see Supplementary Material for details). Autopsy did not show any evidence of bowel atresia, but did confirm widespread severe apoptotic enterocolitis as identified previously by endoscopy.

In Family 2, an infant male was born at 36 weeks' gestation to non-consanguineous Caucasian parents. Shortly after birth, the infant presented with symptoms of small bowel obstruction due to short-segment jejunal atresia. Despite surgical resection, the intestinal disease progressed

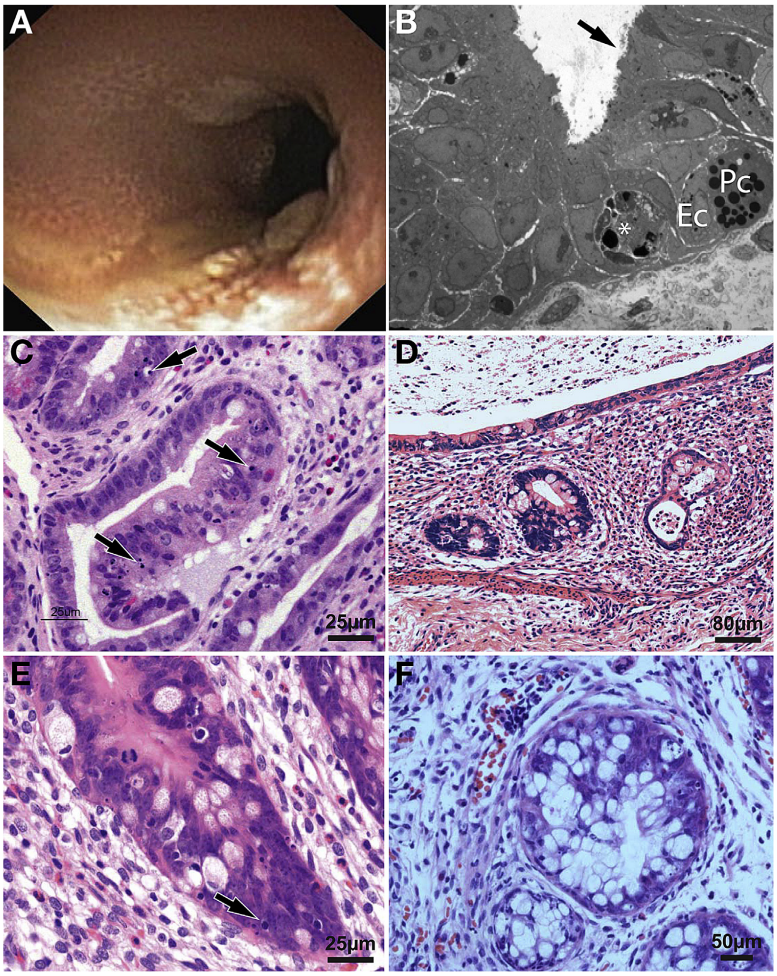

Figure 1. Histologic and endoscopic characteristics of intestine of patients with *TTC7A* mutations. (*A*) Colonoscopy showed severe inflammation characterized by continuous grade 2 colitis and multiple areas of exfoliation and sloughing of the surface epithelium from Family 1. (*B*) Low-magnification electron micrograph of crypt epithelium from the same biopsy shown in *panel C* from Family 1. Among regenerating crypt cells, apoptotic cell (*white asterisk*), enteroendocrine cell (EC), and Paneth cell (PC) are present. Crypt enterocytes showed sparse brush border microvilli (*arrow*). (*C*) High magnification of duodenal crypt epithelium showed extensive apoptosis from Family 1 (*arrows*) (H&E stain). Low (*D*) and high (*E*) magnification of cecum epithelium showed extensive apoptosis from Family 2 (*arrow*) (H&E stain). (*F*) High magnification of cecum epithelium showed extensive apoptosis from Family 3 (H&E stain).

and the patient was found to have recurrent multiple atretic areas that also required resection. The disease continued to progress and the patient died of cardiac arrest before 3 months of age. A second child from the same family also had jejunal atresia at birth, which was initially resected. The intestinal disease progressed and ultimately resulted in the patient's death at the age of 19 months. Both children had evidence of immunodeficiency with lymphopenia and T-cell deficiency. Pathologic analysis showed loss of intestinal architecture, focal scarring, and severe inflammation with increased apoptosis reminiscent of graft-vs-host-disease, as described in Family 1 (Figure 1*D* and *E*).

Family 3 had 2 infant daughters from consanguineous parents who presented with diarrhea and failure to thrive shortly after birth. Both children had no evidence of overt immunodeficiency and pathologic analysis of colonic biopsies showed similar loss of intestinal architecture, focal scarring, and severe inflammation with increased enterocyte apoptosis (Figure 1*F*) and areas where surface epithelium was detached, as described in Family 1 and Family 2. The younger girl died before the age of 1 year due to uncontrolled candida sepsis and the older girl is presently being partially treated with total parenteral nutrition (see Supplementary Material for details; summarized in Table 1).

Whole Exome Sequencing

Whole exome sequencing of Family 1 resulted in >80 times coverage of exomes and the subsequent identification of a nonsynonymous variant in exon 2 inherited from the father, and a nonsense mutation in exon 14 inherited from the mother in the *TTC7A gene* (Figure 2*A*). The nonsynonymous mutation in exon 2 at c.211 G>A resulted in a glutamic acid to lysine substitution at amino acid position 71 (p.E71K; rs147914967). The mutant allele is not found in either the National Center for Biotechnology Information database or the 1000 Genomes database, and is only found in 1 heterozygous allele from 6503 healthy individuals genotyped in the National Heart, Lung, and Blood Institute's Exome Sequencing Project (http://evs.gs.washington.edu). The mutation was predicted to be highly deleterious with a Polyphen[14] score of 0.99 and is located in a highly conserved α-helical region (Figure 2*D* and Supplementary Figure 1). The second *TTC7A* mutation in exon 14 at c.1944 C>T transition resulted in a nonsense mutation causing the premature termination of the protein at amino acid 526 (p.Q526X). This nonsense mutation has not been described previously in the datasets mentioned.

In siblings from Family 2 with severe apoptotic enterocolitis, we also identified heterozygous *TTC7A* mutations. The c.844-1 G>T mutation in the splice acceptor site of exon 7 was inherited from the mother and a c.1204-2 A>G mutation in splice acceptor site of exon 10 was inherited from the father (Figure 2*B*). These *TTC7A* mutations were predicted to result in loss of the splice acceptor sites for both exons 7 and 10, leading to skipping of both exon 7 and 10, respectively, and causing premature stop codons that would disrupt tetratricopeptide repeat (TPR) domains (Figure 2*D*). These splice mutations have not been previously described

Table 1. Summary of *TTC7A* Mutations and Clinical Features

	Age at presentation	Sex	CS	Clinical features	Immune workup	Outcome	*TTC7A* mutation	TTC7A mutated protein
Patient 1 (Family 1)	At birth	Female	No	Bloody diarrhea; AE	Lymphopenia, hypogammaglobulinemia	Died at 11 mo of age	c.211 G>A c.1944 C>T	p.E71K p.Q526X
Patient 2 (Family 2)	At birth	Male	No	Obstruction, stricture, AE	Lymphopenia	Died at 3 mo of age	c.844-1 G>T c.1204-2 A>G	Loss of the splice acceptor sites for exons 7 and 10
Patient 3 (Family 2)	At birth	Female	No	Obstruction, stricture, AE	Lymphopenia	Died at 19 mo of age	c.844-1 G>T c.1204-2 A>G	Loss of the splice acceptor sites for exons 7 and 10, respectively
Patient 4 (Family 3)	At birth	Female	Yes	Bloody diarrhea; AE	Normal	Died at 11 mo of age	c.2494 G>A	p.A832T
Patient 5 (Family 3)	At birth	Female	Yes	Bloody diarrhea; AE	Normal	Alive, TPN for partial control	c.2494 G>A	p.A832T

AE, apoptotic enterocolitis; CS, consanguinity; TPN, total parental nutrition.

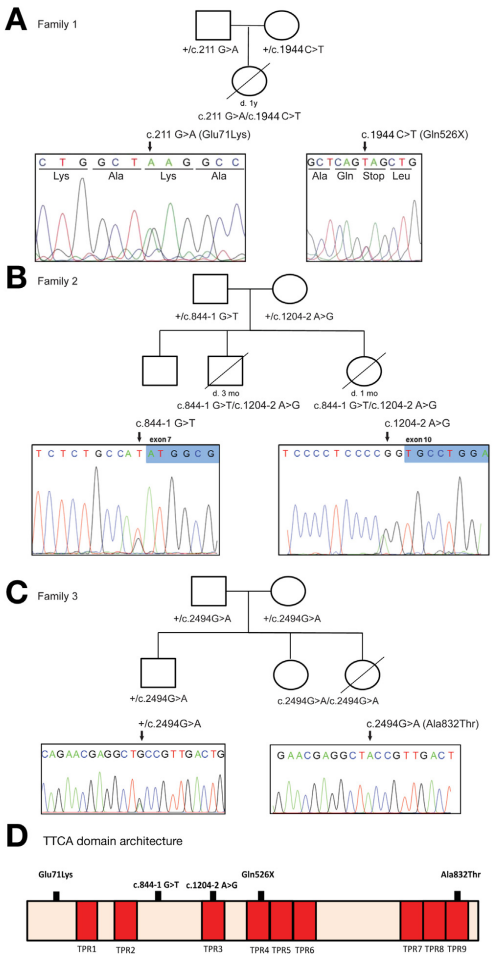

Figure 2. *TTC7A* genetic analysis. (*A*) Pedigree and *TTC7A* mutations in Family 1. Patient from Family 1 was heterozygous for 211G>A (p.E71K) inherited from her father and c.1944 C>T (p.Q526X) inherited from her mother. (*B*) Pedigree and *TTC7A* mutations in Family 2. Siblings from Family 2 were heterozygous for a novel c.844-1 G>T TTC7A mutation in splice acceptor site of exon 7 inherited from the mother and a novel c.1204-2 A>G TTC7A mutation in splice acceptor site of exon 10 inherited from the father. A third sibling was found to be negative for both mutations. (*C*) Pedigree and *TTC7A* mutations in Family 3. Siblings from Family 2 were homozygous for a nonsynonymous mutation in exon 20 at c.G2494A resulted in a alanine acid to threonine substitution at amino acid position 832 (p.A832T). (*D*) Location of TTC7A mutations in patients. Illustration of TTC7A protein with TPR domains in *red* and identified mutations are *highlighted*.

in the datasets mentioned and it is likely that these mutations will result in nonsense-mediated decay of the TTC7A messenger RNA.

In siblings from Family 3 with severe apoptotic enterocolitis, we identified a homozygous nonsynonymous mutation in exon 20 at c.2494 G>A (Figure 2*C*) that resulted in an alanine to threonine substitution at amino acid position 832 (p.A832T). The mutation was predicted to be highly deleterious with a Polyphen[14] score of 0.99 and is located in a highly conserved region of the ninth TPR domain (Figure 2*D*; Supplementary Figure 1) and has not been described previously in the datasets mentioned (see Table 1 for a summary).

Functional Analysis of TTC7A Mutations in Enterocytes

Immunostaining of TTC7A from healthy human control intestinal tissue (duodenum, ileum, and colon) showed that TTC7A was strongly expressed in enterocytes with areas of discreet localization at the plasma membrane and only few lamina propria cells stained positive (Figure 3*A*). This observed pattern of intestinal expression suggests a primary role for TTC7A in enterocyte homeostasis. To determine if the mutation identified in Family 1 and Family 3 resulted in abnormal TTC7A cellular localization, we transiently transfected Caco-2 cells with Myc-tagged WT, E71K, Q526X, and A832T TTC7A. Immunostaining using anti-Myc antibody demonstrated that E71K, Q526X, and A832T TTC7A mutants appeared to accumulate in cytoplasmic puncta, and the WT-TTC7A localized diffusely in the cytoplasm (Figure 3*B*). In addition, biopsies from the Family 2 patient with the *TTC7A* splice acceptor site mutations predicted to result in complete loss of the protein showed loss of TTC7A in enterocytes, as expected, indicating that these mutations might result in nonsense-mediated decay of the TTC7A messenger RNA (Figure 3*C*).

Knockdown of TTC7A by shRNA resulted in loss of cobblestone morphology, typical of human Henle-407 cells with the development of fibroblastoid morphology with spindle-like features (Figure 3*D* and Supplementary Figure 2). In addition, overexpression of E71K, A832T, and Q526X TTC7A in Caco-2 cells demonstrated cytoplasmic accumulations of Myc-TTC7A in addition to disrupted cortical actin staining suggestive of adhesion defects or loss of cellular polarity (Supplementary Figure 3). Reduced expression of TTC7A in the enterocytes also resulted in detachment during trypsinization (Figure 4*A*), impaired adhesion to collagen and fibronectin (Figure 4*B*), and increased apoptosis, as measured by caspase-3 (Figure 4*C*) and Annexin V (Figure 4*D*). These cellular changes are reminiscent of the apoptosis and mucosal exfoliation described in our patient.

TTC7A Binding Partners

Tandem mass spectrometry was performed on proteins co-immunoprecipitated (co-IP) from HEK293T cells expressing human TTC7A, with the aim of identifying TTC7A binding partners. Isolated proteins were digested with trypsin to generate peptide fragments and analyzed by tandem mass spectrometry (Supplementary Figure 4). To

refine this list to TTC7A binding partners, spectral hit counts were compared between WT TTC7A and the E71K mutation samples, and determined that phosphatidylinositol 4-kinase IIIα (PI4KIIIα) protein fragments were able to co-IP with WT TTC7A, but were significantly reduced with E71K TTC7A mutation (Figure 5*A* and Supplementary Figure 4). This PI4KIIIα and TTC7A interaction was supported by a weighted coexpression network[15] from small bowel gene expression data demonstrating that Ttc7a falls within a subnetwork (module) of the mouse small bowel network that included Pi4kca (murine form of PI4KIIIα) (Supplementary Tables 1–4; Supplementary Figure 5). The additional hits identified in the tandem mass spectrometry screen (Supplementary Figure 4) implicated several proteins associated with ubiquitination pathways, including E3 ligases (HUWE1, HECTD1, UBR5), and proteins that function in the ubiquitin-proteasome system (USP9X, PSMD1, VCP).

Loss of TTC7A Results in PI4KIIIα Dysfunction

As TTC7A has been implicated previously in PI4KIIIα regulation in yeast,[16,17] and confirmed through the tandem mass spectrometry and network analysis of mouse small bowel, we next confirmed through co-IP experiments that TTC7A and PI4KIIIα interacted in human cell lines. We found that Myc-Flag-tagged WT TTC7A was able to co-IP PI4KIIIα, indicating that these proteins interact either directly or indirectly in a larger complex (Figure 5*B*). We also observed reduced co-IP of PI4KIIIα with the TTC7A Q526X and E71K mutated proteins identified in Family 1 and the A832T TTC7 mutation identified in Family 3 (Figure 5*B*). As the splice variants identified in Family 2 were assumed to be unstable, we would predict that the gene product of these *TTC7A* mutations would also not bind to PI4KIIIα.

We next examined human PI4KIIIα in intestinal tissue of healthy controls and found that PI4KIIIα was abundantly expressed in both enterocytes and immune cells, including lymphocytes (Figure 5*C*, *left panel*). In our patients with TTC7A deficiency, the severe disruption of the bowel architecture with sloughing of the majority of enterocytes made interpretation of PI4KIIIα localization difficult; however, in areas with relatively preserved epithelial architecture, we observed overall reduced PI4KIIIα expression in a patient from Family 2 (while lamina propria expression was preserved; Figure 5*C*). To confirm these results, we transiently co-transfected TTC7A and TTC7A shRNA into Henle-407 cells and observed a reduction in PI4KIIIα (Figure 5*D* and *E*). These results indicate that loss of TTC7A resulted in aberrant subcellular localization of PI4KIIIα in enterocytes.

Finally, we determined that knockdown of TTC7A in human Henle-407 cell lines resulted in decreased phosphatidylinositol 4-phosphate, the end product of PI4KIIIα enzyme, in both the cytoplasm (Figure 5*E*) and at the plasma membrane (Figure 5*F*). Together these results indicate that TTC7A is required for PI4KIIIα localization to the plasma membrane and that TTC7A deficiency results in loss of PI4KIIIα signaling in enterocytes.

Discussion

Our index case (Family 1) had severe infantile apoptotic enterocolitis with a presentation significantly different from previously described cases of VEOIBD with *IL10* and *IL10R* mutations that are invariably present with colitis and perianal disease.[4,5,18–20] The severe enterocolitis with friability and exfoliative mucosal changes along with villous atrophy, gland dropout, and crypt apoptosis led to our genetic exploration through whole exome sequencing and identification of *TTC7A* as the causative gene.

The TPR domain is defined by a degenerate consensus sequence of 34 amino acids[21] and 4 of the 5 *TTC7A* mutations found in our patients resulted in disruption of these TPR domains. TPR domains mediate protein–protein interactions and the assembly of multi-protein complexes that are involved in the regulation of cell cycle, transcription, and protein transport.[22] Our tandem mass spectrometry and intestinal network experiments demonstrated an association between TTC7A and PI4KIIIα that was previously only described in yeast.[16,17] In yeast, the TTC7 ortholog, *YPP1*, is essential and has been shown to rescue a lethal α-synuclein (αSyn-A53T) yeast mutant.[23] Ypp1 (TTC7) directly binds to Stt4 (PI4KIIIα), and this binding is critical to maintaining phosphatidylinositol 4-phosphate levels and PI4KIIIα stability at the plasma membrane.[16,17] In addition, in yeast, the phenotypes of *YPP1* (TTC7) and *STT4* (PI4KIIIα) conditional mutants are identical and both mutants result in cell wall destabilization and defective organization of actin. Overexpression of *STT4* (PI4KIIIα) also suppresses the temperature-sensitive growth defect observed in *YPP1* (TTC7) mutants.[17] The role of TTC7A in PI4KIIIα recruitment to the plasma membrane was also recently confirmed in mammalian cell lines[24] and we demonstrate for the first time that TTC7A and PI4KIIIα directly interact in human cell lines. Because TTC7A is required for proper localization of PI4KIIIα at the plasma membrane,[24] we propose that TTC7A mutations result in disease through loss of PI4KIIIα at the plasma membrane and subsequent reduction of phosphatidylinositol 4-phosphate that is required for cell polarity and survival. In support of this model, down-regulation of PI4KIIIα results in increased apoptosis[25] and, in addition, intestinal-specific murine knockout of Pi4kca (PI4KIIIα) results in a strikingly severe intestinal phenotype with widespread mucosal epithelial degeneration[26] reminiscent of our patients with *TTC7A* mutations. Therefore, our results demonstrate a direct interaction between PI4KIIIα and TTC7A. And similar to the phenotype observed in TTC7A-deficient patients, TTC7A knockdown in human intestinal-like cell lines resulted in decreased adhesion and increased apoptosis. These results indicate that disruption of the PI4KIIIα–TTC7A pathway results in a combined T-cell and enterocyte defect that results in the intestinal phenotype described here (Figure 6).

The EFR3 homolog B (*EFR3B;* ENSG00000084710) gene product EFR3B tethers TTC7A (and TTC7B) to the plasma membrane and is essential for both TTC7A and PI4KIIIα function.[24] In addition, knockdown of EFR3B results in the loss of both TTC7A and PI4KIIIα at the plasma membrane

and is critical for PI4KIIIα signaling.[24] Interesting, several *EFR3B* single nucleotide polymorphisms located both in the *EFR3B* gene and its flanking regions were reported to be associated with Crohn's disease (http://www.ibdgenetics.org; Supplementary Table 5; lead single nucleotide polymorphism rs1077492; $P = 1.9 \times 10^{-14}$, odds ratio, 1.11). This locus on chromosome 2 at 25.12 Mb was recently reported in the International Inflammatory Bowel Disease Genetics Consortium meta-analysis as an IBD locus.[27] In silico analyses carried out by the International Inflammatory Bowel Disease Genetics Consortium suggested ADCY3 as a potential candidate at this locus[27]; however, EFRB3's role in regulating PI4KIIIα-TTC7A implicates *EFRB3* as a plausible causative IBD gene at this locus and that this

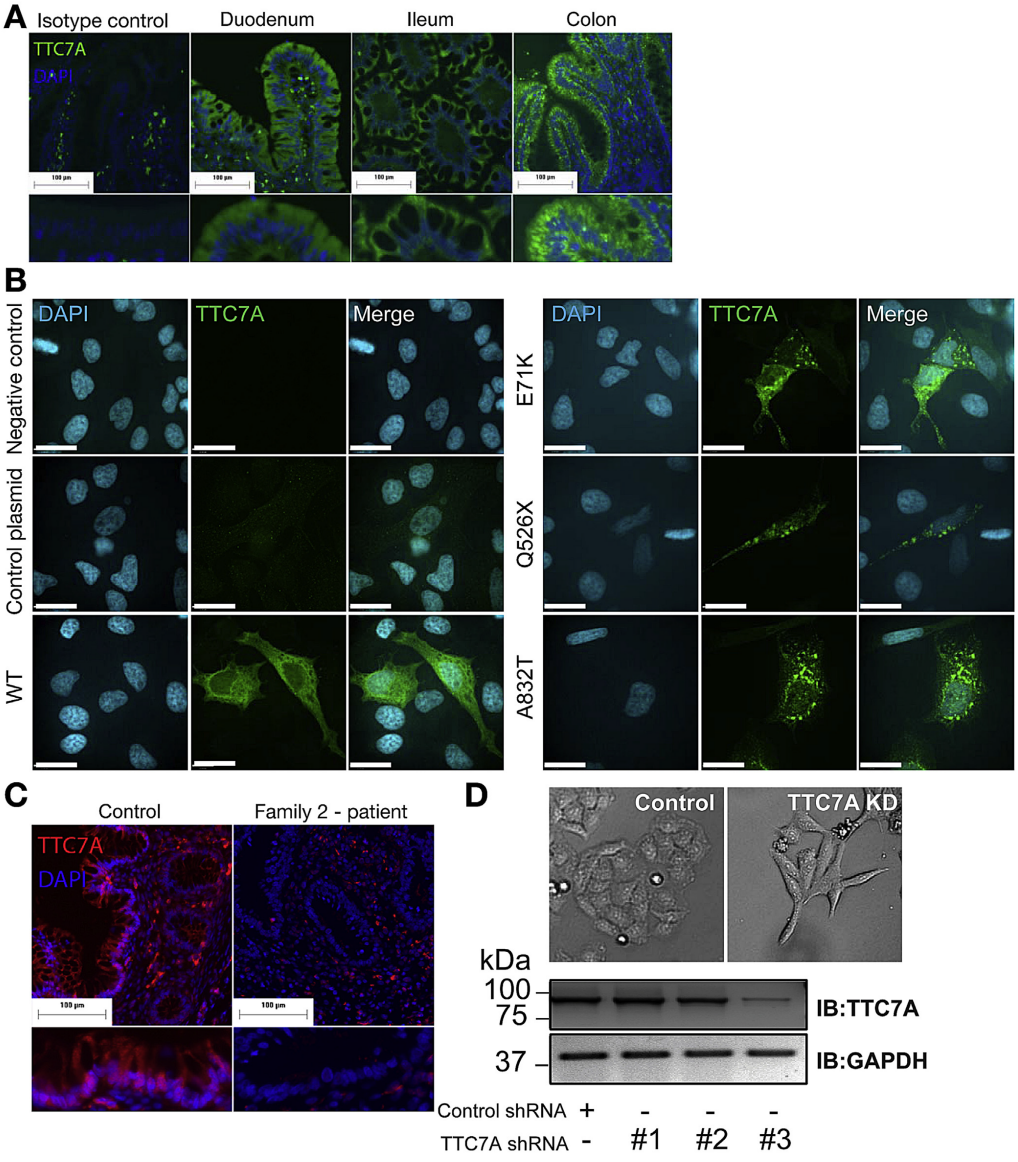

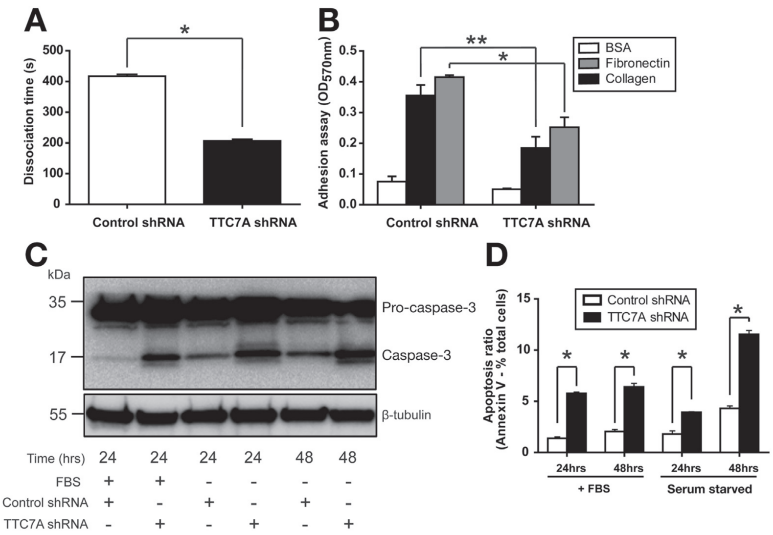

Figure 4. (*A*) Impaired cell adhesion in TTC7A-depleted cells. The total dissociation time, defined as the time required for complete dissociation of all cells from the tissue culture plate, was markedly reduced in TTC7A-depleted Henle-407 cells compared with control cells. Dissociation assay (n = 6, biological replicates; Student *t* test, **P* = .0022). (*B*) Impaired cell adhesion to collagen and fibronectin in TTC7A-depleted cells. Cell adhesion assays were performed using crystal violet staining. Control and TTC7A-depleted Henle-407 cells were seeded on 96-well plates coated with either collagen or fibronectin. Adhesion was assessed on the basis of optical density (OD) at 570 nm. n = 3; adhesion assay (n = 3) biological replicates, Student *t* test, **collagen: *P* = .027 and *fibronectin: *P* = .0077. (*C*) TTC7A-depletion in Henle-407 cells results in greater caspase-dependent apoptosis. To investigate the impact of TTC7A suppression on the induction of apoptosis, the activation of caspase-3 was measured by Western blot. Specific cleavage of pro-caspase 3 (32 kDa) into the active caspase-3 fragments (17 kDa) was increased in cells serum starved for 24 and 48 hours. n = 3; *P* = .012, analysis of variance. (*D*) TTC7A-depletion in Henle-407 cells results in greater apoptosis measured by flow cytometric analysis of Annexin V. To examine the significance of TTC7A suppression, after loss of attachment, flow cytometric analysis was conducted to quantity the extent of apoptosis in cells starved for 24 and 48 hours. Cells were stained with Annexin V-phycoerythrin and 7-aminoactinomycin D (viability marker); apoptotic cells were identified as Annexin V^+ 7-aminoactinomycin D^- cells. In TTC7A-depleted cells, the proportion of cells in early apoptosis increased to approximately 4.5% at 24 hours and 11.2% at 48 hours of serum-starvation compared to 1.3% (24 hours) and 4.1% (48 hours) in control cells. Annexin V apoptosis assay n = 3 biological replicates, Student *t* test, fetal bovine serum (FBS), 24 hours: **P* = .0018; FBS, 48 hours: **P* = .0076; serum starved, 24 hours: **P* = .021; serum starved, 48 hours: **P* = .0034. BSA, bovine serum albumin.

PI4KIIIα-TTC7A-EFRB3 pathway plays a broader role in adult-onset IBD.

Mutations in a *Ttc7a* TPR domain[28–30] result in flaky skin (*fsn*) mice and the associated pleiotropic abnormalities, including severe weight loss with diarrhea and intestinal apoptosis, being reported infrequently.[31,32] In addition, the intestinal-specific knockout of Pi4kca (PI4KIIIα) in mice resulted in a severe intestinal phenotype with widespread

Figure 3. Functional TTC7A enterocyte studies. (*A*) TTC7A expression in intestinal enterocytes. Immunofluorescence microscopy performed on human tissue sections immunostained using anti-TTC7A antibody (and 4′,6-diamidino-2-phenylindole [DAPI]) demonstrates TTC7A expression in enterocytes within the duodenum, ileum, and colon. *Lower inset* panels represent zoomed images of the corresponding panel above. *Scale bars* = 100 μm. (*B*) E71K, Q526X, and A832T mutations in TTC7A. Caco-2 cells were transiently transfected with Myc-tagged WT, E71K, Q526X, and A832T TTC7A, immunostained using anti-Myc antibody and visualized using confocal microscopy. Negative control panels represent staining with secondary antibody only. The control plasmid represents an empty vector sham transfection. *Scale bars* = 25 μm. (*C*) TTC7A in enterocytes from patient cecum (Family 2). Immunofluorescence microscopy was performed on TTC7A-immunostained (and DAPI) cecal tissues sections from both control and patient (Family 2) biopsies. Compared to control staining (*left panel*), TTC7A expression is reduced in the patient sample (*right panel*). *Scale bar* = 100 μm. (*D*) Stable knockdown of *TTC7A* resulted in morphological changes in Henle-407 cells. Expression of TTC7A in stably transfected Henle-407 cells was reduced (70%–80%) compared with Henle-407 cells stably transfected with control shRNA. The impact on cellular morphology of control and *TTC7A* shRNA knockdown was examined in Henle-407 cells by contrast microscopy (100× magnification) under normal culture conditions. Knockdown of TTC7A resulted in a loss of cobblestone morphology and development of fibroblastoid morphology with spindle-like features. GAPDH, glyceraldehyde-3-phosphate dehydrogenase.

mucosal epithelial degeneration.[26] The intestinal phenotype observed in these 2 mouse models is reminiscent of the phenotype seen in our infantile patients who had massive shedding of enterocytes with increased apoptosis; however, none of the patients developed psoriasis or other skin abnormalities like the *fsn* mice. TTC7A has been investigated in human psoriasis and found not to be associated with human dermatological disease.[30] Therefore, psoriasis might only be observed in the *fsn* mice and might not be part of the human disorder.

We have shown that TTC7A is expressed in enterocytes and has a role in enterocyte survival and function, suggesting that the physiological abnormalities observed in both mice and humans with TTC7A mutations result, at least in part, from epithelial dysfunction. However, as Chen et al[11] also demonstrated, TTC7A is expressed in the thymus with a marked reduction of thymocytes and lymphoid depletion in 1 patient with TTC7A deficiency, TTC7A plays a critical role in modulating immune homeostasis and the immunodeficiency also contributes to the pathogenesis of *TTC7A*

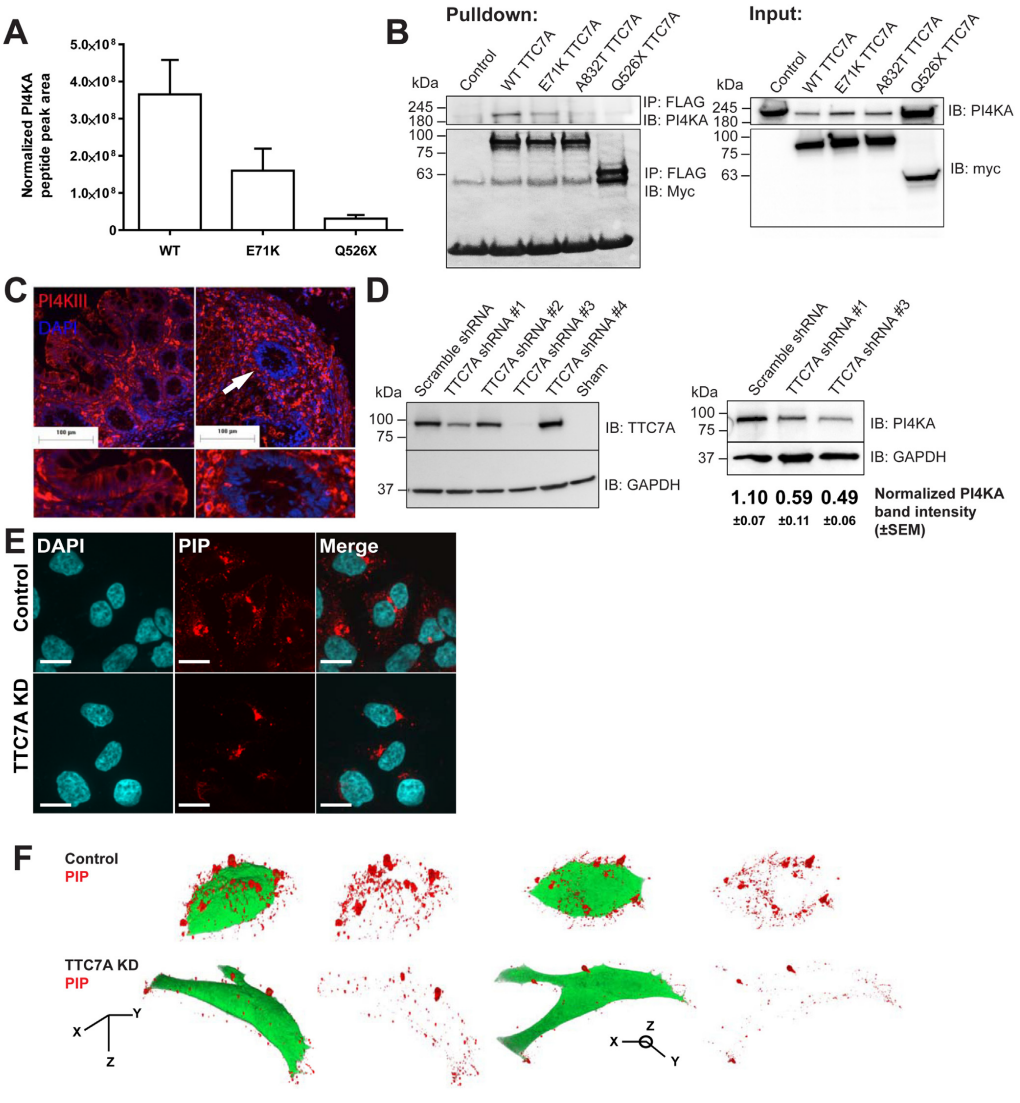

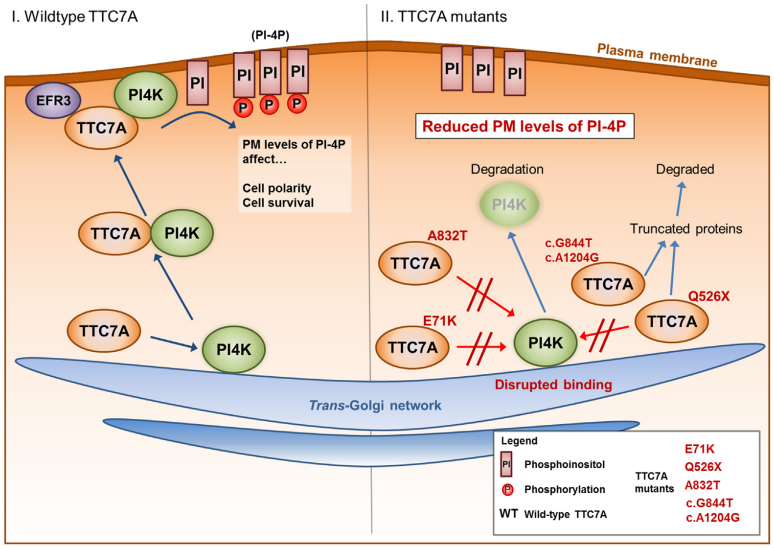

Figure 6. Summary of TTC7 mutations. Schematic representation of the role of TTC7A in the trafficking of PI4KIIIα to the plasma membrane from the *trans*-Golgi network. The *left panel* represents WT TTC7A in enterocytes wherein TTC7A binds to and facilitates the transport of PI4KIIIα from the *trans*-Golgi to the plasma membrane. At the membrane, PI4KIIIα can catalyze the production of PtdIns-4P(PI-4P). PI-4P levels at the plasma membrane have been implicated in cell survival and the maintenance of cell polarity. In the *right panel*, the various TTC7A mutations identified in the patients are depicted. E71K, Q526X, and A832T TTC7A all demonstrated reduced binding to PI4KIIIα, which could reduce the interaction between TTC7A and PI4KIIIα, hindering transport to the plasma membrane (PM). Consequently, this will lead to reduced plasma membrane levels of PI-4P, a dysregulation that would affect downstream signaling pathways.

Figure 5. (*A*) Tandem mass spectrometry. E71K and Q526X mutations reduce the ability of TTC7A to immunoprecipitate PI4KA. Selected peptides from PI4KA and TTC7A were analyzed to determine the area under their MS1 peaks to assess the relative abundance of each peptide. The PI4KA present in each sample was normalized to the total TTC7A in each technical replicate to allow comparisons among biological replicates (n = 3). These normalized values were averaged over all experiments. Error bars represent the standard error. (*B*) PI4KIIIα-TTC7A co-immunoprecipitate. HEK293T cells were transiently transfected with Myc-tagged WT (WT-TTC7A), E71K, Q526X, and A832T TTC7A constructs. Lysates were immunoprecipated with anti-Myc antibody, and then immunoblotted using anti-PI4KIIIα and anti-Myc (for TTC7A) antibodies. The control lane represents transfection with an empty vector. (*C*) Expression and localization of PI4KIIIα is altered in patients with TTC7A deficiency. Immunofluorescence microscopy was performed on both control and patient colonic tissue sections immunostained with anti-PI4KIIIα antibodies. In the *left panel*, immunohistochemistry demonstrated that PI4KIIIα is highly expressed in enterocytes and immune cells from healthy human intestine. *Inset panel* depicts zoomed view of *left panel*, demonstrating PI4KIIIα expression at the plasma membrane of enterocytes. In the patient tissues, immunohistochemistry demonstrated that PI4KIIIα is dysregulated in enterocytes. *Inset panel* (representing region indicated by *white arrow*) demonstrates loss of PI4KIIIα at the plasma membrane of enterocytes bordering the intestinal crypt. *Scale bar* = 100 μm. (*D*) shRNA-mediated knockdown of TTC7A expression leads to decreased PI4KIIIα levels. To test the efficacy of the TTC7A shRNA, Henle-407 cells were transiently co-transfected with WT TTC7A and the various knock-down constructs, labeled #1 through #4, including a scrambled shRNA control and sham transfection. shRNA #1 and #3 showed reduction in TTC7A expression (*left panels*). shRNA containing the same targeting sequences were used to lentivirally infect Henle-407 cells where expression of PI4KIIIα was assessed in cell lysates by Western blot (*right panels*). Glyceraldehyde-3-phosphate dehydrogenase (GAPDH) was stained as loading control for all blots. The intensity of each PI4KIIIa band was normalized to the GADPH loading control by densitometry. Quantitation of band intensities (listed below each lane) demonstrates a statistically significant reduction in PI4KIIIa expression after TTC7A knockdown (Student *t* test, n = 3, *P* = .0234). Each normalized band intensity is presented as $\pm$SEM. (*E*) TTC7A depletion results in decreased cytoplasmic phosphatidylinositol 4-phosphate (PI-4P) production. TTC7A knockdown and control Henle-407 cells were stained with antibodies against PtdIns4P (*in red*; Z-P004, IgM, Cedarlane, Burlington, NC) and 4′,6-diamidino-2-phenylindole (DAPI) (*in blue*) to visualize nuclei. (*F*) TTC7A knockdown Henle-407 cells have reduced plasma membrane immunostaining for PI-4P compared with controls. For control and TTC7A knockdown (KD), Henle-407 cells Z-stack images were generated at 0.2-mm intervals and recapitulated using Volocity to generate a 3-dimensional model to illustrate cell surface levels of PIP. Unconjugated green fluorescent protein, expressed from the control and knockdown plasmids, was visualized and used to approximate the morphology of the cells. Each pair of images represents 2 views of the same cell according to axes depicted.

deficiency, as seen in Family 1 and Family 2. These results are consistent with those seen in the MIA patients described with SCID,[11,12,33] and points to a severe defect in both enterocyte and T-cell function; however, patients from Family 3 did not have an overt T-cell defect and patients with MIA described previously[11,12,33] had varying degrees of immunodeficiency, with some patients exhibiting mild T-cell lymphopenia in Chen et al,[11] who also suggested an enterocyte defect based on the high frequency of bloodstream infections with intestinal microbes.

Therefore, our studies also suggest that mutations in the *TTC7A* gene can result in a spectrum of intestinal disease ranging from VEOIBD with apoptotic enterocolitis, as first described here, to MIA with SCID, as described here and previously.[11,12,33] In support of this, *TTC7A* mutations were found to cause hereditary MIA with SCID[11,12,33]; however, apoptotic enterocolitis has not been reported. The patients from Family 1 and Family 3, with apoptotic enterocolitis with no evidence of MIA or stricturing disease on autopsy, had mutations that would be predicted to reduce TTC7A expression but not completely abolish function. In support, we also demonstrated that the mutations identified in Family 1 and Family 3 reduced TTC7A binding to PI4KIIIα. Therefore, it is possible that the disease observed in patients from Family 1 and Family 3 represents a hypomorphic state, where some residual TTC7A activity in both enterocytes and the thymus results in severe enterocolitis without MIA and with or without lymphopenia.

All TTC7A-deficiency patients, including the patients described here, died in infancy due to their progressive bowel disease, failed allogeneic hematopoietic stem cell transplantation, or survived with short gut and total parenteral nutrition.[11,12] Interestingly, both Chen et al[11] and Samuels et al[12] described an MIA TTC7A-deficiency patient who had hematopoietic stem cell transplantation and developed severe recurrence of MIA post transplantation. The recurrence of MIA after resection in our Family 2 patients and those presented by Chen et al and Samuels et al,[11,12] suggests that TTC7A deficiency results in a severe intestinal inflammatory process driven by a combined epithelial and T-cell defect that continues post resection of atretic regions, and the enterocyte defect will not respond to hematopoietic stem cell transplant. Therefore, as we have demonstrated that an enterocyte defect is also found in patients with *TTC7A* deficiency, transplantation of allogeneic hematopoietic stem cells might not be warranted in TTC7A-deficient patients. However, our study opens the possibility of pharmacologically targeting the PI4KIIIα–TTC7A–EFR3B pathway as a potential therapeutic approach. The identification of *TTC7A* as a candidate gene for a unique and unrecognized variant of severe apoptotic enterocolitis expands the genetic diversity of VEOIBD and the need to tailor therapeutic approaches for individual subtypes.

Supplementary Material

Note: To access the supplementary material accompanying this article, visit the online version of *Gastroenterology* at www.gastrojournal.org, and at http://dx.doi.org/10.1053/j.gastro.2014.01.015.

References

1. Muise AM, Snapper SB, Kugathasan S. The age of gene discovery in very early onset inflammatory bowel disease. Gastroenterology 2012;143:285–288.
2. Griffiths AM. Specificities of inflammatory bowel disease in childhood. Best Pract Res Clin Gastroenterol 2004;18:509–523.
3. Heyman MB, Kirschner BS, Gold BD, et al. Children with early-onset inflammatory bowel disease (IBD): analysis of a pediatric IBD consortium registry. J Pediatr 2005;146:35–40.
4. Glocker EO, Kotlarz D, Boztug K, et al. Inflammatory bowel disease and mutations affecting the interleukin-10 receptor. N Engl J Med 2009;361:2033–2045.
5. Kotlarz D, Beier R, Murugan D, et al. Loss of interleukin-10 signaling and infantile inflammatory bowel disease: implications for diagnosis and therapy. Gastroenterology 2012;143:347–355.
6. Glocker EO, Frede N, Perro M, et al. Infant colitis—it's in the genes. Lancet 2010;376(9748):1272.
7. Worthey EA, Mayer AN, Syverson GD, et al. Making a definitive diagnosis: successful clinical application of whole exome sequencing in a child with intractable inflammatory bowel disease. Genet Med;13:255–262.
8. Blaydon DC, Biancheri P, Di WL, et al. Inflammatory skin and bowel disease linked to ADAM17 deletion. N Engl J Med;365:1502–1508.
9. Matute JD, Arias AA, Wright NA, et al. A new genetic subgroup of chronic granulomatous disease with autosomal recessive mutations in p40 phox and selective defects in neutrophil NADPH oxidase activity. Blood 2009;114:3309–3315.
10. Muise AM, Xu W, Guo CH, et al. NADPH oxidase complex and IBD candidate gene studies: identification of a rare variant in NCF2 that results in reduced binding to RAC2. Gut 2012;61:1028–1035.
11. Chen R, Giliani S, Lanzi G, et al. Whole-exome sequencing identifies tetratricopeptide repeat domain 7A (TTC7A) mutations for combined immunodeficiency with intestinal atresias. J Allergy Clin Immunol 2013;132:656–664.e17.
12. Samuels ME, Majewski J, Alirezaie N, et al. Exome sequencing identifies mutations in the gene TTC7A in French-Canadian cases with hereditary multiple intestinal atresia. J Med Genet 2013;50:324–329.
13. Krieger JR, Taylor P, Gajadhar AS, et al. Identification and selected reaction monitoring (SRM) quantification of endocytosis factors associated with Numb. Mol Cell Proteomics 2013;12:499–514.
14. Dixon AL, Liang L, Moffatt MF, et al. A genome-wide association study of global gene expression. Nat Genet 2007;39:1202–1207.
15. Zhang B, Horvath S. A general framework for weighted gene co-expression network analysis. Stat Appl Genet Mol Biol 2005;4:Article17.
16. Baird D, Stefan C, Audhya A, et al. Assembly of the PtdIns 4-kinase Stt4 complex at the plasma membrane requires Ypp1 and Efr3. J Cell Biol 2008;183:1061–1074.
17. Zhai C, Li K, Markaki V, et al. Ypp1/YGR198w plays an essential role in phosphoinositide signalling at the plasma membrane. Biochem J 2008;415:455–466.

18. Begue B, Verdier J, Rieux-Laucat F, et al. Defective IL10 signaling defining a subgroup of patients with inflammatory bowel disease. Am J Gastroenterol 2011;106:1544–1555.
19. Engelhardt KR, Shah N, Faizura-Yeop I, et al. Clinical outcome in IL-10- and IL-10 receptor-deficient patients with or without hematopoietic stem cell transplantation. J Allergy Clin Immunol 2013;131:825–830.
20. Moran CJ, Walters TD, Guo CH, et al. IL-10R polymorphisms are associated with very-early-onset ulcerative colitis. Inflamm Bowel Dis 2013;19:115–123.
21. Cortajarena AL, Regan L. Ligand binding by TPR domains. Protein Sci 2006;15:1193–1198.
22. D'Andrea LD, Regan L. TPR proteins: the versatile helix. Trends Biochem Sci 2003;28:655–662.
23. Flower TR, Clark-Dixon C, Metoyer C, et al. YGR198w (YPP1) targets A30P alpha-synuclein to the vacuole for degradation. J Cell Biol 2007;177:1091–1104.
24. Nakatsu F, Baskin JM, Chung J, et al. PtdIns4P synthesis by PI4KIIIalpha at the plasma membrane and its impact on plasma membrane identity. J Cell Biol 2012;199:1003–1016.
25. Ma H, Blake T, Chitnis A, et al. Crucial role of phosphatidylinositol 4-kinase IIIalpha in development of zebrafish pectoral fin is linked to phosphoinositide 3-kinase and FGF signaling. J Cell Sci 2009;122:4303–4310.
26. Vaillancourt FH, Brault M, Pilote L, et al. Evaluation of phosphatidylinositol-4-kinase IIIalpha as a hepatitis C virus drug target. J Virol 2012;86:11595–11607.
27. Jostins L, Ripke S, Weersma RK, et al. Host-microbe interactions have shaped the genetic architecture of inflammatory bowel disease. Nature 2012;491:119–124.
28. White RA, McNulty SG, Nsumu NN, et al. Positional cloning of the Ttc7 gene required for normal iron homeostasis and mutated in hea and fsn anemia mice. Genomics 2005;85:330–337.
29. Takabayashi S, Iwashita S, Hirashima T, et al. The novel tetratricopeptide repeat domain 7 mutation, Ttc7fsn-Jic, with deletion of the TPR-2B repeat causes severe flaky skin phenotype. Exp Biol Med (Maywood) 2007;232:695–699.
30. Helms C, Pelsue S, Cao L, et al. The Tetratricopeptide repeat domain 7 gene is mutated in flaky skin mice: a model for psoriasis, autoimmunity, and anemia. Exp Biol Med (Maywood) 2005;230:659–667.
31. Sundberg JP, France M, Boggess D, et al. Development and progression of psoriasiform dermatitis and systemic lesions in the flaky skin (fsn) mouse mutant. Pathobiology 1997;65:271–286.
32. Nüesch U, Seger R, Pachlopnik Schmid J. Clinical and histological features of flaky skin (fsn) mice. Presented at the XXIX Meeting of the Swiss Immunology PhD Students, Schloss Wolfsberg, April 2–4, 2012.
33. Bigorgne AE, Farin HF, Lemoine R, et al. TTC7A mutations disrupt intestinal epithelial apicobasal polarity. J Clin Invest 2013 Dec 2 [Epub ahead of print].

Received October 2, 2013. Accepted January 3, 2014.

Reprint requests
Address requests for reprints to: Aleixo Muise, MD, PhD, The Hospital for Sick Children, 555 University Avenue, Toronto, Ontario, Canada, M5G 1X8. e-mail: aleixo.muise@utoronto.ca; fax: (416) 813-6531.

Acknowledgments
The authors thank the families of the patients described here from Canada, Germany, and Iran. International Early Onset Pediatrics IBD Cohort Study participants (www.NEOPICS.org): Yaron Avitzur, Conghui Guo, Lucas A. Mastropaolo, Abdul Elkadri, Sandeep Dhillon, Ryan Murchie, Ramzi Fattouh, Hien Huynh, Fiona Powrie, Thomas D. Walters, John H. Brumell, Anne M. Griffiths, Dermot P. B. McGovern, Holm H. Uhlig, Eric Schadt, Christoph Klein, Scott B. Snapper, and Aleixo M. Muise.

Conflicts of interest
The authors disclose no conflicts.

Funding
AMM is supported by an Early Researcher Award from the Ontario Ministry of Research and Innovation and funded by a Canadian Institute of Health Research Operating Grant (MOP119457). SBS is supported by National Institutes of Health grants HL59561, DK034854, and AI50950 and the Wolpow Family Chair in IBD Treatment and Research. SP is supported by Lupus Research Institute Novel Grant Program and University of Southern Maine/Maine Economic Improvement Fund Development Grant program. This work was supported by DFG SFB1054, the Gottfried-Wilhelm-Leibniz program, BaySysNet (CK) and the Care-for-Rare Foundation (EB, DK). IBD Research at Cedars-Sinai is supported by US Public Health Service grant PO1DK046763 and the Cedars-Sinai F. Widjaja Foundation Inflammatory Bowel and Immunobiology Research Institute Research Funds. Genotyping at Cedars-Sinai Medical Center is supported in part by the National Center for Research Resources grant M01-RR00425, UCLA/Cedars-Sinai/Harbor/Drew Clinical and Translational Science Institute grant (UL1 TR000124-01), the Southern California Diabetes and Endocrinology Research Grant (DK063491). In addition, DPBM is supported by The Leona M. and Harry B. Helmsley Charitable Trust, The European Union, the Crohn's and Colitis Foundation of America, and The Joshua L. and Lisa Z. Greer Chair in IBD Genetics. Subject ascertainment and data and sample processing was also supported by DK062413 and DK084554 and supplements to activities of the National Institute of Diabetes and Digestive and Kidney Diseases IBD Genetics Consortium. Partial funding is provided Harvard Institute of Translational Immunology (HITI) to AMM and SBS. This work was funded in part by a Leona M. and Harry B. Helmsley Charitable Trust grant to AMM, SBS, CK, DPBM, FP, and ES.

8. Declaration of contribution as co-author

LMU KLINIKUM DER UNIVERSITÄT MÜNCHEN

CAMPUS INNENSTADT

KINDERKLINIK UND KINDERPOLIKLINIK
IM DR. V. HAUNERSCHEN KINDERSPITAL

Klinikum der Universität München, Kinderklinik und Kinderpoliklinik im Dr. von Haunerschen Kinderspital Lindwurmstr. 4 80337 München

Prof. Dr. Christoph Klein
Direktor

Kinderklinik und Kinderpoliklinik
im Dr. von Haunerschen Kinderspital
Klinikum der Universität München
Campus Innenstadt
Sekretariat: Gerlinde Graf

Tel.: +49 (0)89 4400-57701
Fax: +49 (0)89 4400-57702
christoph.klein@med.uni-muenchen.de
www.klinikum.uni-muenchen.de

Postanschrift:
Lindwurmstr. 4
D-80337 München

Ihr Zeichen: Unser Zeichen: ck/gg

Declaration of contribution as co-author

This is to declare contribution of Ehsan Bahrami as a co-author in manuscripts entitled "*Chromatin remodeling factor SMARCD2 regulates transcriptional networks controlling differentiation of neutrophil granulocytes*" and "*Mutations in Tetratricopeptide Repeat Domain 7A (TTC7A) result in a severe form of very early onset inflammatory bowel disease*".

- SMARCD2 manuscript: Ehsan performed endogenous immunoprecipitation (IP) experiments, helped in ectopic IP, helped in cloning and optimization of the lentiviral plasmid (pET), and assisted in designing qPCR primers for chromatin IP experiments.
- TTC7A manuscript: Ehsan carried out experiments and analyzed data on family 2.

Munich, April 11, 2017

Prof. Dr. med. Christoph Klein
Direktor der Kinderklinik und Kinderpoliklinik
im Dr. von Haunerschen Kinderspital

Munich, April 11, 2017

Ehsan Bahrami

9. Discussion

9.1.1. Identification of premature stop codon mutation in *MYSM1* and its clinical relevance.

In our study, we used the power of whole exome sequencing to identify the underlying genetic defect in two patients with an unusual presentation of bone marrow failure. The mutation in *MYSM1* (NM_001085487: c.1168G>T) results in a premature stop codon mutation in aa 390 (p.E390*). Detailed, genetic, clinical, and immunological findings for the individual patients are provided in the manuscript #1. MYSM1-deficient patients share several phenotypic aspects with Mysm1$^{-/-}$ mice, including BMF, severe B cell deficiency, anemia and neutropenia [106, 107, 115, 138]. These data support and build upon previous findings regarding the importance of MYSM1 in hematopoiesis, notably in B cell development. It is possible that the hematopoiesis defect, in particular the B deficiency, observed in MYSM1-deficient patients results from a transcriptional deregulation of key factors involved in hematopoiesis and B-cell development, as found in Mysm1$^{-/-}$ mice [107-109, 139]. However, investigations on transcription regulation in bone marrow cells of our patients were not feasible due to the lack of HSCs in bone marrow of the patients

In contrast to the other reported MYSM1-deficient patient, who showed reduced number of CD3^{+}, CD4^{+} and CD8^{+} cells in periphery [116], we did not observe any consistent T cell phenotype in our patients. However, the clinical need to undergo allogeneic HSC transplantation prevented us from performing extensive T cell studies. In depth analysis of human T cell differentiation and function will be needed in the future, when additional patients with MYSM1 deficiency will be identified.

Dysplastic findings of red and white blood precursors are quite common in BMF syndromes such as FA, DBA, SDS, and SCN. Cytogenic investigations on BM specimens of our patients revealed MDS findings including Pseudo Pelger-Huet anomaly as well as multinucleated erythroblasts, cytoplasmic bridges and ectopic nuclear morphology of erythroblast (Manuscript #1). Dysplastic findings of erythroid and megakaryocytes had been also noted in the first reported MYSM1-deficient patient [115]. Indeed, lack of MYSM1 function is correlated to dysplastic features of blood cells precursor cells. Thus, studying the role of

MYSM1 may help to unravel molecular mechanisms preventing dysplasia of blood cells in healthy individuals. It remains currently unknown whether dysplasia in MYSM1-deficiency is associated with clonal aberrations. Further studies with gene marked human hematopoietic stem cells transplanted in immunodeficient mice will help to address this important question in the future.

Studies of Mysm1$^{-/-}$ mice disclosed that Myms1 function is not restricted to BM and B cells, but may also affects other immune and nonimmune cells [110, 112, 113]. Our patients had growth retardation and mild neurocognitive impairment, possibly related to MYSM1 deficiency. It is however not easy to differentiate these potentially MYSM1-related effects from other genetic factors in highly consanguineous pedigrees.

Our investigations were of relevance to the clinical management and thus are an example of how molecular studies in patients with rare diseases can be directly helpful for the therapy of individual patients. In view of the progressive bone marrow failure and cellular immunodeficiency, both patients received transplantation of HLA matched healthy hematopoietic stem cells. Conditioning regimens vary a lot and should be adapted to the underlying disease. For example, patients with defects in genomic integrity (i.e. Fanconi anemia) require less intensive conditioning and avoidance of irradiation. Patients with auto-inflammatory disorders such as IL10R deficiency need intensive immunosuppression [140]. The fact that we could show increased stress responses and delayed re-equilibration of cellular homeostasis in MYSM1 deficient cells led us to choose a targeted conditioning approach using reduced intensity conditioning (fludarabine (150mg/m²), treosulfan (42g/m²), alemtuzumab (0,4mg/kg)). Of note, the success of this approach also documents that the bone marrow stromal cells appear not to be affected in MYSM1 deficiency. As expected, the neurological anomalies could not be cured by re-establishing a healthy hematopoietic system.

9.1.2. Increased stress response in MYSM1-deficient patient cells

Following DNA damage, ubiquitination of H2A at ɣ-H2AX containing foci resulting in activation of cellular repair mechanisms has been shown previously [141, 142]. The role of DUB enzymes in regulation of DNA damage response (DDR) has been studied by different groups. USP3 and USP6 deficiencies have been associated with accumulation of spontaneous DNA damages and stable and silencing of the genes near DNA-damaged sites [103, 143,

144]. The role of the other de-ubiquitination enzymes, such as MYSM1, in DDR is largely unknown. Studying spontaneous and induced DNA damage in MYSM1-deficient cells provided us an opportunity to shed light on the role of DUBs in DDR and genome stability.

Elevation of ɣ-H2AX has been documented in HSCs and blood progenitors of Mysm1$^{-/-}$ mice [107]. In accordance with these findings in mice, the cells from MYSM1-deficient patients also were characterized by elevated levels of ɣ-H2AX, reflecting increased genome instability. Moreover, increased levels of ɣ-H2AX were detected in patient cells following genotoxic stress induction such as UV light. These data are in line with the findings of Nishi *et al*. showing MYSM1 is recruited to the site of DNA damage and is involved in cell cycle checkpoint regulation [145]. However, due to the lack of suitable MYSM1 antibody for immunofluorescence studies, we were not able to study co-localization of MYSM1 and ɣ-H2AX in primary patient cells. Further investigations are required to define the molecular mechanism of elevated DNA instability in MYMS1-deficient mice and human cells.

Following genotoxic stress induction in MYSM1-deficient patient cells, increased rate of apoptosis, elevation of ROS production, cell cycle arrest and increased genome instability were observed, which demonstrate that MYSM1 is involved also in cell survival, genome repair and cell cycle progression.

Mysm1 may be linked to the tumor suppressor protein p53. Two independent groups generated Mysm1$^{-/-}$ p53$^{-/-}$ double-deficient mice that showed almost complete recovery of hematopoietic defects observed in *Mysm1*$^{-/-}$ mice [117, 121]. Furthermore, co-localization of p53 and Mysm1 in p53 correlated genes, such as Bbc3/PUMA and Cdkn1a/p21, has been documented by Belle *et al* [122]. The established link between MYSM1 and p53 may be helpful with respect to the identification of pharmacological compounds.

Cross-activation of p53 and p38 has been shown to play a key role in genotoxic stress responses [146-149]. In order to analyze p53 and p38 activation in MYSM1-deficient cells, we studied p38 activation and p38-mediated stress responses in fibroblast cells of our patient. This analysis suggested that MYSM1 is involved in fine-tuning stress response equilibration, as MYSM1-deficient cells showed sustained induction of Phosphorylated-p38 (P-p38). Our reconstitution data unequivocally prove that the increased susceptibility to genotoxic stress is caused by MYSM1 deficiency. Further investigations are required to define p38 p53 interaction and the mechanism of p38 regulation by MYSM1. Based on our findings and the published data about MYSM1, we propose that MYSM1 regulates hematopoiesis, B cell

development and genotoxic responses through controlling of histone de-ubiquitination and regulation of transcription (Figure 10)

Taken together our study on MYSM1-deficient patient cells showed that lack of MYSM1 leads to the hypersensitivity of cells to genotoxicity which indicates MYSM1 plays an essential role in stress-induced responses and cell survival.

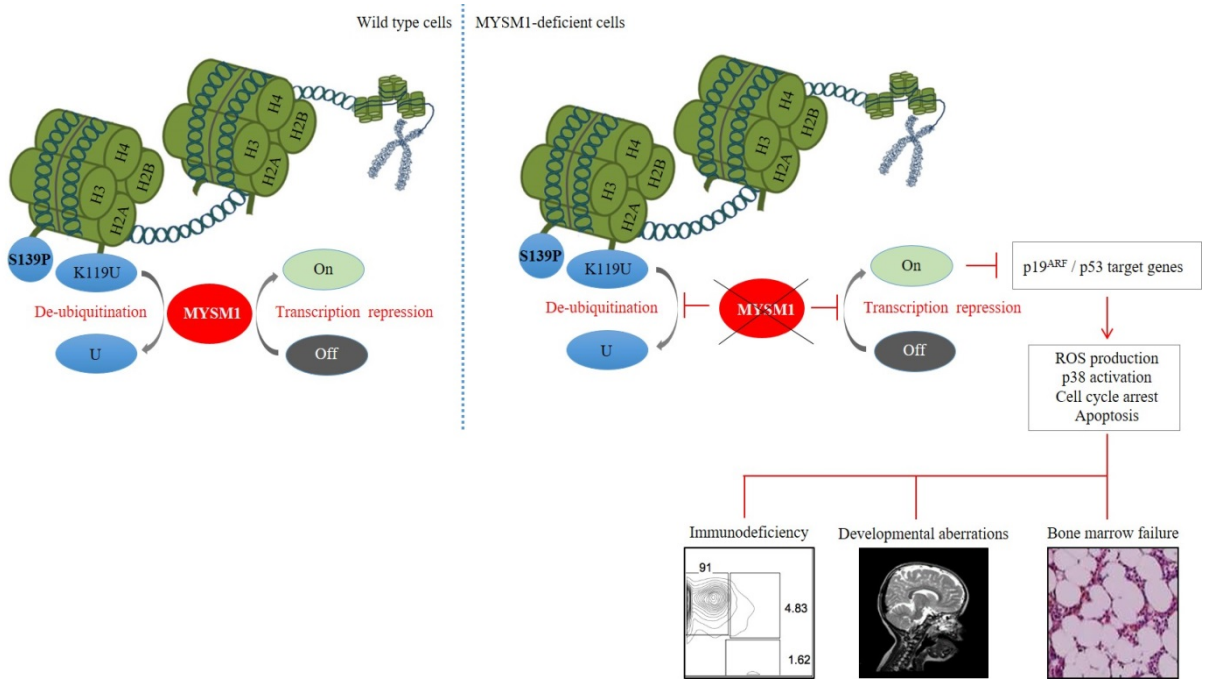

Figure 10: MYSM1-deficiency in human leads to immunodeficiency, developmental aberrations and BMF. In wild type cells MYSM1 properly regulates de-ubiquitination of H2A and transcription repression. De-ubiquitination of H2A and transcription repression of p53 and its target genes are impaired in MYSM1-deficient cells leading to elevation of ROS, apoptosis, sustained induction of p38 and cell cycle arrest, consequently resulting in developmental aberrations, immunodeficiency and BMF. The figure is taken from http://dx.doi.org/10.1016/j.jaci.2016.10.053

9.1.3. Chromatic remodeling complex can cause SGD and neutropenia

Previously it has been shown that rare mutation in CEBPE can cause SGD, elucidating the importance of CRCs for hematopoiesis and neutrophil maturation [132]. Our group has identified a new genetic defect associated with specific granule deficiency in 3 unrelated

families (Manuscript #2, Nature Genetics, in press). Using homozygosity mapping and NGS we discovered mutations in SMARCD2, an integral member of the SWI/SNF complex, known to control nucleosome positioning and chromatin reassembly.

Our biochemical studies could document SMARCD2 interacts with CEBPE, disclosing a direct functional correlation of SMARCD2 and CEBPE. SMARCD2 appears to bring CEPBE to relevant promotor sites, thus orchestrating the transcription of CEBPE-dependent genes in neutrophil granulocytes. However, the phenotype of SMRACD2 deficiency does not completely match the phenotype of CEBPE deficiency which is limited to anomalies of neutrophil granulocytes. SMARCD2 also affects hematopoietic stem cells (where it acts as transcriptional repressor, in contrast to its role as transcriptional activator in more mature precursor cells of neutrophil granulocytes) and non-hematopoietic systems such as bones.

We tried to establish a SMARCD2-deficient myeloid cell using CRISP/Cas9 mediated gene editing. However, our attempts failed probably due to the toxicity of SMARCD2 loss in cell lines. Only SMARCD2 knockdowns (using shRNA) gave rise to viable derivative clones. Further investigations are required to characterize SMARCD2 function in cell survival and development. Similar to patients with MYSM1 deficiency, patients with SMACD2 deficiency showed signs of myelodysplasia. The clinical picture thus highlights a critical role of chromatin remodeling/epigenetic control in both monogenic diseases.

9.1.4. Outlook – Basic lessons in biology from studying inherited rare diseases of the immune system

Inherited BMF syndromes comprise a heterogeneous group of deficiencies characterized by hematopoietic stem cell defects, with or without affecting other organ systems. This work extends the spectrum of known BMF disorders and highlights novel principles governing hematopoietic stem cell renewal and differentiation.

Investigations of FA eventuated in a better understanding of genome integrity and DNA repair mechanisms. Molecular inspections revealed interaction of FA proteins with proteins involved in other rare genetic chromosome instability syndromes such as ATM (ataxia-telangiectasia mutated), MRE11 (MRE11 meiotic recombination 11 homolog) and ATR (ATM and Rad3-

related), which play essential roles in DNA damage response and the pathogenesis of genome instable disorders [150]. Further investigations of FA associated genes linked them to cancer pathogenesis and disclosed that acquired mutations in FA genes presents in a wide variety of human cancers [151-154].

Telomere biology was first linked to medicine by the discovery of telomerase genes mutants in DC. BM and skin which have a high cell turnover are the most affected tissues in DC. Critically, shortened telomeres subsequently lead to activation of DNA damage machinery, cell cycle arrest, genome instability, chromosomal breakage and senescence [155-158]. It has been hypothesized that the combination of genomic instability and subsequent somatic mutations allowing further irregular cellular proliferation can result in oncogenesis [159]. These valuable insights about importance of telomeres in biology of the cells became apparent after investigation on DC and the underlying genetic cause.

Despite recent advances in the understanding of the genetic etiology of inherited BMF syndromes, in as many as about 40% of patients the underlying genetic cause remains unknown [160]. This work has shown that by the combination of next generation sequencing technology in association with basic biology investigations, new diseases can be identified and their molecular pathomechanisms can be understood. MYSM1 deficiency is characterized by a decreased capacity of cells to withstand genotoxic stresses, whereas SMARCD2 deficiency is caused by defective chromatin remodeling machinery. Even though the observations reported in our papers do not yet provide direct cues for novel therapies for affected patients, our research is aimed towards the development of cures for patients with currently still incurable diseases. It is conceivable that drugs can be developed that specifically affect the function of MYSM1 or SMARCD2. At this point, the only curative approach for these patients consists in transplantation of AHSC – but this procedure remains associated with severe comorbidities and its effects are limited to the hematopoietic system. Future studies are needed to develop novel therapeutic strategies.

10. Acknowledgements

Over the past years I was fortunate enough to work in Christoph Klein's laboratory and I would like to express my gratitude for his contributions of time, ideas, and funding to make my Ph.D possible.

I would like to thank Heinrich Leonhardt for his support as the internal supervisor of my thesis and the committee members: Thomas Cremer, Wolfgang Enard, John Parsch, Angelika Böttger, and Martin Parniske for their willingness to examine my thesis.

I also appreciate help of Rolf Meino and Imran Hause for revising of my thesis. I would like also to acknowledge Tomas Racek, for teaching and mentoring. I would like to thank Maximilian Witzel and Naschla Greif-Kohistani for the great help in the clinical part of my project.

I am deeply grateful to Jacek Puchalka for continuously kind help and support from the first minute of my work in the lab till the last day of his life.

A special thanks to my family. Words cannot express how beholden I am to my father, mother, and my wife for their help and support.

11. Curriculum vitae

Ehsan Bahrami
Date of birth: July/07/1984

EDUCATION

- Master of Science in Biology-Microbiology, University of Isfahan, Isfahan, Iran. (2007-2010). GPA: 17.20 out of 20. Graduate program, Department of Biology, Faculty of Science, University of Isfahan, Isfahan, Iran. (M.S. Thesis: The relationship among Multiple Sclerosis, leptin serum level and Epstein-Barr virus infection. Supervisor: Dr. Hamid Zarkesh-Esfahani .Score: 19.33 out of 20)

- Bachelor of Science in Cellular and Molecular Biology, Azad University, Iran (2002-2006) GPA: 16.33 out of 20.

PUBLICATIONS

- MYSM1 deficiency - genotoxic stress-associated bone marrow failure and developmental aberrations. Ehsan Bahrami, Maximilian Witzel, Tomas Racek, Jacek Puchałka, Sebastian Hollizeck, Naschla Greif-Kohistani, Daniel Kotlarz, Hans-Peter Horny, Regina Feederle, Heinrich Schmidt, Roya Sherkat, Doris Steinemann, Gudrun Göhring, Brigitte Schlegelbeger, Michael H. Albert, Waleed Al-Herz, and Christoph Klein. Journal of Allergy and Clinical Immunology 2017 (doi: 10.1016/j.jaci.2016.10.053.)

- Chromatin remodelling factor SMARCD2 (BAF60B) regulates transcriptional networks controlling differentiation of neutrophil granulocytes. Maximilian Witzel, Daniel Petersheim, Yanxin Fan, Ehsan Bahrami, Tomas Racek, Meino Rohlfs, Jacek Puchałka, Christian Mertes, Julien Gagneur, Christoph Ziegenhain, Wolfgang Enard, Asbjørg Stray-Pedersen, Peter D. Arkwright, Miguel R. Abboud, Vahid Pazhakh, Graham J. Lieschke, Peter M. Krawitz, Maik Dahlhoff, Marlon R. Schneider, Eckhard Wolf, Hans-Peter Horny, Heinrich Schmidt, Alejandro A. Schaffer and Christoph Klein. Nature Genetics 2017 (accepted paper in press)

- Mutations in Tetratricopeptide Repeat Domain 7A Result in a Severe Form of Very Early Onset Inflammatory Bowel Disease. Avitzur Y, Guo C, Mastropaolo LA, Bahrami E, Chen H, Zhao Z, Elkadri A, Dhillon S, Murchie R, Fattouh R, Huynh H, Walker JL, Wales PW, Cutz E, Kakuta Y, Dudley J, Kammermeier J, Powrie F, Shah N, Walz C, Nathrath M, Kotlarz D, Puchaka J, Krieger JR, Racek T, Kirchner T, Walters TD, Brumell JH, Griffiths AM, Rezaei N, Rashtian P, Najafi M, Monajemzadeh M, Pelsue S,

McGovern DP, Uhlig HH, Schadt E, Klein C, Snapper SB, Muise AM. Gastroenterology 2014, Apr; 146 (4):1028-39.

- Insulin and leptin levels in overweight and normal-weight Iranian adolescents: The CASPIAN-III study. Bahrami E, Mirmoghtadaee P, Ardalan G, Zarkesh-Esfahani H, Tajaddini MH, Haghjooy-Javanmard S, Najafi H, Kelishadi R. Journal of Research in Medical Sciences 2014, May;19 (5):38790.

- Leptin hormone level in serum of opticospinal, neuromyelitisoptica and multiple sclerosis patients. Ehsan Bahrami, Sayyed Hamid Zarkesh-Esfahani, Mohammad T. Kardi, Maryam Mostajeran, Alexa Triot, Majid Bouzari, Amir H. Maghzi, Masoud Etemadifar. Clinical and Experimental Neuroimmunology 2014, Feb (5) 77–83.

- Double-chimera proteins to enhance recruitment of endothelial cells and their progenitor cells. Behjati M, Kazemi M, Hashemi M, Zarkesh-Esfahanai SH, Bahrami E, Hashemi-Beni B, Ahmadi R. International Journal of Cardiology 2012, Aug 20; 167 (4):1560-9.

- Seroprevalence of NMO-IgG among patients with neuromyelitis optica and opticospinal multiple sclerosis. M.Etemadifar, M.Mollabashi, A.Chitsaz, O.Behnamfar, E.Bahrami, A.M.Maghzi:. Clinical Neurology and Neurosurgery 2011, Jan; 114 (1):17-20.

- Restricted leptin antagonism as a therapeutic approach to treatment of autoimmune diseases. A.Babaei, Babaei A, Zarkesh-Esfahani SH, Bahrami E, Ross RJ. Hormones 2011, Jan-Mar; 10 (1):16-26.

SEMINARS AND PRESENTATIONS

- SWI/SNF Protein SMARCD2 Orchestrates Transcriptional Networks Controlling Hematopoiesis and Neutrophil Granulocytes in Humans, Mice and Zebrafish. Maximilian Witzel, Daniel Petersheim, Yanxin Fan, Ehsan Bahrami, Tomas Racek, Meino Rohlfs, Jacek Puchalka, Christian Mertes, Julien Gagneur, Christoph Ziegenhain, Wolfgang Enard, Asbjorg Stray-Pedersen, Peter D Arkwright, Miguel R Abboud, Vahid Pazhakh, Graham J Lieschke, Peter K Krawitz, Maik Dahlhoff, Marlon R Schneider, Eckhard Wolf, Hans-Peter Horny, Heinrich Schmidt, Alejandro A Schäffer, Christoph Klein. 58th ASH meeting USA 2016 (American Society of Hematologists)

- A Human Bone Marrow Failure Syndrome Caused By a Homozygous Mutation in MYSM1. Ehsan Bahrami, Tomas Racek, Maximilian Witzel, Jacek Puchalka, Naschla Greif-Kohistani, Daniel Kotlarz, Michael Orth, Kirsten Lauber, Christoph Walz, Waleed

Al Herz, Hans-Peter Horny, Heinrich Schmidt, Michael H. Albert, Christoph Klein. 57th ASH meeting USA (American Society of Hematologists) Blood 2015 126:1204;

- Leptin serum levels in different subtypes of multiple sclerosis, dose it play a central role in progression of MS. The 98th annual meeting of the American Association of Immunologists, 2011 USA.

HONORS AND AWARDS

Five year research fellowship in Immunology, Care for rare foundation, Children Hospital of Munich, Germany, 2012-2016.

12. References

1. Maximow, A., *Der Lymphozyt als gemeinsame Stammzelle der verschiedenen Blutelemente in der embryonalen Entwicklung und im postfetalen Leben der Säugetiere.* Folia Haematologica, 1909. **8**: p. 125-134.
2. Lorenz, E., et al., *Modification of irradiation injury in mice and guinea pigs by bone marrow injections.* J Natl Cancer Inst, 1951. **12**(1): p. 197-201.
3. Till, J.E. and C.E. Mc, *A direct measurement of the radiation sensitivity of normal mouse bone marrow cells.* Radiat Res, 1961. **14**: p. 213-22.
4. Dexter, T.M. and L.G. Lajtha, *Proliferation of haemopoietic stem cells in vitro.* Br J Haematol, 1974. **28**(4): p. 525-30.
5. Moore, M.A., N. Williams, and D. Metcalf, *In vitro colony formation by normal and leukemic human hematopoietic cells: characterization of the colony-forming cells.* J Natl Cancer Inst, 1973. **50**(3): p. 603-23.
6. Civin, C.I., et al., *Antigenic analysis of hematopoiesis. III. A hematopoietic progenitor cell surface antigen defined by a monoclonal antibody raised against KG-1a cells.* J Immunol, 1984. **133**(1): p. 157-65.
7. Strauss, L.C., et al., *Antigenic analysis of hematopoiesis. V. Characterization of My-10 antigen expression by normal lymphohematopoietic progenitor cells.* Exp Hematol, 1986. **14**(9): p. 878-86.
8. Doulatov, S., et al., *Hematopoiesis: a human perspective.* Cell Stem Cell, 2012. **10**(2): p. 120-36.
9. Notta, F., et al., *Isolation of single human hematopoietic stem cells capable of long-term multilineage engraftment.* Science, 2011. **333**(6039): p. 218-21.
10. Lessard, J. and G. Sauvageau, *Bmi-1 determines the proliferative capacity of normal and leukaemic stem cells.* Nature, 2003. **423**(6937): p. 255-60.
11. Shojaei, F., et al., *Hierarchical and ontogenic positions serve to define the molecular basis of human hematopoietic stem cell behavior.* Dev Cell, 2005. **8**(5): p. 651-63.
12. Nutt, S.L., et al., *Dynamic regulation of PU.1 expression in multipotent hematopoietic progenitors.* J Exp Med, 2005. **201**(2): p. 221-31.
13. Zhu, J. and S.G. Emerson, *Hematopoietic cytokines, transcription factors and lineage commitment.* Oncogene, 2002. **21**(21): p. 3295-313.
14. LeBien, T.W. and T.F. Tedder, *B lymphocytes: how they develop and function.* Blood, 2008. **112**(5): p. 1570-80.
15. Coutinho, A. and G. Moller, *Thymus-independent B-cell induction and paralysis.* Adv Immunol, 1975. **21**: p. 113-236.
16. Nemazee, D., *Receptor editing in lymphocyte development and central tolerance.* Nat Rev Immunol, 2006. **6**(10): p. 728-40.
17. Blom, B. and H. Spits, *Development of human lymphoid cells.* Annu Rev Immunol, 2006. **24**: p. 287-320.
18. Santos, P., et al., *Transcriptional and epigenetic regulation of B cell development.* Immunol Res, 2011. **50**(2-3): p. 105-12.
19. Ng, S.Y., et al., *Genome-wide lineage-specific transcriptional networks underscore Ikaros-dependent lymphoid priming in hematopoietic stem cells.* Immunity, 2009. **30**(4): p. 493-507.
20. Mansson, R., et al., *Molecular evidence for hierarchical transcriptional lineage priming in fetal and adult stem cells and multipotent progenitors.* Immunity, 2007. **26**(4): p. 407-19.
21. Adolfsson, J., et al., *Identification of Flt3+ lympho-myeloid stem cells lacking erythro-megakaryocytic potential a revised road map for adult blood lineage commitment.* Cell, 2005. **121**(2): p. 295-306.
22. Forsberg, E.C., et al., *New evidence supporting megakaryocyte-erythrocyte potential of flk2/flt3+ multipotent hematopoietic progenitors.* Cell, 2006. **126**(2): p. 415-26.

23. Friedman, A.D., *Transcriptional control of granulocyte and monocyte development.* Oncogene, 2007. **26**(47): p. 6816-28.
24. Laslo, P. and T. Stopka, *Transcriptional and Epigenetic Regulation in the Development of Myeloid Cells: Normal and Diseased Myelopoiesis*, in *Transcriptional and Epigenetic Mechanisms Regulating Normal and Aberrant Blood Cell Development*. 2014, Springer. p. 223-245.
25. Moreau-Gachelin, F., A. Tavitian, and P. Tambourin, *Spi-1 is a putative oncogene in virally induced murine erythroleukaemias.* Nature, 1988. **331**(6153): p. 277-80.
26. Back, J., et al., *Visualizing PU.1 activity during hematopoiesis.* Exp Hematol, 2005. **33**(4): p. 395-402.
27. Scott, E.W., et al., *Requirement of transcription factor PU.1 in the development of multiple hematopoietic lineages.* Science, 1994. **265**(5178): p. 1573-7.
28. Dakic, A., et al., *PU.1 regulates the commitment of adult hematopoietic progenitors and restricts granulopoiesis.* J Exp Med, 2005. **201**(9): p. 1487-502.
29. Iwasaki, H., et al., *Distinctive and indispensable roles of PU.1 in maintenance of hematopoietic stem cells and their differentiation.* Blood, 2005. **106**(5): p. 1590-600.
30. DeKoter, R.P. and H. Singh, *Regulation of B lymphocyte and macrophage development by graded expression of PU.1.* Science, 2000. **288**(5470): p. 1439-41.
31. Hagman, J. and K. Lukin, *Transcription factors drive B cell development.* Curr Opin Immunol, 2006. **18**(2): p. 127-34.
32. Busslinger, M., *Transcriptional control of early B cell development.* Annu Rev Immunol, 2004. **22**: p. 55-79.
33. Rossi, M.I., et al., *B lymphopoiesis is active throughout human life, but there are developmental age-related changes.* Blood, 2003. **101**(2): p. 576-84.
34. Nutt, S.L., et al., *Commitment to the B-lymphoid lineage depends on the transcription factor Pax5.* Nature, 1999. **401**(6753): p. 556-62.
35. Santos, P.M. and L. Borghesi, *Molecular resolution of the B cell landscape.* Curr Opin Immunol, 2011. **23**(2): p. 163-70.
36. Cobaleda, C., et al., *Pax5: the guardian of B cell identity and function.* Nat Immunol, 2007. **8**(5): p. 463-70.
37. Nutt, S.L., et al., *Essential functions of Pax5 (BSAP) in pro-B cell development: difference between fetal and adult B lymphopoiesis and reduced V-to-DJ recombination at the IgH locus.* Genes Dev, 1997. **11**(4): p. 476-91.
38. Nutt, S.L., et al., *Identification of BSAP (Pax-5) target genes in early B-cell development by loss- and gain-of-function experiments.* EMBO J, 1998. **17**(8): p. 2319-33.
39. Aronheim, A., et al., *The E2A gene product contains two separable and functionally distinct transcription activation domains.* Proc Natl Acad Sci U S A, 1993. **90**(17): p. 8063-7.
40. Massari, M.E., P.A. Jennings, and C. Murre, *The AD1 transactivation domain of E2A contains a highly conserved helix which is required for its activity in both Saccharomyces cerevisiae and mammalian cells.* Mol Cell Biol, 1996. **16**(1): p. 121-9.
41. Bain, G., et al., *E2A proteins are required for proper B cell development and initiation of immunoglobulin gene rearrangements.* Cell, 1994. **79**(5): p. 885-92.
42. Zhuang, Y., P. Soriano, and H. Weintraub, *The helix-loop-helix gene E2A is required for B cell formation.* Cell, 1994. **79**(5): p. 875-84.
43. Kee, B.L., M.W. Quong, and C. Murre, *E2A proteins: essential regulators at multiple stages of B-cell development.* Immunol Rev, 2000. **175**: p. 138-49.
44. Park, S.J., et al., *Stem cell factor protects bone marrow-derived cultured mast cells (BMCMC) from cytocidal effect of nitric oxide secreted by fibroblasts in murine BMCMC-fibroblast coculture.* Biochem Mol Biol Int, 1996. **40**(4): p. 721-9.
45. Kee, B.L. and C. Murre, *Induction of early B cell factor (EBF) and multiple B lineage genes by the basic helix-loop-helix transcription factor E12.* J Exp Med, 1998. **188**(4): p. 699-713.

46. Quong, M.W., et al., *E2A activity is induced during B-cell activation to promote immunoglobulin class switch recombination.* EMBO J, 1999. **18**(22): p. 6307-18.
47. Lin, H. and R. Grosschedl, *Failure of B-cell differentiation in mice lacking the transcription factor EBF.* Nature, 1995. **376**(6537): p. 263-7.
48. Bain, G., et al., *Both E12 and E47 allow commitment to the B cell lineage.* Immunity, 1997. **6**(2): p. 145-54.
49. Lin, Y.C., et al., *A global network of transcription factors, involving E2A, EBF1 and Foxo1, that orchestrates B cell fate.* Nat Immunol, 2010. **11**(7): p. 635-43.
50. Treiber, T., et al., *Early B cell factor 1 regulates B cell gene networks by activation, repression, and transcription- independent poising of chromatin.* Immunity, 2010. **32**(5): p. 714-25.
51. Decker, T., et al., *Stepwise activation of enhancer and promoter regions of the B cell commitment gene Pax5 in early lymphopoiesis.* Immunity, 2009. **30**(4): p. 508-20.
52. Walter, K., C. Bonifer, and H. Tagoh, *Stem cell-specific epigenetic priming and B cell-specific transcriptional activation at the mouse Cd19 locus.* Blood, 2008. **112**(5): p. 1673-82.
53. Dokal, I. and T. Vulliamy, *Inherited bone marrow failure syndromes.* Haematologica, 2010. **95**(8): p. 1236-40.
54. Collins, J. and I. Dokal, *Inherited bone marrow failure syndromes.* Hematology, 2015. **20**(7): p. 433-4.
55. Shimamura, A. and B.P. Alter, *Pathophysiology and management of inherited bone marrow failure syndromes.* Blood Rev, 2010. **24**(3): p. 101-22.
56. Fanconi, G., *Familiäre infantile perniziosaartige Anämie (perniziöses Blutbild und Konstitution)*. 1927: Karger.
57. Green, A.M. and G.M. Kupfer, *Fanconi anemia.* Hematol Oncol Clin North Am, 2009. **23**(2): p. 193-214.
58. Wang, W., *Emergence of a DNA-damage response network consisting of Fanconi anaemia and BRCA proteins.* Nat Rev Genet, 2007. **8**(10): p. 735-48.
59. Yoshida, K. and Y. Miki, *Role of BRCA1 and BRCA2 as regulators of DNA repair, transcription, and cell cycle in response to DNA damage.* Cancer Sci, 2004. **95**(11): p. 866-71.
60. Xia, B., et al., *Control of BRCA2 cellular and clinical functions by a nuclear partner, PALB2.* Mol Cell, 2006. **22**(6): p. 719-29.
61. Yu, X., et al., *The BRCT domain is a phospho-protein binding domain.* Science, 2003. **302**(5645): p. 639-42.
62. Duncan, J.A., J.R. Reeves, and T.G. Cooke, *BRCA1 and BRCA2 proteins: roles in health and disease.* Mol Pathol, 1998. **51**(5): p. 237-47.
63. Alter, B.P., et al., *Malignancies and survival patterns in the National Cancer Institute inherited bone marrow failure syndromes cohort study.* Br J Haematol, 2010. **150**(2): p. 179-88.
64. Parikh, S. and M. Bessler, *Recent insights into inherited bone marrow failure syndromes.* Curr Opin Pediatr, 2012. **24**(1): p. 23-32.
65. Vulliamy, T.J., et al., *Mutations in dyskeratosis congenita: their impact on telomere length and the diversity of clinical presentation.* Blood, 2006. **107**(7): p. 2680-5.
66. Calado, R.T. and N.S. Young, *Telomere diseases.* N Engl J Med, 2009. **361**(24): p. 2353-65.
67. Townsley, D.M., B. Dumitriu, and N.S. Young, *Bone marrow failure and the telomeropathies.* Blood, 2014. **124**(18): p. 2775-83.
68. Vlachos, A., et al., *Diagnosing and treating Diamond Blackfan anaemia: results of an international clinical consensus conference.* Br J Haematol, 2008. **142**(6): p. 859-76.
69. Draptchinskaia, N., et al., *The gene encoding ribosomal protein S19 is mutated in Diamond-Blackfan anaemia.* Nature genetics, 1999. **21**(2): p. 169-175.
70. Vlachos, A., et al., *Clinical utility gene card for: Diamond Blackfan anemia.* Eur J Hum Genet, 2011. **19**(5).
71. Dror, Y. and M.H. Freedman, *Shwachman-diamond syndrome.* Br J Haematol, 2002. **118**(3): p. 701-13.

72. Dror, Y. and M.H. Freedman, *Shwachman-Diamond syndrome: An inherited preleukemic bone marrow failure disorder with aberrant hematopoietic progenitors and faulty marrow microenvironment.* Blood, 1999. **94**(9): p. 3048-54.
73. Rawls, A.S., et al., *Lentiviral-mediated RNAi inhibition of Sbds in murine hematopoietic progenitors impairs their hematopoietic potential.* Blood, 2007. **110**(7): p. 2414-22.
74. Ball, H.L., et al., *Shwachman-Bodian Diamond syndrome is a multi-functional protein implicated in cellular stress responses.* Hum Mol Genet, 2009. **18**(19): p. 3684-95.
75. Dror, Y., et al., *Immune function in patients with Shwachman-Diamond syndrome.* Br J Haematol, 2001. **114**(3): p. 712-7.
76. Orelio, C. and T.W. Kuijpers, *Shwachman-Diamond syndrome neutrophils have altered chemoattractant-induced F-actin polymerization and polarization characteristics.* Haematologica, 2009. **94**(3): p. 409-13.
77. Kostmann, R., *Hereditär reticulos-en ny systemsjukdom.* Svenska Läkartideningen, 1950. **47**: p. 2861-2868.
78. Klein, C., *Genetic defects in severe congenital neutropenia: emerging insights into life and death of human neutrophil granulocytes.* Annu Rev Immunol, 2011. **29**: p. 399-413.
79. Donadieu, J., et al., *Congenital neutropenia: diagnosis, molecular bases and patient management.* Orphanet J Rare Dis, 2011. **6**: p. 26.
80. Klein, C., *Congenital neutropenia.* Hematology Am Soc Hematol Educ Program, 2009: p. 344-50.
81. Klein, C., et al., *HAX1 deficiency causes autosomal recessive severe congenital neutropenia (Kostmann disease).* Nat Genet, 2007. **39**(1): p. 86-92.
82. Devriendt, K., et al., *Constitutively activating mutation in WASP causes X-linked severe congenital neutropenia.* Nat Genet, 2001. **27**(3): p. 313-7.
83. Person, R.E., et al., *Mutations in proto-oncogene GFI1 cause human neutropenia and target ELA2.* Nat Genet, 2003. **34**(3): p. 308-12.
84. Vilboux, T., et al., *A congenital neutrophil defect syndrome associated with mutations in VPS45.* N Engl J Med, 2013. **369**(1): p. 54-65.
85. Triot, A., et al., *Inherited biallelic CSF3R mutations in severe congenital neutropenia.* Blood, 2014. **123**(24): p. 3811-7.
86. Boztug, K., et al., *A syndrome with congenital neutropenia and mutations in G6PC3.* N Engl J Med, 2009. **360**(1): p. 32-43.
87. Boztug, K., et al., *JAGN1 deficiency causes aberrant myeloid cell homeostasis and congenital neutropenia.* Nat Genet, 2014. **46**(9): p. 1021-7.
88. Toriello, H.V., *Thrombocytopenia-absent radius syndrome.* Semin Thromb Hemost, 2011. **37**(6): p. 707-12.
89. Sato, T., et al., *Clinical manifestations and enzymatic activities of mitochondrial respiratory chain complexes in Pearson marrow-pancreas syndrome with 3-methylglutaconic aciduria: a case report and literature review.* Eur J Pediatr, 2015. **174**(12): p. 1593-602.
90. Bannister, A.J. and T. Kouzarides, *Regulation of chromatin by histone modifications.* Cell Res, 2011. **21**(3): p. 381-95.
91. Goldknopf, I.L., et al., *Isolation and characterization of protein A24, a "histone-like" non-histone chromosomal protein.* J Biol Chem, 1975. **250**(18): p. 7182-7.
92. Nickel, B.E. and J.R. Davie, *Structure of polyubiquitinated histone H2A.* Biochemistry, 1989. **28**(3): p. 964-8.
93. West, M.H. and W.M. Bonner, *Histone 2A, a heteromorphous family of eight protein species.* Biochemistry, 1980. **19**(14): p. 3238-45.
94. Wang, H., et al., *Role of histone H2A ubiquitination in Polycomb silencing.* Nature, 2004. **431**(7010): p. 873-8.
95. Zhou, W., et al., *Histone H2A monoubiquitination represses transcription by inhibiting RNA polymerase II transcriptional elongation.* Mol Cell, 2008. **29**(1): p. 69-80.

96. Sparmann, A. and M. van Lohuizen, *Polycomb silencers control cell fate, development and cancer.* Nat Rev Cancer, 2006. **6**(11): p. 846-56.
97. Vissers, J.H., et al., *The many faces of ubiquitinated histone H2A: insights from the DUBs.* Cell Div, 2008. **3**: p. 8.
98. Hershko, A. and A. Ciechanover, *The ubiquitin system.* Annu Rev Biochem, 1998. **67**: p. 425-79.
99. Joo, H.Y., et al., *Regulation of cell cycle progression and gene expression by H2A deubiquitination.* Nature, 2007. **449**(7165): p. 1068-72.
100. Wunsch, A.M., A.L. Haas, and J. Lough, *Synthesis and ubiquitination of histones during myogenesis.* Dev Biol, 1987. **119**(1): p. 85-93.
101. McClurg, U.L. and C.N. Robson, *Deubiquitinating enzymes as oncotargets.* Oncotarget, 2015. **6**(12): p. 9657-68.
102. Coyne, E.S. and S.S. Wing, *The business of deubiquitination - location, location, location.* F1000Res, 2016. **5**.
103. Nicassio, F., et al., *Human USP3 is a chromatin modifier required for S phase progression and genome stability.* Curr Biol, 2007. **17**(22): p. 1972-7.
104. Zhu, P., et al., *A histone H2A deubiquitinase complex coordinating histone acetylation and H1 dissociation in transcriptional regulation.* Mol Cell, 2007. **27**(4): p. 609-21.
105. Komander, D., M.J. Clague, and S. Urbe, *Breaking the chains: structure and function of the deubiquitinases.* Nat Rev Mol Cell Biol, 2009. **10**(8): p. 550-63.
106. Jiang, X.X., et al., *Control of B cell development by the histone H2A deubiquitinase MYSM1.* Immunity, 2011. **35**(6): p. 883-96.
107. Nijnik, A., et al., *The critical role of histone H2A-deubiquitinase Mysm1 in hematopoiesis and lymphocyte differentiation.* Blood, 2012. **119**(6): p. 1370-1379.
108. Demarco, I.A. and H. Singh, *The A-MYSM power of deubiquitinases.* Immunity, 2011. **35**(6): p. 847-9.
109. Wang, T., et al., *The control of hematopoietic stem cell maintenance, self-renewal, and differentiation by Mysm1-mediated epigenetic regulation.* Blood, 2013. **122**(16): p. 2812-22.
110. Won, H., et al., *Epigenetic control of dendritic cell development and fate determination of common myeloid progenitor by Mysm1.* Blood, 2014. **124**(17): p. 2647-2656.
111. Forster, M., et al., *Deubiquitinase MYSM1 Is Essential for Normal Fetal Liver Hematopoiesis and for the Maintenance of Hematopoietic Stem Cells in Adult Bone Marrow.* Stem Cells Dev, 2015. **24**(16): p. 1865-77.
112. Nandakumar, V., et al., *Epigenetic control of natural killer cell maturation by histone H2A deubiquitinase, MYSM1.* Proceedings of the National Academy of Sciences of the United States of America, 2013. **110**(41): p. E3927-E3936.
113. Li, P., et al., *Deubiquitinase MYSM1 Is Essential for Normal Bone Formation and Mesenchymal Stem Cell Differentiation.* Sci Rep, 2016. **6**: p. 22211.
114. DiTommaso, T., et al., *Identification of genes important for cutaneous function revealed by a large scale reverse genetic screen in the mouse.* PLoS Genet, 2014. **10**(10): p. e1004705.
115. Alsultan, A., et al., *MYSM1 is mutated in a family with transient transfusion-dependent anemia, mild thrombocytopenia, and low NK- and B-cell counts.* Blood, 2013. **122**(23): p. 3844-5.
116. Le Guen, T., et al., *An in vivo genetic reversion highlights the crucial role of Myb-Like, SWIRM, and MPN domains 1 (MYSM1) in human hematopoiesis and lymphocyte differentiation.* J Allergy Clin Immunol, 2015.
117. Gatzka, M., et al., *Interplay of H2A deubiquitinase 2A-DUB/Mysm1 and the p19(ARF)/p53 axis in hematopoiesis, early T-cell development and tissue differentiation.* Cell Death Differ, 2015. **22**(9): p. 1451-62.
118. Liu, Y., et al., *p53 regulates hematopoietic stem cell quiescence.* Cell Stem Cell, 2009. **4**(1): p. 37-48.

119. Milyavsky, M., et al., *A distinctive DNA damage response in human hematopoietic stem cells reveals an apoptosis-independent role for p53 in self-renewal.* Cell Stem Cell, 2010. **7**(2): p. 186-97.
120. Wang, J., et al., *A differentiation checkpoint limits hematopoietic stem cell self-renewal in response to DNA damage.* Cell, 2012. **148**(5): p. 1001-14.
121. Belle, J.I., et al., *p53 mediates loss of hematopoietic stem cell function and lymphopenia in Mysm1 deficiency.* Blood, 2015. **125**(15): p. 2344-8.
122. Belle, J.I., et al., *Repression of p53-target gene Bbc3/PUMA by MYSM1 is essential for the survival of hematopoietic multipotent progenitors and contributes to stem cell maintenance.* Cell Death Differ, 2016. **23**(5): p. 759-75.
123. Clapier, C.R. and B.R. Cairns, *The biology of chromatin remodeling complexes.* Annu Rev Biochem, 2009. **78**: p. 273-304.
124. Romero, O.A. and M. Sanchez-Cespedes, *The SWI/SNF genetic blockade: effects in cell differentiation, cancer and developmental diseases.* Oncogene, 2014. **33**(21): p. 2681-9.
125. Brownlee, P.M., C. Meisenberg, and J.A. Downs, *The SWI/SNF chromatin remodelling complex: Its role in maintaining genome stability and preventing tumourigenesis.* DNA Repair (Amst), 2015. **32**: p. 127-33.
126. Feng, B., et al., *Purification and Characterization of Phospholipase A(2) from the Venom of Snake Trimeresurus stejnegeri Schmidt.* Sheng Wu Hua Xue Yu Sheng Wu Wu Li Xue Bao (Shanghai), 1996. **28**(2): p. 201-205.
127. Lickert, H., et al., *Baf60c is essential for function of BAF chromatin remodelling complexes in heart development.* Nature, 2004. **432**(7013): p. 107-12.
128. Lou, X., et al., *Smarcd3b and Gata5 promote a cardiac progenitor fate in the zebrafish embryo.* Development, 2011. **138**(15): p. 3113-23.
129. Meng, Z.X., et al., *Baf60c drives glycolytic metabolism in the muscle and improves systemic glucose homeostasis through Deptor-mediated Akt activation.* Nat Med, 2013. **19**(5): p. 640-5.
130. Meng, Z.X., et al., *The Baf60c/Deptor pathway links skeletal muscle inflammation to glucose homeostasis in obesity.* Diabetes, 2014. **63**(5): p. 1533-45.
131. Hsiao, P.W., et al., *BAF60a mediates critical interactions between nuclear receptors and the BRG1 chromatin-remodeling complex for transactivation.* Mol Cell Biol, 2003. **23**(17): p. 6210-20.
132. Lekstrom-Himes, J.A., et al., *Neutrophil-specific granule deficiency results from a novel mutation with loss of function of the transcription factor CCAAT/enhancer binding protein epsilon.* J Exp Med, 1999. **189**(11): p. 1847-52.
133. Stewart, M.J., et al., *The role of CCAAT/enhancer-binding protein in the differential transcriptional regulation of a family of human liver alcohol dehydrogenase genes.* J Biol Chem, 1991. **266**(18): p. 11594-603.
134. Ramji, D.P. and P. Foka, *CCAAT/enhancer-binding proteins: structure, function and regulation.* Biochem J, 2002. **365**(Pt 3): p. 561-75.
135. Antonson, P., et al., *A novel human CCAAT/enhancer binding protein gene, C/EBPepsilon, is expressed in cells of lymphoid and myeloid lineages and is localized on chromosome 14q11.2 close to the T-cell receptor alpha/delta locus.* Genomics, 1996. **35**(1): p. 30-8.
136. Chumakov, A.M., et al., *Cloning of the novel human myeloid-cell-specific C/EBP-epsilon transcription factor.* Mol Cell Biol, 1997. **17**(3): p. 1375-86.
137. Lekstrom-Himes, J. and K.G. Xanthopoulos, *CCAAT/enhancer binding protein epsilon is critical for effective neutrophil-mediated response to inflammatory challenge.* Blood, 1999. **93**(9): p. 3096-105.
138. Le Guen, T., et al., *An in vivo genetic reversion highlights the crucial role of Myb-Like, SWIRM, and MPN domains 1 (MYSM1) in human hematopoiesis and lymphocyte differentiation.* J Allergy Clin Immunol, 2015. **136**(6): p. 1619-26 e1-5.

139. Jiang, X.X., et al., *Control of B Cell Development by the Histone H2A Deubiquitinase MYSM1.* Immunity, 2011. **35**(6): p. 883-896.
140. Kotlarz, D., et al., *Loss of interleukin-10 signaling and infantile inflammatory bowel disease: implications for diagnosis and therapy.* Gastroenterology, 2012. **143**(2): p. 347-55.
141. Huen, M.S., et al., *RNF8 transduces the DNA-damage signal via histone ubiquitylation and checkpoint protein assembly.* Cell, 2007. **131**(5): p. 901-14.
142. Mailand, N., et al., *RNF8 ubiquitylates histones at DNA double-strand breaks and promotes assembly of repair proteins.* Cell, 2007. **131**(5): p. 887-900.
143. Lancini, C., et al., *Tight regulation of ubiquitin-mediated DNA damage response by USP3 preserves the functional integrity of hematopoietic stem cells.* J Exp Med, 2014. **211**(9): p. 1759-77.
144. Shanbhag, N.M., et al., *ATM-dependent chromatin changes silence transcription in cis to DNA double-strand breaks.* Cell, 2010. **141**(6): p. 970-81.
145. Nishi, R., et al., *Systematic characterization of deubiquitylating enzymes for roles in maintaining genome integrity.* Nat Cell Biol, 2014. **16**(10): p. 1016-26, 1-8.
146. Gong, X.W., et al., *UV-induced interaction between p38 MAPK and p53 serves as a molecular switch in determining cell fate.* Febs Letters, 2010. **584**(23): p. 4711-4716.
147. She, Q.B., N.Y. Chen, and Z.G. Dong, *ERKs and p38 kinase phosphorylate p53 protein at serine 15 in response to UV radiation.* Journal of Biological Chemistry, 2000. **275**(27): p. 20444-20449.
148. Bulavin, D.V., et al., *Phosphorylation of human p53 by p38 kinase coordinates N-terminal phosphorylation and apoptosis in response to UV radiation.* Embo Journal, 1999. **18**(23): p. 6845-6854.
149. Huang, C.S., et al., *p38 kinase mediates UV-induced phosphorylation of p53 protein at serine 389.* Journal of Biological Chemistry, 1999. **274**(18): p. 12229-12235.
150. Taniguchi, T. and A.D. D'Andrea, *Molecular pathogenesis of Fanconi anemia: recent progress.* Blood, 2006. **107**(11): p. 4223-33.
151. Tischkowitz, M., et al., *Bi-allelic silencing of the Fanconi anaemia gene FANCF in acute myeloid leukaemia.* Br J Haematol, 2003. **123**(3): p. 469-71.
152. Marsit, C.J., et al., *Inactivation of the Fanconi anemia/BRCA pathway in lung and oral cancers: implications for treatment and survival.* Oncogene, 2004. **23**(4): p. 1000-4.
153. van der Heijden, M.S., et al., *Functional defects in the fanconi anemia pathway in pancreatic cancer cells.* Am J Pathol, 2004. **165**(2): p. 651-7.
154. Turner, N., A. Tutt, and A. Ashworth, *Hallmarks of 'BRCAness' in sporadic cancers.* Nat Rev Cancer, 2004. **4**(10): p. 814-9.
155. Zou, Y., et al., *Does a sentinel or a subset of short telomeres determine replicative senescence?* Mol Biol Cell, 2004. **15**(8): p. 3709-18.
156. Mieczkowski, P.A., et al., *Genetic regulation of telomere-telomere fusions in the yeast Saccharomyces cerevisae.* Proc Natl Acad Sci U S A, 2003. **100**(19): p. 10854-9.
157. McClintock, B., *The Stability of Broken Ends of Chromosomes in Zea Mays.* Genetics, 1941. **26**(2): p. 234-82.
158. Ballew, B.J. and S.A. Savage, *Updates on the biology and management of dyskeratosis congenita and related telomere biology disorders.* Expert Rev Hematol, 2013. **6**(3): p. 327-37.
159. Hanahan, D., *Benefits of bad telomeres.* Nature, 2000. **406**(6796): p. 573-4.
160. Yu, Q.H., S.Y. Wang, and Z. Wu, *Advances in genetic studies of inherited bone marrow failure syndromes and their associated malignancies.* Transl Pediatr, 2014. **3**(4): p. 305-9.